



**MODELLING THE IMPACT OF COASTAL DEFENCE
STRUCTURES ON THE NEARSHORE
MORPHODYNAMICS**

A thesis submitted to Cardiff University

in candidature for the degree of

Doctor of Philosophy

by

Fernando Alvarez-Martinez

Hydro-environmental Research Centre

School of Engineering

Cardiff University

2016

ACKNOWLEDGEMENTS

I would like to express my appreciation to the people and organisations that supported and accompanied me in this long journey.

- To the School of Engineering of Cardiff University for supporting this PhD programme.
- To all Cardiff University staff in the Research, Finance and Teaching offices for their support to all PhD students, making things easier for all during the process.
- To family and friends that always supported me and encouraged me to keep going until the end.
- To Dr. Shunqi Pan for his patience, advice and support during all the stages of this PhD and to Professor Roger A. Falconer for his support.

MODELLING THE IMPACT OF COASTAL DEFENCE STRUCTURES ON THE NEARSHORE MORPHODYNAMICS

Fernando Alvarez-Martinez

ABSTRACT

Coastal areas are heavily populated in countries around the world and are a source of economic activity, both recreational and industrial. Waves and tides interact with sediments in a dynamic equilibrium which leads to coastal morphological changes at different temporal and spatial scales. Natural or human-induced changes in this equilibrium may lead to an alteration of the coastline causing environmental or economic impacts. Coastal defences are often needed in order to protect specific areas and reduce such impacts. Therefore, understanding the impact that coastal defence structures have on coastal morphological changes is important for coastal managers.

There are different methods to study morphological changes in coastal areas. Process-based numerical models are powerful and precise tools but they are more effective for small to medium spatial scales (km) and short to medium-term temporal scales. Data-driven methods have been proven useful to study morphological changes in the long-term. However, data is not always available in the quantity or quality needed for such methods to provide meaningful results. This study uses jointly process-based numerical models, COAST2D, and data-driven methods, Empirical Orthogonal Functions method (EOF), taking advantage of the strengths of both methods to overcome their own weaknesses. A novel methodology for EOF components extrapolation, named Dynamic EOF method, is developed.

Results show that, COAST2D is an efficient tool to simulate morphological changes in the scale of months and kilometres. These scales exceed the ones reached previously by the model, increasing the confidence on its capabilities. The Dynamic EOF method, which extrapolates both temporal and spatial EOF components, was found to yield better results than previous attempts using the EOF method to extrapolate results beyond the training period based on EOF temporal component extrapolation only.

Keywords: EOF method, Dynamic EOF method, forecasting, shore-parallel breakwaters, morphological changes, COAST2D.

TABLE OF CONTENTS

Acknowledgements	i
Abstract	ii
Table of Contents	iii
List of Figures	v
List of Tables.....	x
List of Publications	xi
1 Introduction	1
2 Literature Review	5
2.1 Introduction	5
2.2 Coastal Morphology	17
2.3 Process-based Modelling.....	20
2.4 Reduced-physics Modelling	22
2.5 Data-Driven Modelling	22
2.6 Aims and Objectives	30
3 Methodology	32
3.1 Introduction	32
3.2 EOF Method	32
3.3 Dynamic EOF Method	39
3.3.1 EOF Spatial Component extrapolation	40
3.3.2 EOF Temporal Component extrapolation.....	43
3.4 Summary	45
4 Process-based Model.....	47
4.1 Introduction	47
4.2 Model Description	47
4.2.1 Currents	48
4.2.2 Waves.....	48
4.2.3 Sediment transport	50

4.3	Model Re-Validation	51
4.3.1	Study Area.....	51
4.3.2	Model Setup	52
4.3.3	Results and Discussion.....	55
4.3.4	Summary	62
5	Data Generation	63
5.1	Introduction	63
5.2	Idealised Study Domain	63
5.2.1	Boundary Conditions	65
5.2.2	Model Results	66
5.3	Data preparation	74
5.3.1	Shoreline Changes.....	75
5.3.2	Volumetric changes – alongshore sections	76
5.3.3	Volumetric changes – computational cells	81
5.4	Summary	84
6	Dynamic EOF Analysis	86
6.1	Introduction	86
6.2	1D Approach	86
6.3	2D Approach	96
6.4	Dynamic EOF method advantages and limitations	109
6.5	Summary	112
7	Conclusions and Future Research	113
7.1	Conclusions	113
7.2	Future Research.....	116
8	References	118

LIST OF FIGURES

Figure 2.1. Coastal Regions patterns in the European Union. Error! Bookmark not defined.	
Figure 2.2. Managed realignment in Little Haven beach, South Shield, UK. Beach in 2012 before the works (left) and beach in 2015 after the works (right).	10
Figure 2.3. Schematic shore-parallel breakwater scheme. Initial shoreline (dashed line) and final shoreline (solid line).....	13
Figure 2.4. Beam deformation when a punctual external force is applied..... Error! Bookmark not defined.	
Figure 2.5. Design parameters shore-parallel breakwaters.	14
Figure 2.6. Predicted VS observed shoreline response of different breakwater schemes across UK (Environment Agency 2010a). Observed tombolos (squares), observed salients (triangles), no sinuosity (cross).	15
Figure 2.7. Railway damage after storm in January 2014(The Guardian).....	18
Figure 2.8. Sediment transport motion. Fluids forces causing sediment motion (Reeve et al. 2011).....	19
Figure 3.1. Example for EOF matrix construction.....	34
Figure 3.2. Schematic diagram of the dynamic EOF approach (c) in comparison with the method of Horrillo-Caraballo et al. (2014) (b) and standard EOF method (a).	40
Figure 3.3. Concept for Dynamic EOF spatial component extrapolation.....	41
Figure 3.4. Example of EOF spatial component extrapolation.	42
Figure 3.5. Example of standard EOF temporal extrapolation.	43
Figure 3.6. Example of inadequate EOF temporal extrapolation.	44

Figure 3.7. Example of Dynamic EOF temporal extrapolation.	45
Figure 4.1. Validation study area.	52
Figure 4.2. Initial computational domain for the model COAST2D. Initial shoreline position is indicated in blue.....	53
Figure 4.3. Offshore significant wave height at Leixoes station.....	54
Figure 4.4. Wave direction rose at Leixoes station.....	54
Figure 4.5. Significant wave height VS wave period at Leixoes station.	54
Figure 4.6. Significant wave height at the Aerao Groyne on the 11th October 2013 with offshore significant wave height 0.82m during high tide (calm conditions).	56
Figure 4.7. Currents at the Aerao Groyne on the 11th October 2013 with offshore significant wave height 0.82m during high tide (calm conditions).....	56
Figure 4.8. Sediment transport rates at the Aerao Groyne on the 11th October 2013 with offshore significant wave height 0.82m during high tide (calm conditions).	57
Figure 4.9. Significant wave height at the Aerao Groyne on the 26th October 2013 with offshore significant wave height 5.3m during high tide (storm conditions).....	58
Figure 4.10. Currents at the Aerao Groyne on the 26th October 2013 with offshore significant wave height 5.3m during high tide (storm conditions).	58
Figure 4.11. Sediment transport rates at the Aerao Groyne on the 26th October 2013 with offshore significant wave height 5.3m during high tide (storm conditions).....	59
Figure 4.12. Initial (blue) and final (red) measured shoreline and final modelled shoreline (green).....	60
Figure 4.13. Net measured (top panel) and modelled (bottom panel) advance-recess of the shoreline.	61
Figure 4.14. Net shoreline advance/recess values (m) for each area.	61

Figure 5.1. Model domain. Shoreline ($z=0$) represented by black dashed line.....	63
Figure 5.2. Model domain definitions.....	64
Figure 5.3. Computational domain and reduced domain for EOF analysis (red square).	65
Figure 5.4. Wave height distribution for the cases S101 (top), S102 (middle) and S103 (bottom).....	67
Figure 5.5. Wave height distribution for cases S104 (top), S105 (middle) and S106 (bottom).....	68
Figure 5.6. Bathymetric changes after 750h for cases S101 (top), S102 (middle) and S103 (bottom).	69
Figure 5.7. Bathymetric changes after 750h for cases S104 (top), S105 (middle) and S106 (bottom).	70
Figure 5.8. Wave height for $t=1h$ (top panel) and $t=750h$ (bottom panel).....	71
Figure 5.9. Alongshore sediment transport for $t=100h$	71
Figure 5.10. Bathymetry for $t=1h$ (top panel) and $t=750h$ (bottom panel).	72
Figure 5.11. Shoreline for $t=750h$	73
Figure 5.12. Bed level changes for $t=750h$	73
Figure 5.13. 1D shoreline changes issues. Horn-shaped salients (top panel). Shoreline discontinuous jumps.....	76
Figure 5.14. Cumulative bed levels per section for $t=750h$ at each section.	78
Figure 5.15. 1 st and 2 nd EOF spatial components for the 750h period analysis.	79
Figure 5.16. 1 st and 2 nd EOF temporal components for the 750h period analysis.	80
Figure 5.17. 1 st and 2 nd EOF spatial components for the 750h period analysis.	83

Figure 5.18. 1 st and 2 nd EOF temporal components for the 750h period analysis.	84
Figure 6.1. Samples of the 1st spatial EOF components for 66 analysis, 1D case.	88
Figure 6.2. Temporal evolution of the first spatial EOF component at location x=1775m.	89
Figure 6.3. 1D extrapolation for section 71, x=1775m.	90
Figure 6.4. 1 st EOF spatial component extrapolation using the Dynamic EOF method.	91
Figure 6.5. 1 st EOF temporal component for different sub-intervals.	92
Figure 6.6, 1 st EOF temporal component extrapolation. Standard method (top panel). Dynamic EOF method (bottom panel).	93
Figure 6.7. 1D unit volumetric changes extrapolation using standard method (blue line) and dynamic EOF extrapolation (red line).	94
Figure 6.8. Measured vs reconstructed shoreline at t=1500h using extrapolated EOF components.	95
Figure 6.9. First EOF component as 2D for the 750h period analysis.	97
Figure 6.10. 1 st EOF components for 66 analyses at one particular location.	98
Figure 6.11. Example of exponential extrapolation with 50 points.	100
Figure 6.12. Example of linear extrapolation with 20 points.	101
Figure 6.16. Dynamic EOF extrapolation for the 1 st EOF spatial component in 2D.	102
Figure 6.14. Percentage of error histogram for the extrapolated 1 st EOF component using the Dynamic EOF extrapolation method vs no extrapolation method.	103
Figure 6.15. Extrapolation type selected by the Dynamic EOF method.	104
Figure 6.16. Number of points selected by the Dynamic EOF method.	104

Figure 6.17. Correlation coefficient for each cell using the Dynamic EOF method. .	105
Figure 6.18. Temporal extrapolation using Dynamic EOF method (top panel) and standard method (bottom panel).....	106
Figure 6.19. Extrapolation results at t=1500h using the standard EOF method.	107
Figure 6.20. Extrapolation results at t=1500h using the Dynamic EOF method.	108
Figure 6.21. Difference (percentage) between measured an extrapolated unit volumetric changes at t=1500h for both the Dynamic EOF extrapolation method (blue) and the standard EOF extrapolation method (red).	109

LIST OF TABLES

Table 1. Number of datasets used for fitting VS validation.....	29
Table 2. Incident waves parameters	65
Table 3. Parameters used for COAST2D.....	66
Table 4. Percentage of variance explained by each component for the 1D unit volumetric changes 750h period analysis.	79
Table 5. Depth of closure values.....	81
Table 6. Percentage of variance explained by each component for the 2D unit volumetric changes 750h period analysis.	83
Table 7. 1 st EOF temporal component values for 1D unit volumetric changes.	93
Table 8. 1 st EOF temporal component values for 2D unit volumetric changes.	106

LIST OF PUBLICATIONS

Journal Articles

Alvarez, F. and Pan, S. (2016) ‘Predicting coastal morphological changes with empirical orthogonal function method’, *Water Science and Engineering*, 9(1), 14-20 [DOI: 10.1016/j.wse.2015.10.003].

Alvarez, F., Pan, S., Coelho, C., Baptista, P. (to be submitted) ‘Modelling of shoreline changes at Aveiro, Portugal using a process-based numerical model: COAST2D’

Conference Proceedings

Alvarez, F. and Pan, S. (2014) ‘Modelling long-term coastal morphology using EOF method’, *Coastal Engineering Proceedings*, (34).

Alvarez, F. and Pan, S. (2015). ‘Modelling long-term morphological changes using EOF method on volumetric changes’ in: *Proceedings of the 3rd International IMA Conference on Flood Risk 2015*, Swansea, UK

Conferences attended

3rd IMA International Conference on Flood Risk, Swansea, UK (March, 2015)

XI Young Coastal Scientist and Engineers Conference, Manchester, UK (March, 2015)

34th International Conference on Coastal Engineering, Seoul, South Korea (June, 2014)

X Young Coastal Scientist and Engineers Conference, Cardiff, UK (March, 2014)
(Member of the Local Academic Organising Committee)

IX Young Coastal Scientist and Engineers Conference, Aberdeen, UK (March, 2013)

1 INTRODUCTION

Coastlines around the world are heavily populated. The increase in population living by the sea together with the economic importance of the coastline due to tourism, recreational and industrial areas or environmental preservation turn coastal morphological changes assessment into a main consideration for coastal engineers and managers.

Waves and tides generate currents that lift and draft sediments both in the cross-shore and alongshore directions. These processes are especially important in the breaking and swash zones. Whereas sediment is moved at a higher rate it is replenished, erosion will occur. On the contrary, where sediment is replenished faster than it is washed away, accretion happens. Despite the conceptually simple description of the process a precise mathematical description of sediment transport processes remains challenging.

Human activity interaction with the environment may lead to an alteration of morphodynamics patterns affecting greatly the sediment transport equilibrium in the area. Sea level rise and changes in meteorological patterns may also affect the dynamic equilibrium between waves, tides and sediment sources. These factors have played an important role in the recent decades. Where the sediment balance is altered, coastal erosion and accretion occur. Both situations could represent an issue not just for the local area but at a regional scale. For these reasons morphological changes remain one of the most important issues in coastal areas. Therefore, it is crucial to understand any impact to the coastal morphodynamics system, from dam construction upstream a river, channel dredging for navigation, coastal defence structures or artificial nourishments.

Coastal morphodynamics has been classically seen as an empirical science as it is complex to define clear generic relationships between external forces and effects. Many of the design criteria for coastal works have been based, until recent decades, in 'good practice' manuals based in previous experience (Environment Agency 2010a). Coastal erosion is one of the aspects to be considered as it causes many economic losses every year, representing life-threatening events in some cases. Where the

coastline needs to be protected from coastal erosion coastal defences are often considered.

Shore-parallel breakwaters have been widely used to protect the shoreline. There are some benefits over other structures but defining their effects on the shoreline remains challenging. These structures are often dominated by current related transport. However wave-current interaction in the surrounding of these structures is complex, especially when large tidal ranges are acting in the area. Typically, design guidelines have been proposed for different countries/areas depending on their own previous experience. Most likely, extrapolating those guidelines to different countries or conditions might yield inaccurate results. This has been the case for the United Kingdom. Using the design criteria that have been developed for micro-tidal conditions might have resulted in undesirable shoreline shapes being developed under the meso or macro-tidal conditions in the UK (Thomalla and Vincent 2004).

In order to study morphological changes in coastal areas and specifically around coastal defence structures, different approaches can be followed. Numerical models have played a very important role during the last decades in predicting coastal hydrodynamics and morphodynamics. However, it is important to fully understand the limitations of these models in order to adequately interpret their results, especially when studying sediment transport (Hanson et al. 2003). In most cases, sediment transport equations are still based on empirical experience, and depending on the chosen set of equations results may vary. These issues are especially important when assessing long-term morphological changes. Among the inherent difficulties to parameterize coastal morphological changes there is the stochastic nature of waves and precipitations that makes it difficult for deterministic models to assess a range of possible case scenarios.

There are other techniques to assess coastal changes based on historical data analysis rather than on building-up results with process-based models. These are often referred to as data-driven methods. Such methods rely on data acquired in the past years or decades trying to explain the changes experienced by the system during such period and in some cases, extrapolating those results into the future, at least qualitatively. The Empirical Orthogonal Functions (EOF) Method is one of those methods. It has been

applied to different disciplines from oceanography, meteorology and also, coastal morphology. The use of EOF method in coastal morphology has several benefits. The EOF method provides components that are independent in time and space, which facilitates understanding the changes experienced by the system. Those components can often be related to physical processes. The components provided by the EOF method are sorted so the first pair of components, spatial and temporal, explains the majority of the data variance. The second pair explains the majority of the remaining variability and so on. This feature allows explaining most of the data variance with, typically, a low number of components. The EOF method in coastal areas has been used to study different features, from cross-shore profiles to alongshore profiles and more recently 2D bed level changes, such as sandbanks.

However, the EOF method requires a high-quality data set in order to provide meaningful results. Due to the characteristics of coastal areas it is often difficult to obtain appropriate datasets in order to apply the EOF method intensively. Data availability is more concerning when structures have not been yet constructed. Recently the usage of video cameras has helped obtaining better data-set which yields to better interpretation of the EOF method results (Fairley et al. 2009). The improvements on satellites, image and communication is rapidly increasing the quality of data collection while reducing their acquisition cost which will certainly improve the accuracy of data-driven methods.

EOF components allow describing changes that have occurred during the training period. More recently, effort has been made in describing the EOF components extrapolation techniques in order to quantitatively assess the data variability beyond the training period. However, the experience is limited to the EOF temporal component extrapolation only, assuming the EOF spatial components calculated for the training period are valid for times beyond such period (Reeve and Karunarathna 2011).

This study aims to develop a methodology for the EOF component extrapolation, named Dynamic EOF method, in order to improve the accuracy of the predictions of the longer term coastal morphological changes under the combined wave and tide conditions in presence of coastal structures.

The Dynamic EOF method is intended for long-term predictions. The Dynamic EOF method shares some of the limitations of the EOF standard method. Although it has the capability of explaining physical processes related with the variable of study, it is not always possible to back track those processes and explain them individually, especially if those processes are not known beforehand. Also, the extrapolation function used to extrapolate the EOF components is critical and its definition might not be straightforward for all the cases. Moreover, some processes can not be extrapolated due to the uncertainties on the forcing, especially if such forcing is rapidly and constantly changing. Finally, as it happens with the standard EOF method, the Dynamic EOF data requirements are critical as it needs a high temporal resolution in order to produce meaningful results.

The main objectives of this study are: (i) to use a well calibrated process-based numerical model to generate high quality data under well controlled conditions for Dynamic EOF method, (ii) to develop an approach to improve EOF extrapolation for both the spatial and temporal components in order to increase the accuracy of longer term coastal morphological predictions; and (iii) to further understand the impacts of shore-parallel breakwaters schemes on meso-tidal environments. This thesis is organised as follows:

Chapter 2 reviews the existing research closely relevant to this study, through which the knowledge gaps are identified. It covers a description of morphological changes and coastal protection strategies. Focus is set on shore-parallel breakwaters, a typology of structure widely used worldwide but with limited examples in the UK. Finally, methods for coastal morphology description are shown, including numerical models and data-driven methods such as the EOF method. Chapter 3 describes the novel methodology used in this study, the Dynamic EOF method. Chapter 4 describes the process-based numerical model used to generate the required datasets for the dynamic EOF analysis. Chapter 5 describes the numerical model setup for data generation as well as the application of the standard EOF method to data generated. Chapter 6 presents the application of the Dynamic EOF method to two case studies, 1D and 2D bed level changes. Finally, Chapter 7 summarises the key conclusions of this study stating the advantages and disadvantages of the proposed methodology, the Dynamic EOF method, and proposes recommendations for future research.

2 LITERATURE REVIEW

2.1 INTRODUCTION

This chapter provides the necessary background to understand the scope and purpose of this thesis. The first section, on coastal morphology and erosion, describes the processes involved and the impact of coastal erosion for coastal communities. The second section, on coastal management, describes the main strategies and structures available to protect and enhance the coastline. The following sections describe methods for monitoring and predicting coastal morphological changes including process-based numerical models and data-driven models. An in-depth description of one of those data-driven methods, the Empirical Orthogonal Functions Method is provided as it is a key part on this thesis. To conclude the scope and objectives of the thesis are defined.

Coastal erosion is a natural phenomenon that could potentially happen anywhere. However, when coastal erosion alters human interests, it becomes a concern for scientists and engineers. In the following paragraphs a review of the main concerns that coastal erosion represents for Europe and especially for the United Kingdom is presented.

Europe has an intrinsic relationship with the sea. Eurostat (2009) provides an idea of the weight that coastal communities have in Europe. There are 22 countries with a seacoast in the European Union. These countries have a sea border with four seas, Mediterranean, Baltic, North and Black sea. The total length of the European shoreline is 136.101km. In terms of population, 199 million people live in these coastal areas, and 70 million live in coastal municipalities.

The EuroSION Project, promoted by the European Commission (2004) states that 20% of the European coast faces serious impacts from coastal erosion. The comprehensive study is a solid initial point to understand coastal erosion as a global problem for Europe. Two findings can be highlighted from that report; 1) the importance of systematically monitoring coastal erosion that already affects around 15.000km along Europe and 2) the difficulty of dealing with coastal erosion as the study identifies

2900km of coastline that even protected by any form of coastal protection, are still being eroded.

According to the EuroSION project (EuroSION 2004), the value of assets located within 500m from the shoreline is around 500-1000 billion euros. The same study states that just in 2001, 3500 million euro were spent on coastal erosion and flooding just considering the assets at imminent risk. The Inter-Governmental Panel for Climate Change (IPCC-United Nations) estimates however that the average expenditure per year from 1990-2020 will be 5400 million euros.

Another in-depth study was carried out more recently by the CONSCIENCE consortium. This project, launched in 2007, tested the recommendations given by EuroSION (2004). Many documents were derived from this project and they can be consulted in the CONSCIENCE website (Conscience website). Here, some ideas of special interest for this thesis are highlighted. In the Conscience report, “Conscience report for policy makers” (Marchand 2010) provided some examples of expenditures related to coastal erosion problems along Europe. For instance, France spends every year around 41 million euro just in mitigation measurements. Netherlands expend around 20 million euros on beach nourishment. Another example is given in Portugal where between the municipalities of Aveiro and Vagueira, a 20 km coast stretch, 500 million euros has been spent since 1995 on hard structures and dune stabilization.

In 2002, a report titled “Safeguarding our seas” was published by Department of Food and Rural Affairs (DEFRA 2002) . According to the Secretary of State for Environment, Food and Rural Affairs of the United Kingdom, this report sets the vision for the British marine environment and tackles the need for coherent and integrated approach to face threats and preserve marine biodiversity. The report mentioned coastal erosion as a threat, especially for England and Wales. It also stressed the concept of coastal sediment cells and the need for Shoreline Management Plans to tackle coastal issues as a regional issue rather than a local problem. This report mentioned the European project “Living with the Sea”, which is a sign on how European policies adapt to each particular country. However, this report does not provide figures on coastal erosion and focusses more on other issues such as water pollution, marine renewable energies or marine biodiversity.

In 2005, another report was published by DEFRA (2005), “Charting Progress: An integrated assessment of the state of UK seas” that continues with the vision stated in 2002 (DEFRA, 2002). According to the Minister of State for Environment and Agri-Environment, Elliot Morley, “Charting Progress provides the first integrated assessment of the state of the seas across the whole of the UK Continental Shelf”. This report goes further on describing coastal erosion as a main issue for four out of the eight British regions defined in the report. Coastal erosion is described as an issue generally although some specific figures are given. For instance, the report states that half of English and Welsh coastline varies up to 10cm per year with 25% of the cliff eroding from 10cm to 2m per year. However, an in-depth coastal erosion analysis is yet to be provided.

The Environment Agency (EA) published in 2008 a “Review of International Best Practice” (Environment Agency 2008). This review studied the coastal management policies and experiences in other countries in order to better assess British coastal communities. This report examines policies in United States of America, France, The Netherlands and Australia in order to find the strategies that better worked in other places and their possible application to the United Kingdom. This report does not deal with coastal erosion processes but with mitigation measures through coastal urban planning. This approach is interesting since coastal erosion becomes a major problem especially when properties are affected resulting in economic losses. Therefore, urban planning in coastal communities can be seen as a main coastal erosion mitigation measurement. Seven recommendations are drawn by the authors of this report although just 3 are highlighted here. They all referred to the concepts of risk and planning. Quoting from the report:

- “Systematic use of ‘planned retreat’ to allow time-limited development on the coast providing a mechanism for risk informed decisions” (based on Australian practice).
- Requirement for local planning authorities to systematically adopt restrictive zoning policies for coastal erosion (such as in Australia and French Risk Prevention Plans).
- Acquisition and lease back of coastal lands at risk. Under such schemes, local government acquires land at risk and leases it to existing or future users for a

specified period of time, after which the land reverts to public ownership (based on Australian practice).

The importance of these recommendations lie on the concept of coastal erosion as a long-term uncertain process that has to be treated as such, giving a main role to urban coastal planning as a tool to mitigate coastal erosion by applying prevention measurements rather than mitigation measurements. In December 2014, Defra launched a 6 year programme (2015-2021) with the objective of reducing flood risk and coastal erosion in UK.

Climate change and sea level rise (SLR) will affect sediment transport and therefore coastal morphology. The former, will increase the mean sea level exposing new areas to the action of waves. According to Masselink (2013) the sea SLR could range between 30 to 50cm by 2100. Climate change could also induce a modification in the storminess varying, the frequency, locations and intensity. For instance, the expected increase of significant wave height will be in the range of 0.5 to 1m (Masselink and Russell., 2013). Also, greater storm frequency can be expected (20-fold increase possible by 2100) (Welsh Coastal monitoring Centre, 2011). These changes in storms will consequently produce a shift in the wave climate altering the balance between sediment availability and potential erosion rates.

These considerations on climate change add even more uncertainty to the prediction of long-term morphological changes. Nevertheless, climate change should be taken into consideration when designing coastal defence structures, coastal flood schemes or coastal planning. The UK government have a system of provisions to take into account these effects (EA, 2011). These provisions increase by a certain percentage the active forces used in the design process to allow for possible effects of climate changes and sea level rise, considering different scenarios ranging from lower expected increase to higher expected increase.

Nicholls (2013) provides a list with the expected impact for different coastal features and coastal structures. Masselink (2013) argues that in the future the most likely strategy to prevent coastal erosion problems will be managed realignment. Therefore, climate change, including sea level rise should be considered in coastal planning both in the regional scale and in the individual coastal defence scheme scale.

As it was discussed, the shoreline management plans (SMP) are the guidance for coastal management in the UK. The SMP provide four different policies to be followed by coastal municipalities. As described by DEFRA (DEFRA 2006) those policies are:

Hold the existing defence line by maintaining or changing the standard of protection. This policy should cover those situations where work or operations are carried out in front of the existing defences to improve or maintain the standard of protection provided by the existing defence line.

Advance the existing defence line by building new defences on the seaward side of the original defences. Using this policy should be limited to those policy units where significant land reclamation is considered. *Managed realignment* by allowing the shoreline to move backwards or forwards, with management to control or limit movement.

Managed realignment by allowing the shoreline to move backwards or forwards, with management to control or limit movement

No active intervention where there is no investment in coastal defences or operations.

Although prior to the definition of the SMP in 1996, an example of advance the existing defence line can be found at Sea Palling, Norfolk. After the flooding events in 1953 it was decided to build a seawall along the coast to work as the primary coastal defence structure on the area. Also, further north, groynes were built Eccles to protect the beaches in that area. As a results, beaches increased their size in Eccles but blocking the alongshore sediment transport downdrift and therefore starving the Sea Palling area. As a result, the foundation of the seawall at Sea Palling was regularly eroded. In 1992 a new beach management plan was defined including the construction of rock revetments to protect the sea wall and also the construction of shore-parallel breakwaters to increase the beach size (advance the line) increasing the protection against storms (Gee 2005).

A case of managed realignment can be found in the Little Haven beach, in South Shield, UK (Figure 2.1). In this case, the seawall was being damaged every year and the car park was systematically flooded causing an economic impact to the council. The approach taken was to reconsider the shape of the seawall, allowing the shoreline to reach its natural position, minimising the erosion issues on the foundation of the sea wall. In the picture below it can be clearly seen how the new scheme (right image) adapts to the natural shape of the shoreline whereas previously the seawall and car park were invading the beach space causing the erosion issue. The scheme has been a success (Royal HaskoningDHV, 2015) and highlights the efficiency of the managed realignment policy.

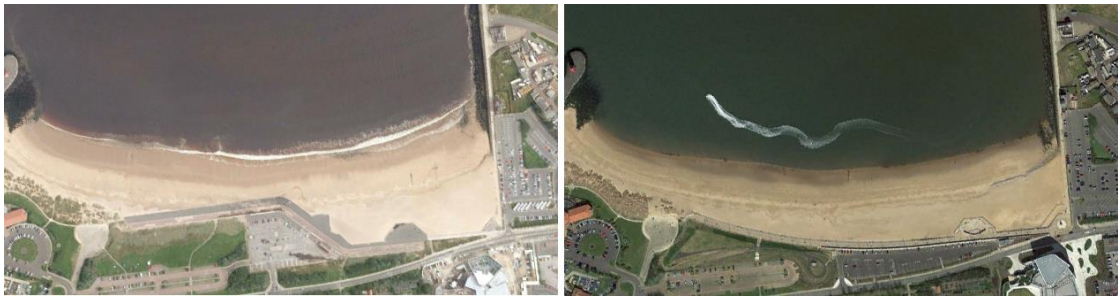


Figure 2.1. Managed realignment in Little Haven beach, South Shield, UK. Beach in 2012 before the works (left) and beach in 2015 after the works (right).

No active intervention would be suggested for those areas where no assets are at risk and therefore either the existing defences are considered enough or no defences are present but are also not required. An example of this policy can be seen in the SMP for Essex and Suffolk (Environment Agency 2010b)

These four policies vary on the degree of intervention provided to the shoreline. The need and justification of one policy over the others will vary widely between sites and each particular case should be assessed individually. However, the Shoreline Management Plans do not specify how to apply the above mentioned strategies and it remains a decision of the Local Authorities and relevant stakeholders to decide what type of defences will be applied in order to meet the SMP specifications.

There are numerous coastal defence structures and strategies that are typically divided into three categories as follows:

Hard Engineering Defences, consisting mainly in concrete or rock defences such as seawalls, groynes, detached breakwaters or revetment. Sometimes wooden groynes can also be found having the same effect than rock groynes. According to EuroSION (2004) more than 70% of the shoreline protected in Europe is protected with Hard Engineering Defences. The same report states that 63% of the new eroding shorelines (eroded in 2001 but not in 1986) are located less than 30km from another defended shoreline. This figure highlights the importance of designing adequately new schemes as they can defend the intended area but produce new coastal erosion issues somewhere else.

Soft Engineering Defences, consisting of typically in beach nourishment but also dune stabilisation or using vegetation to reduce the energy reaching the coast. Beach nourishment is becoming popular against hard engineering measures. In 2004, there were around 600 sites in Europe that were refilled with sand (Hanson et al. 2002) (Hamm et al., 2004). They require in general a lower initial investment although they require a maintenance plan over the years. A case of dune stabilisation can be found in North Portugal (Carvalho 2004) where dune stabilisation was achieved by using wood fences, vegetation and public access management and signposting.

Van Rijn Van Rijn (2011) carried out an assessment of the costs and benefits of using hard engineering measures, mainly groynes and detached breakwaters, and soft engineering approaches such beach nourishment. It was concluded that groynes are not very affective in most sites, the decision should be taken between beach nourishment and detached breakwaters, also known as shore-parallel breakwaters.

In most cases, the breakwaters are displayed parallel to the shoreline thus the name shore-parallel breakwaters. Nevertheless, when wave incidence angle is oblique, >30 degrees, breakwaters might be placed parallel to the incoming waves (Dally and Pope 1986)

The main concept behind shore parallel breakwater is that they reduce the amount of energy reaching the coastline while allowing alongshore sediment transport between them and the shoreline. This fact overcome the main problem with perpendicular structures to the shoreline such as groynes, reducing, in principle, the negative effects on the surrounding beach like sediment blockage leading to increased erosion. The

effects that shore parallel breakwater can produce on the shoreline can be categorise differently. According to Rosati (Rosati 1990) the effects on the shoreline can be; no significant effects, moderate effect or salient; large influence or tombolos. This classification is a simplification to that proposed by Pope (Pope and Dean 1986) that included more cases for the salient response: no sinuosity, subdued salient; well-developed salient; periodic tombolos and permanent tombolos. Although Pope's classification is more precise, in this thesis Rosati's classification will be used and salient will be referred as a unique response without differentiating their size.

The fact that wave energy is reduced at the lee of the breakwaters reduces the sediment transport rates increasing the deposition and therefore inducing the shoreline to advance towards the breakwaters forming what is called salients (Figure 2.2). This situation produces two benefits. Firstly, the size of the beach behind the breakwaters increases which enhances leisure activities. Secondly, the additional sediments represent a defence itself against storms and a supply of sediment to replenish naturally the nearby areas after storm periods.

Nevertheless, shore-parallel breakwater can also produce negative effects on the shoreline. When more than one breakwater is built, the area between them is named embayments. In these embayments, the shoreline typically suffers from erosion. While this is a known fact that can be accounted for during the design phase, the embayment erosion heavily varies on the wave conditions and scheme design. If not design properly, the erosion in the embayment can represent a major threat than prior to the scheme.

When designing shore parallel breakwaters, it may occur as a salient is developed excessively, eventually reaching the breakwaters, the formation of a tombolo. The impact of tombolo formation depends on the overall sediment transport direction in the area. If there is a predominant alongshore sediment transport direction and a tombolo is formed, the sediment can be blocked acting the tombolo like a groyne (Dolphin et al. 2012). If there is not a clear predominant wave direction, tombolo formation becomes less relevant.

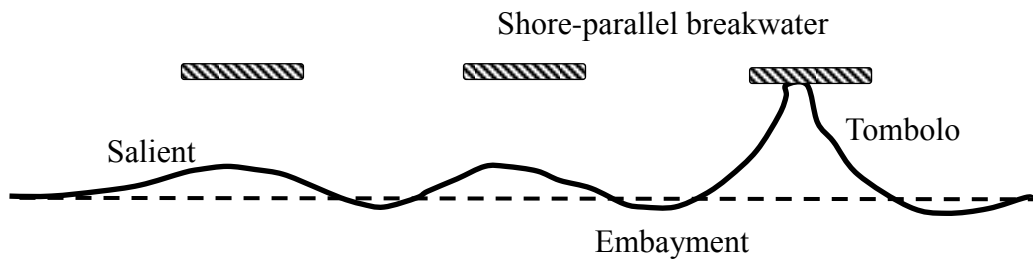


Figure 2.2. Diagram for shore-parallel breakwater scheme. Dashed line indicates the initial shoreline and solid line indicates the final shoreline.

Therefore, when designing shore parallel breakwater schemes the key criteria is to produce as much salient as possible while reducing the size of the embayments and the erosion on the edges of the scheme. Also avoiding tombolo formation can be other key criteria depending on the sediment transport climate.

The shore-parallel breakwater design can be divided into two different stages the structural design and the functional design. Structural design accounts for constructing the breakwater so it can resist the impacts of waves without moving or changing its form and to do so for the design live of the structure. However, the main function of a shore-parallel breakwater is not to resist the wave impacts but to generate a certain response in the shoreline. Therefore, no attention is paid to structural design of the breakwaters as it is out of the scope of this thesis.

The functional design stage contributing to the shoreline response is based on the geometrical layout of the scheme. Geometrical layout refers to length of the breakwaters, gap distance between breakwaters or offshore distance among other geometrical variables that will be explain later on. Depending on these factors, the wave climate and sediment availability in the area, the shoreline response will vary accordingly.

An exhaustive description of the parameters described for shore parallel breakwaters schemes can be found in many references, for instance USACE (2003) or an Environment Agency report on breakwater design criteria (Environment Agency 2010a). Some relevant parameters are shown in Figure 2.5.

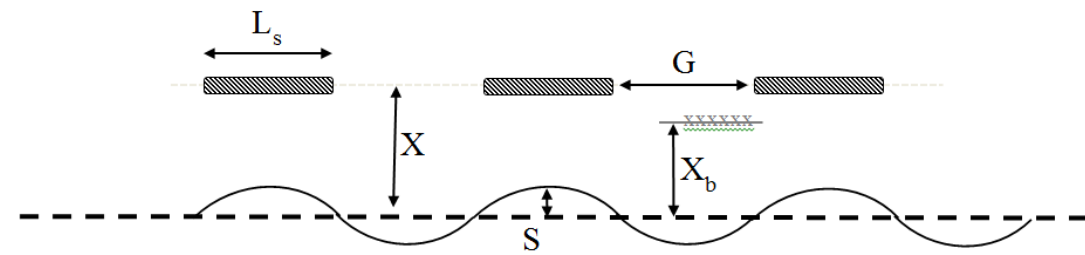


Figure 2.3. Design parameters shore-parallel breakwaters.

L_s is defined as the breakwater length, referring to the length on an individual breakwater. G is the gap distance between breakwaters in case there is more than one. X , is the offshore distance considered from the initial shoreline position (dashed line). X_b is the distance from the shoreline to the wave breaking line or surf zone. This value depends obviously on the considered waves and provides an idea on the amount of sediment trapped by the breakwaters. S , is the magnitude of the salient produced as a response to the breakwaters.

In a qualitative manner, it can be discussed that the smaller X , the chances of generating a tombolo increase. On the contrary, if breakwater is situated far from the shoreline, large X , their impacts can be unnoticeable. The larger the gap, G , more energy reaches the shoreline and more eroded the embayments will be. The longer are breakwaters, L_s , more coastline length is protected but the chances of tombolo formation increase. The ratio of X_b/X provides an idea of the littoral drift affected by the breakwaters. This ratio can be used initially to calculate the amount of sediment that will move downstream unaffected by the breakwaters. While these relationships have a common acceptance, quantifying their value is not straight forward.

Classically engineers used relations based on field experience. Dally (1986) state in a CERC report that design of these structures is an empirical process. The same year, the Japanese Ministry of Construction (JMC 1986) published a design guide for off-shore breakwaters based in 1552 projects alongside the Japanese coast. From that experience, relationships between geometrical parameters and shoreline responses were defined and a step by step guide for breakwaters design was proposed. Experimental relationships have the issue that those might not be valid for a different location with different conditions. In 1990, Rosati reviewed the JMC methodology and applied it to some of the 17 schemes built in USA at that time (Rosati 1990). Both

cases Japan and USA are located in non-tidal or micro-tidal areas. This fact implicates their design guidance might not be valid in other environments with larger tides.

More recently, the DEFRA and the EA published a report aimed to discuss the state of the design guidance for shore-parallel breakwaters in the UK (Environment Agency 2010a). This report reviewed the current design criteria based on field experience and applied it to the existing British schemes. Their findings reveal that design criteria based on field experience in other countries is not valid to explain the shoreline behaviour under the British wave and tide conditions. A figure is shown in the report showing the expected shoreline response using the current design criteria vs the observed shoreline response in the British scheme. Figure 2.6 represent the figure from the report.

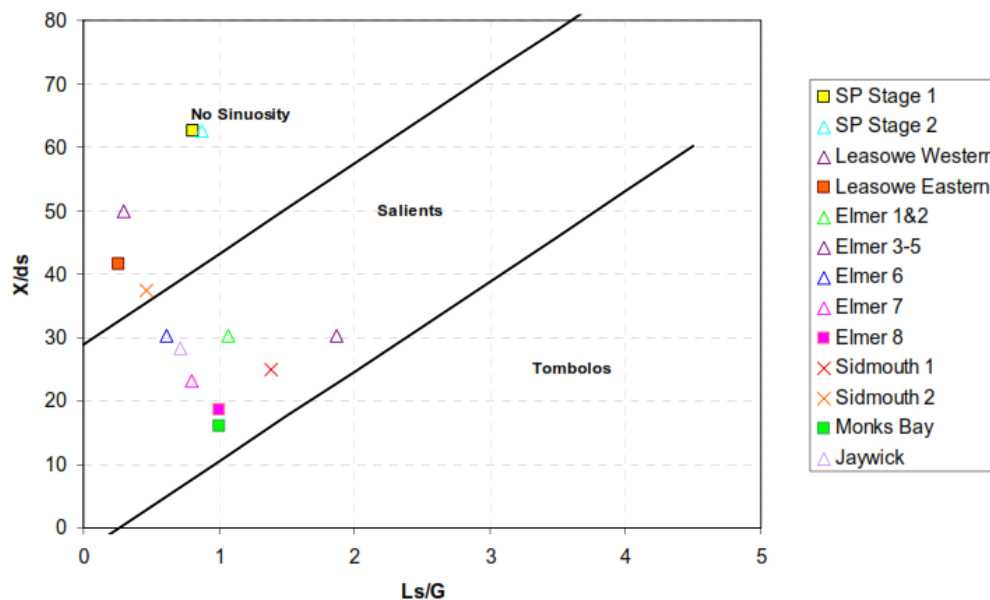


Figure 2.4. Predicted VS observed shoreline response of different breakwater schemes across UK (Environment Agency 2010a). Observed tombolos (squares), observed salients (triangles), no sinuosity (cross).

Figure 2.4 shows the predicted vs the observed shoreline response in different breakwater schemes within UK based in the Pope and Dean diagram for coastal response (triangles for observed salient, squares for observed tombolo and x for no sinuosity). It can be seen for instance that for the case of Sea Palling scheme, no sinuosity was expected according to the design criteria whereas salient and tombolo were observed in the field. Similar situation is found in Leasowe where no sinuosity is predicted and tombolo is observed in the field. Other examples such Elmer or Monk's

Bay presented tombolos where just salient where expected. The discrepancies between predicted and observed results are linked to the fact that previous field experience does not consider the effect of the tides. This study revealed the need to further develop the design criteria for shore parallel breakwaters in the UK.

In order to field that gap, the before mentioned report proposed a number of process-based numerical model simulations aimed to set up new relationships between the geometrical parameters of the scheme and the coastal responses. However, the study is limited in the number of cases studied and also by the intrinsic limitations of the numerical models to represent long-term changes in the shoreline.

It has been shown there is not a clear design criteria for these structures. Moreover, it is not clear either how to assess the success of an already built scheme. For instance, the shore parallel breakwater scheme built at Sea Palling consisting of 9 breakwaters built in two phases has been shown as an example of success and also as the opposite by different authors. The Sea Palling scheme was considered as a success for some authors a few years after its completion (Fleming and Hamer 2000). In such work, mention was made to the ability of computational models to describe the downdrift erosion effects. One year later the optimistic view on the results at Sea Palling focusing on the erosion downdrift the scheme became arguable (Thomalla and Vincent 2001). More than a decade after the completion of such scheme, further study on the Sea Palling scheme showed it a 'less-than-ideal' case for applying the current experimental design criteria (micro-tidal) in the UK coasts (Dolphin et al. 2012). It has been highlighted that the sediment is being deflected towards the sea, by-passing around 2.5km of coast downstream the scheme and therefore causing erosion issues nearby the breakwaters. The difficulty on predicting shoreline response due to breakwaters was also highlighted by Pilarczyk and Zeidler (1996) who "claim that an accurate forecast of shoreline evolution, due to offshore breakwaters, is beyond the ability of simple empirical relationships such as these".

2.2 COASTAL MORPHOLOGY

Coastal erosion, and its opposite, coastal accretion are the natural shoreline responses to the balance between motion forces and sediment supplies. Simplistically, coastal erosion can be described as a natural process by which sediments, sand or shingle, are dragged by the currents, waves and/or tides induced. If there is enough incoming sediment to replace the amount washed away by the currents, the shoreline will remain stable. If there is a lack of incoming sediments, the shoreline will retreat in a process named coastal erosion. If the sediment supply exceeds the amount washed away, the shoreline will move seawards, in a process called accretion. Therefore, there are mainly two areas of knowledge involved on coastal erosion processes, hydrodynamics and sediment transport processes. Both these processes can be altered by human activities modifying the natural equilibrium and therefore inducing coastal erosion and/or accretion. Coastal erosion can include aerial sediment transport related to sand dunes. However, in this thesis, coastal erosion will be referred to only when it is caused by nearshore hydrodynamics only.

Many definitions of coastal erosion can be found in the literature. Two are highlighted here to guide the discussion:

“Coastal erosion is the encroachment upon the land by the sea and is measured by averaging over a period, which is long enough, to eliminate the impacts of weather, storms event and local sediment dynamics”.
(Commission 2004)

Another definition, more precise, can be found as follows:

“Coast erosion is the process of wearing away material from a coastal profile due to imbalance in the supply and export of material from a certain section. It takes place in the form of scouring in the foot of the cliffs or dunes or at the subtidal foreshore. Coastal erosion takes place mainly during strong winds, high waves and high tides and storm surge conditions, and results in coastal retreat and loss of land. The rate of erosion is correctly expressed in volume/length/time e.g. in m³/m/year, but

erosion rate is often used synonymously with coastline retreat and thus expressed in m/year. (Mangor 2004)

According to the first definition, short-term erosive processes such those produced by storms only, are not considered coastal erosion. Figure 2.5 shows the damages caused by a storm period during winter 2014 at Dawlish, Devon, UK. This case can be used as an example of short-term events causing devastating effects on the shoreline and human assets, and therefore it should be considered as a coastal erosive process itself.



Figure 2.5. Railway damage at Dawlish (Devon, UK) after storm in January 2014 (The Guardian)

The second definition, by Mangor (2004), clearly depicts the importance of the sediment balance versus the action of the external forces and does not specify any period of time. This definition is used as a starting point to describe the main dynamics behind coastal sediment transport and therefore behind coastal erosion.

As it was shown in the above definitions, coastal erosion (and accretion) is the result of a balance between forcing and sediment budget. Once wind is neglected as a direct driver for coastal erosion, the main forces considered are waves and tides. As described in many books (Dean and Dalrymple 2004; Kamphuis 2010; Reeve et al. 2011) waves and tides generate currents defined by their velocity. In the nearshore, these velocities eventually start interacting with the seabed. This point is identified as depth of closure which was first defined by Hallermeir (1978) and later defined by Krauss (1998) as:

“The depth of closure (DoC) for a given or characteristic time interval is the most landward depth seaward of which there is no significant change in bottom elevation and no significant net sediment transport between the nearshore and the offshore.”

When the nearshore currents interact with the seabed, they generate a tangential force in the seabed that eventually may mobilize the sediments. A schematically drawing for this process can be found in many books and papers. The one shown in Reeve (2011) is shown here (Figure 2.6).

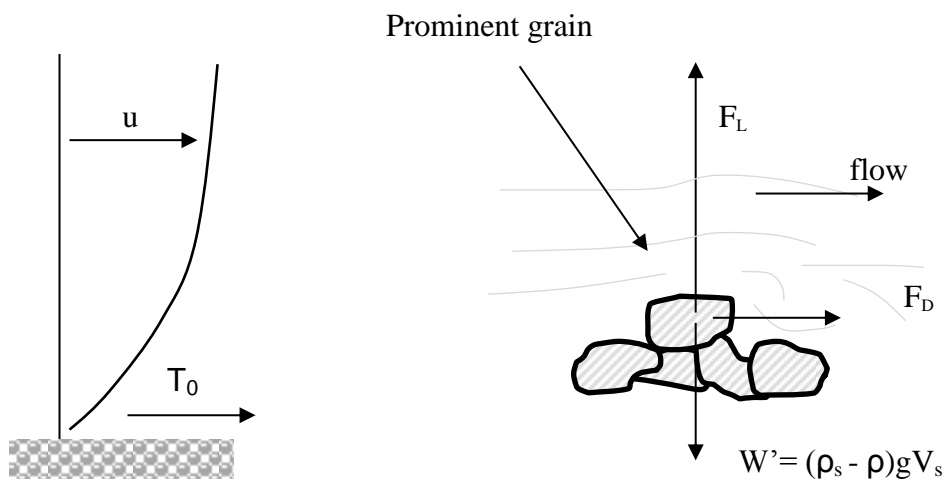


Figure 2.6. Sediment transport motion. Fluids forces causing sediment motion (Reeve et al. 2011).

Once the sediment starts its movement, different motion modes can be described. According to Dean and Dalrymple (2004) three modes are found:

- Bedload transport, that occurring in the seabed either by rolling or by sheet flow.
- Suspended load, that occurring within the water column.
- Swash load, that occurring in the swash zone on the beach.

Other authors (Reeve et al. 2011) would differentiate between rolling (sliding and hopping) and sheet flow as different motion modes therefore defining 4 rather than 3 modes.

It is not yet clear which of these modes is the predominant depending on the conditions and neither if it is relevant to distinguish between them (Dean and

Dalrymple 2004). This uncertainty on sediment motion will be common throughout this thesis, and almost in any work related to coastal sediment transport.

When studying shore-parallel breakwaters other processes become relevant in order to explain coastal morphodynamics. Wave transformation processes such as refraction, diffraction, shoaling and wave breaking play an important role on hydrodynamics and morphodynamics around shore-parallel breakwaters. Also other wave-structure interaction processes such as wave overtopping are critical to be able to accurately represent the morphodynamics behind the structures. Additionally, when studying shore-parallel breakwater it is important to account for processes occurring in the vertical profile such under-toe current than play an important role in carrying sediment from the shore to off-shore areas close to the seabed.

2.3 PROCESS-BASED MODELLING

In order to determine morphological changes in the shoreline process based models have become very popular in the recent decades. They started to be a main research topic in the 80s. De Vriend (1987) provides a summary of the work done on coastal models until that date which already included 2D and 3D modelling. Process-based models describe mathematically and individually each of the processes involved in the system that they are simulating. Typically, coastal process based models include different modules accounting for hydrodynamics, waves, sediment transport, water quality or flood risk. Each of those modules will be based in different sets of equations to describe the processes involved.

Models are a common tool when studying coastal areas not just in research but also in industry. Examples can be found in a variety of fields, for instance; Coastal & Harbour Management (Rusu and Guedes-Soares 2015) studying wave propagation processes inside harbours; Impacts on the hydrodynamics due to coastal structures (Du et al. 2010); Water Quality (Gao et al. 2013) including bacteria transport processes; Marine Renewable Energies studying hydro-environmental impacts of tidal stream turbines or tidal lagoons (Angeloudis et al. 2016); Coastal Structures Impacts on Hydrodynamics Coastal Defence Design (Environment Agency 2010a) studying morphological changes induced by coastal structures; or other Morphological Changes around Structures such beach nourishments (Pan 2011) among other uses.

There are many process-based numerical models available, both developed for commercial or research purposes. A detailed description and review can be found in Amoudry and Souza (2011). As an example of commercial models used in industry DELFT3D, MIKE21 or TELEMAC can be named. There are other models developed for research purposes. COAST2D has been used in a variety of projects including the assessment of the impacts that coastal structures produce on the nearshore morphodynamics. For instance it was used to model nearshore morphodynamics behind a set of shore-parallel breakwater at Sea Palling, UK (Pan et al. 2005; Du et al. 2010; Du et al. 2012) and a set of V-shaped breakwaters (Pan et al. 2013). COAST2D has been also used to assess the behaviour of beach nourishment on a coastal defence scheme under macro-tide conditions (Pan 2011). Other morphological features such as sandbanks have also been studied (Pan et al. 2007).

COAST2D uses a constant rectangular grid. The most common grid size has been 25m for the alongshore direction and 12.5m for the cross-shore direction (Pan et al., 2005; Du et al., 2010; Pan, 2011). Smaller grid size has been also used in Du et al. (2015) where 5m used in both directions. The model has also been used to recreate conditions in an experiment where 0.2m grid size was used in both directions. The covered spatial domain dimensions also vary. The maximum alongshore distance covered has been 5km (Du et al., 2010; Du et al., 2012). The computational time has been increasing along time from 25h in Pan et al., (2005), 55h in Pan (2009), 200h in Du et al., (2010) and 336h in Du et al., (2012).

Process-based models need to be calibrated and validated before can be confident in the results produced. Although powerful for short-medium term and medium size domains (km) numerical models present some limitations for long term or large domains, especially when simulating sediment transport and morphological changes. De Vriend et al. acknowledged the difficulties of describing long-term processes as a limitation of these models (de Vriend et al. 1993). Ten years later, Larson et al., (2003) still recognise such limitations of process based (physic based) as one of the key limitations of process-based models for long-term morphological simulations. Some of those limitations, such as computational performance, could be overcome with time, as computer science is evolving continuously. Nevertheless, due to the construction of numerical models themselves, the equations representing the processes are not exact.

The small errors can be accumulative over time, leading to divergent solutions when little changes in initial conditions are present. Also, additional processes might be present in the long-term that are not modelled in conventional process-based models (Hanson et al. 2003).

Significant effort has been done to overcome these limitations, such as morphodynamic acceleration (Roelvink 2006) or input reduction (Walstra et al. 2013). These techniques are above the scope of this thesis and will not be described here. These limitations prevent numerical models to be a suitable solution for long term simulations and large scales, especially when dealing with sediment transport and morphological changes.

2.4 REDUCED-PHYSICS MODELLING

Reduced-physics models try to reproduce the effects observed in the scale of interest, rather than the basic physics of all processes involved at smaller scales. They are especially useful for season to yearly scales. These scales are often the more interesting for coastal managers and engineers. The one-line model firstly defined by Pelnard-Consideré (1956) is an example of reduced-physics models. It explains the advanced or recess of the shoreline based on the alongshore sediment transport gradient, without paying attention on how those sediments are moved. An example of the application of one-line model can be found in Reeve (2010) where the one-line model is used to define the shoreline behind a set of shore-parallel breakwaters. A different approach can be found in Karunarathna et al. (2015) where diffusion formulation is used to represent morphological changes in beach profiles at the Hasaki Coast, Japan.

2.5 DATA-DRIVEN MODELLING

In the past decades, with the rapid development of the data acquisition and communication techniques, a large amount of high quality field data has been collected. The high quality and long-term field data collected has enabled the development of the data-driven models that determine relationships based purely on a data-set and not on physical processes. Data-driven models are particularly useful when studying long-term phenomena as these cases are beyond the capabilities of

process-based numerical models as explained in the previous section. There are different data-driven models that can be used. A detailed summary on data-driven models can be found in Reeve (Reeve et al. 2016). Although it is not the objective of this thesis to provide an exhaustive description on these models, a general view is presented.

Data-driven models mainly use the field measurements to determine the relationships between a set of variables by applying various statistical tools. The complexity of the models varies. For example, regression models use regression techniques to define the relationship between two variables and the fitness of the regression is judged by the correlation coefficient 'r', in the range between [-1,1]. More complex models are based on covariance. The covariance matrix generated from these models is decomposed into independent eigenvectors. This allows each eigenvector to be studied independently to gain the insights of the correlations between the defined variables. Examples of these methods are the Empirical Orthogonal Function (EOF) method or the Complex EOF method. Other data-driven methods based on covariance analysis are the 3-mode Principal Component Analysis (PCA) and the Canonical Correlation analysis (CCA). These methods can be very useful to analyse long-term data series and they also can be used for forecasting. Nevertheless, results interpretation is not always straight forward and special care must be taken.

The Empirical Orthogonal Functions (EOF) method is a statistical technique that describes spatial and temporal patterns within a dataset. EOF method is often known as Principal Component Analysis (PCA) (Joliffe, 2002). Typically, the nomenclature 'EOF' is used over PCA in geophysics fields, such as meteorology or coastal engineering, although both can be found in the literature.

The EOF method synthesises the dataset into a number of orthogonal functions. The EOF method has been used widely in different disciplines. Lorenz (1956) first applied the EOF method to the weather prediction, and over the last few decades, a number of studies used the EOF method to analyse the coastal morphodynamics (Winant et al. 1975; Dick and Dalrymple 1984; Larson and Kraus 1994; Short and Trembanis 2004; Reeve and Karunarathna 2011; Alvarez and Pan 2014). When using the EOF method to analyse coastal morphodynamics, the method has mainly been applied to study the

variation or evolution of the cross-shore profile variations, where the different EOF components or eigenvalues from the analysis can be interpreted to represent particular features. For example, in the study of Winant (1975), the first EOF spatial component was defined as ‘mean beach’; the second as ‘berm-bar’ function describing seasonal changes in the cross-shore profile; and the third component as the terrace function indicating changes in the low tide location. Similarly, Aubrey (1979) and Losada (1991) also found the EOF components of the cross-shore profiles having the same presentations for the first three EOF components. However, other authors described the second component as being related to beach rotation (Short and Trembanis 2004; Turki et al. 2013) induced by the physical characteristics of the beach and not by seasonal changes in wave conditions. Alongshore changes have been typically less explored using the EOF method. Dick and Dalrymple (1984) performed the EOF analysis on cross-shore profiles independently at different alongshore locations and linked the alongshore variations to describe alongshore beach morphological changes. (Munoz-Perez et al. 2001) analysed directly shoreline position data during 3 years in a beach in South Spain. In their work, the first EOF components represent a 99.51% when mean is not removed and a 65% when mean value is removed from the matrix. Fairley et al. also performed an EOF analysis on shoreline changes at Sea Palling, UK, behind a scheme of shore-parallel breakwaters (Fairley et al. 2009). In that work, the first component, once the mean as removed, accounts for the 59% of the variability. Karunarathna et al. compared sand-gravel beaches cross-shore profiles behaviour at two different locations using the EOF method (Karunarathna et al. 2012). More recently, Turki et al. (2013), studied shoreline changes in 3 different beaches using the EOF obtaining around a 70% of the variability explain by the first EOF components, when the mean was removed.

Despite cross-shore positions and along-shore position have been commonly used in the past, other coastal morphological variables have been also studied. Aubrey (1985) used the EOF components to perform a spectral analysis in order to study the most energetic frequency finding that one year cycle was the most dominant in his study area. Pruszek studied the relationship between EOF components and the Dean’s profile (Pruszek 1993). Medina et al. (1994) studied the relation between morphological changes in the cross-shore profile and the sediment size gradation in

North Spain. They concluded stating that sediment size variation is a key factor in coastal morphological changes. Reeve et al. studied volumetric changes in a sandbank in UK (Reeve et al. 2001). The first component in that case represented the 97% which is the mean value. Miller and Dean (2007b) related EOF components to wave parameters such wave energy (E), wave energy fluxes or wave steepness among others. Karunarathna et al. studied morphological changes in an estuary (Karunarathna et al. 2008). In that case, the first component (mean) represented a 92%. Another example of different morphological variables can be found in Navarro et al. (2011) where the movement of a sand dune is studied. Yuhi et al. studied not just coastal changes but also river changes near the sea (Yuhi et al. 2013).

As pointed out in many studies, there are limitations on temporal and/or spatial resolution when the EOF method is used. Nevertheless, studies applying the EOF method vary largely in term of temporal and spatial areas covered. Large scale studies can be found in Wijnberg and Terwindt (1995), where cross-shore sections along a stretch of coast 115km long was analysed. Distance between profiles was 250m and surveys were taken annually during 30 year. In total 14,000 samples were analysed. In order to simplify the analysis a “moving window” was used averaging sets of four consecutive cross-shore profiles. Karunarathna et al. (2008) performed an analysis over 150 years. However, in such time span, just 20 surveys were available. Short used monthly data over 26 years (Short and Trembanis 2004). Even daily surveys were studied in Turki et al. (2013). Fairley et al. (2009) also tried to analyse daily surveys using video images but they faced visibility problems fog and spray during storm periods. It is interesting to note how the total time span studied is not necessarily an indication of the temporal precision. A large period can be studied with little resolution or short period with high precision. Also, the temporal resolution required depends on the phenoma intended to explain.

Spatial resolution also varies within the literature reviewed. Miller and Dean (2007a) claim cross-shore profiles spaced between 58m and 102m. Wijnberg et al. (1995) consider profiles every 250m Using video images allows highly increasing the spatial resolution with claimed alongshore spacing of 2m according to Fairley et al. (2009). Other examples of video cameras (Turki et al. 2013) were limited to 40m. It can be seen that video cameras allow decreasing the spacing interval providing higher survey

densities. This is particularly important when studying coastal behaviour behind shore-parallel breakwaters or other coastal structures. Hsu et al. used EOF method to study coastal behaviour behind detached breakwaters but profiles were taken just at the centre of the structures so no information in the embayments was taken, limiting the interpretation of the components (Hsu et al. 1986). Fairley et al. (2009) carried out a more intensive surveying behind a set of shore-parallel breakwaters increasing the accuracy of the results. In any case as reported by different authors (Reeve and Karunarathna 2011) the success of the EOF method analysis depends largely on the quality and quantity of the data analysed.

In coastal morphodynamics a common case of 1D analysis is a cross-shore profile analysis. In this case, for the same cross-shore profile bathymetries are taken at different times. Bed elevation, is therefore measured at different locations at different times. This data is used to define the 2D matrix typically analysed with the EOF method. Several examples of this approach can be provided, for instance Winant (1975) studies five different profiles but EOF method is performed independently. The same methodology is followed by Losada et al. (1991), Larson et al. (1994), Short et al (2004) or Loureiro (Loureiro et al. 2012). In order to study alongshore variability, a first approach was to perform the EOF analysis to several cross-shore profiles, but representing the results jointly to identify alongshore trends. Examples of this approach can be found in Dick and Dalrymple (1984), Wijnberg (1995) or Loureiro (2012). Nevertheless it should be noted that this approach calculates EOF components for each profile independently and the interpretation is done jointly. Hsu (Hsu et al. 1986) attempted to provide a more detailed methodology to study the coastal morphological changes behind detached breakwaters as a real 2D variable. Hsu methodology calculates independent EOF components for the cross-shore changes and the alongshore changes that multiplied by each other, can reconstruct the total changes in the 2D domain. This methodology added more complexity to the EOF method as the Hsu acknowledged in 1994 when a simplified approach was presented (Hsu et al. 1986). Hsu suggested that 2D analysis was particularly important especially in areas with shore-parallel breakwaters or other coastal structures. The 2D analysis has been also important to study the behaviour of estuaries (Karunarathna et al. 2008; Horrillo-Caraballo et al. 2014) or other coastal features that vary in 2D as sandbanks (Reeve et

al. 2001; Reeve et al. 2008). The methodology to approach the 2D problem proposed in the later papers consists of a dimension reduction. As explained before the matrix to be analysed by the EOF method consisted columns having information of the variable at different spatial locations and row containing information at different times. Therefore, a 1D variable (i.e. cross-shore elevation) becomes a 2D matrix when including the time. This means that a 2D domain, becomes a 3D matrix when including the time. The regular EOF method cannot deal with tri-dimensional matrices. Reeve (2001) proposed a dimension reduction to overcome this problem allowing analysing 2D domains using a standard EOF analysis.

The EOF method has some disadvantages. For instance it cannot identify wave-like patterns moving within the domain such as bars (de Vriend et al. 1993; Larson et al. 2003). This disadvantage can be overcome by using a modification of the EOF method, the Extended EOF (EEOF) method. An example of EEOF can be found in Weare et al. (Weare and Nasstrom 1982) applied to meteorological variables. The authors stated that EEOF have itself some limitations as high computational cost due to the size of the diagonalization that need to be performed and also an increased difficulty to interpret spatial patterns. Other possibility to overcome the EOF limitations in the description of wave-like patterns is the Complex EOF method (COEF). The COEF method has the potential of identifying moving patterns (de Vriend et al. 1993; Larson et al. 2003; Reeve et al. 2008). However CEOF also presents some disadvantages as it divides the spatial components into phase and amplitude which make it more difficult to interpret the results. A paper from Merrifield and Guza (1990) shows an example of CEOF method applied to coastal-trapped waves. They conclude that while COEF is a robust method for identifying wave propagation in a data set, but the results obtained should be interpreted carefully. Also work has been done applying the EOF method to coastal morphology in cross-shore profiles (Liang et al. 1992). They discuss that results obtained with the COEF are slightly better than those obtained for the EOF method and the same dataset. Nevertheless, they faced the issue of having to interpret both phase and signal. In their case, simple cross-shore profiles were analysed. Therefore, despite the possibility of using the EEOF or COEF the standard EOF has been the most common method used when analysed historical data trends related to coastal morphodynamics. Miller and

Dean (2007a) states that the EOF method is ‘an extremely useful statistical method capable of identifying underlying patterns within noisy data sets’. Another disadvantage is that EOF method requires data to be sampled in constant intervals in order to provide meaningful results (Larson et al. 2003) which sometimes is not possible to achieve in coastal environments. More recently the use of video cameras for surveying (Fairley et al. 2009; Turki et al. 2013) provides better means to increase the temporal and spatial resolution although it brings other issues such as low visibility during storms or loss of spatial resolution the farther from the camera. Also the improvement in telemetry in general in the last decade are a reason to believe that data collection will improve greatly increasing the possibility of obtaining higher spatial and temporal resolution at smaller cost. Moreover, the continuous increment in computational power also allows working with larger matrices. Therefore, the EOF method is likely to continue being of interest for coastal researches.

The EOF method, as seen in the literature reviewed, provides means to explain coastal behaviour within the measurement period. Extrapolation of the results further in the future can be done qualitatively but the method itself does not provide a way to quantitatively extrapolate the results beyond such period. Nevertheless, extrapolating historical trends to the future is of the interest for coastal managers and therefore it is an interesting research topic. The experience extrapolating EOF components for forecasting is limited (Karunarithna et al. 2008; Reeve et al. 2008; Reeve and Karunarithna 2011; Horrillo-Caraballo et al. 2014; Alvarez and Pan 2014; Alvarez and Pan 2016). As seen in the previous section, the EOF method provides spatial and temporal components. In principle, temporal evolution information is contained within the temporal components only, being the spatial component invariant in time. Then, the variable in study can be reconstructed as the sum of the product of spatial and temporal components for different modes (first, second, third, ...). The extrapolation concept behind the current extrapolation techniques is that by extrapolating the temporal components, the variable in study can then be reconstructed beyond the training period as a product of the spatial component and the extrapolated temporal component. According to this idea, forecasting using EOF method is reduced to the problem of extrapolating the temporal component.

In the last decade, work has been done to address this topic. Karunarathna et al. (2008) after carrying out an EOF analysis in the Humber estuary, in United Kingdom, acknowledged in their conclusions that extrapolating the components beyond the sampled will provide a way of estimating the values for bed elevations in the future. The same year, Reeve et al. (Reeve et al. 2008) presented a way to extrapolate the temporal components into the future. Extrapolated temporal components are then used together with the non-extrapolated spatial component to reconstruct morphological changes in the Yarmouth sandbank, in UK. Burg's algorithm was used to extrapolate the components using different 'r' factors and the best fitting was selected. Reeve et al. (Reeve and Karunarathna 2011) continuing the work on Karunarathna (2008) extrapolated the first 3 components using a linear fitting. Despite being a 'simplistic' approach results are promising in morphological changes forecasting based in data-driven methods. Horrillo-Caraballo et al. (2014), uses the Burg's algorithm to extrapolate the temporal components beyond the sampled period in the Deben estuary, UK. The complexity of extrapolating the EOF temporal component varies depending on the variable of study and the data-set available. For instance in Reeve (2011), linear fitting was used to fit the first 3 EOF temporal components. A different approach was followed by Horrillo-Caraballo (2014) where an auto-regression method was used to fit a more complex EOF temporal component. In all cases, a sub-interval of the studied period was used to define the fitting parameters and the rest is used for validation. Once the EOF temporal components are extrapolated, they can be used for forecasting beyond the studied period. To assess how much beyond the studied period a variable can be forecasted a ratio between calibration period and extrapolated period is presented here.

Table 1. Number of datasets used for fitting VS validation.

Author	Used for fitting	Validation	ratio
Reeve et al., 2008	33	3	0.09
Reeve et al., 2011	10	1.6	0.167
Horrillo et al., 2014	12	3	0.25

It is important to note that the EOF method works with surveys equidistant in time, regardless what the gap between surveys is. This means that in principle, from a

mathematical point of view, it does not matter if 10 surveys are taken every year or every hour in order to extrapolate those values. The consistency of the dataset might vary depending on the temporal gap, but the mathematical procedure for the EOF method itself or the extrapolation techniques are independent to the temporal gap between surveys. For instance in Reeve (2008) surveys are separated by decades but in Horillo-Caraballo (2014) surveys are separated by years. However, both authors apply the same extrapolation technique to their corresponding data set. In any case, the approach followed has been the forecasting by extrapolating the EOF temporal components only using the non-extrapolated spatial component when reconstructing beyond the sampled period.

2.6 AIMS AND OBJECTIVES

As indicated from previous studies, it is clear that the EOF offers many advantages over the physical and process-based modelling approaches in studying the coastal morphological changes. It can reveal the main features of the coastal and beach evolution and their relationships between the key influential factors. However, the applications of the EOF method, as a data-driven approach, are hugely limited by the availability of the existing field data, in both quantify and quality. Using the EOF method for long-term predictions of the coastal morphological changes is challenging and an uncharted area of research. Applications of the EOF methods become even impossible for the coastal defence projects in planning, as there are no field measurements being collected yet. To this end, this research aims to develop a dynamic EOF method using the data provided by a process-based model to improve the predictability of longer term morphological changes. The specific objectives of this research are as follows:

- To develop a dynamic EOF method to improve the extrapolation of the EOF components, both temporal and spatial for better predictions;
- To further validate the process-based model (COAST2D) for provision of the data for the EOF analysis required;
- To apply the data provided by the process-based model with the newly developed dynamic EOF method;

- To apply the improved extrapolation of the EOF components for longer term coastal morphological predictions.

3 METHODOLOGY

3.1 INTRODUCTION

As discussed in Chapter 2 EOF method allows studying the behaviour of a given variable within the considered period. However, the EOF method itself does not allow extrapolating results beyond such period and therefore any prediction will be qualitative and not quantitative or objective. Nevertheless, EOF components could be, in principle, be extrapolated beyond the studied period in order to reconstruct the variable of interest beyond such period in a quantitative or objective manner. EOF extrapolation could be of special interest for coastal managers. Long-term data series can be analysed not just to understand how the system evolved in the period of consideration but how it is going to evolve in the future. This Chapter follows that concept studying what has been done so far and developing a new methodology for EOF components extrapolation.

3.2 EOF METHOD

For a given spatially and temporally varying data set, the EOF method calculates a set of orthogonal functions (eigen vectors), or EOF temporal and spatial components, that can be used to reconstruct and interpret the original data set at any location of the domain within the studied period. A key aspect of the EOF method is that it is possible to reproduce variable in study during the training period by using a reduced number of orthogonal functions. Also, the set of functions provided is sorted, so the first couple of functions, temporal and spatial, explain the majority of the data variability. The second couple of functions, spatial and temporal, explain the majority of the remaining variability and so on. Another key feature is that it provides temporal variations and spatial variations separately, allowing studying the behaviour of the variable both in time and space independently.

Detailed information on the Empirical Orthogonal Functions (EOF) method can be found in Joliffe (2004), which provides a detailed mathematical description on the method and Navarra (2010) which provides an explanation of the EOF method from a Climate Data Analysis perspective. The mathematical description of the EOF method based on a practical example is given here.

Let $h(x,t)$ be a quantity varying in 'x' (spatial domain) by 't' (temporal dimension). When the measurements/surveys are taken, it will form a matrix containing the values of 'h', at locations 'x' and time 't' in the form of $h_{ij} = h(x_i, t_j)$. Using the EOF analysis, the measured data $h(x_i, t_j)$ can be represented by functions $X_l(x)$ and $T_l(t)$ as:

$$h_{ij} = H(x_i, t_j) = \sum_{l=1}^N X_l(x_i) \cdot T_l(t_j) \quad (3.1)$$

where $H(x_i, t_j)$ is the measured data; $X_l(x)$ and $T_l(t)$ are the spatial and temporal EOF components respectively; and l represents the number of components/functions considered.

To obtain the $X_l(x)$ and $T_l(t)$ functions, the following eigenvalues and vectors problem have to be solved using:

$$[A - \lambda I]X_l = 0 \quad (3.2)$$

$$[B - \lambda I]T_l = 0 \quad (3.3)$$

To solve Eqs. (3.2) and (3.3), a practical case with shoreline changes as shown in Figure 3.1 is taken as an illustration. Let h_{ij} be the measured shoreline positions to a reference baseline at position x_i and for a specific bathymetric survey: j , where $i = 1 : n_x$; n_x is the number of measurements taken in that alongshore profile; $j = 1 : n_t$; n_t is the number of surveys considered for the analysis.

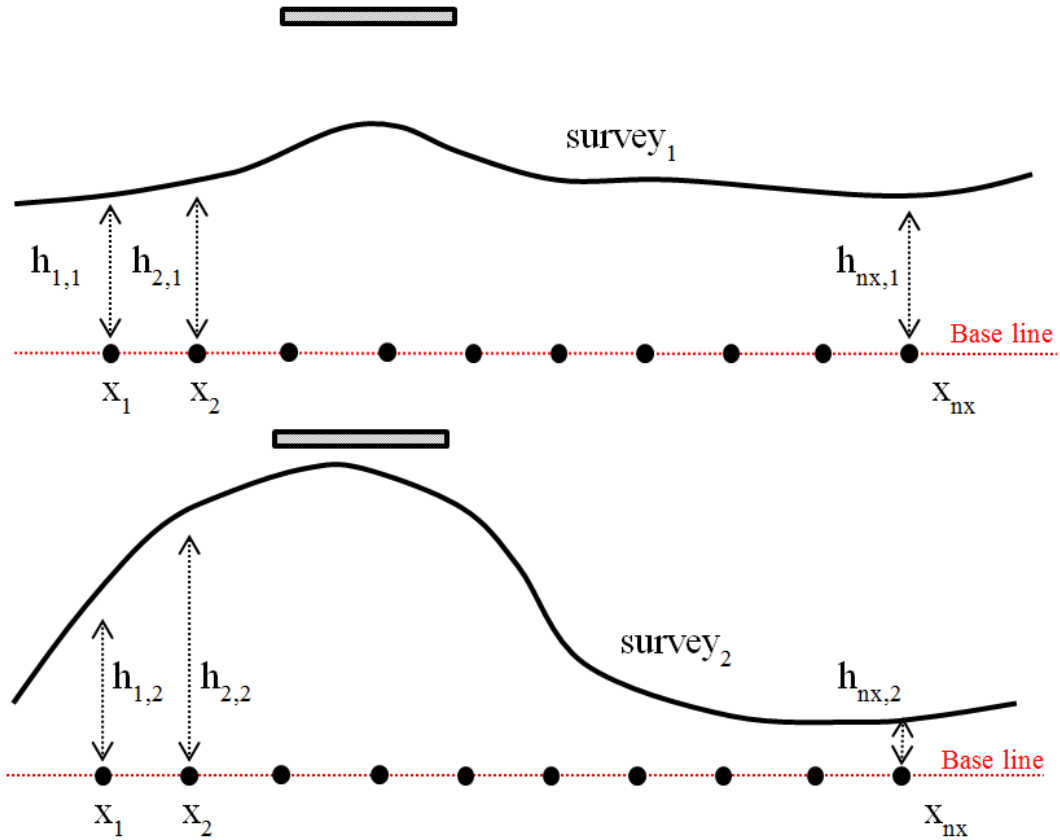


Figure 3.1. Example for EOF matrix construction.

Therefore, the measured shoreline positions, h_{ij} , can be expressed as:

$$h_{ij} = \begin{pmatrix} h_{11} & h_{12} & \cdots & h_{nx,1} \\ h_{12} & h_{22} & & h_{nx,2} \\ h_{1,nt} & h_{2,nt} & & h_{nx,nt} \end{pmatrix} \quad (3.4)$$

The EOF method provides temporal and spatial functions that are able to reconstruct the value of the variable in study, shoreline position in this example, at any time or position within the spatial and temporal boundaries of the study. According to such concept, the following hypothesis is assumed:

There exist two orthogonal functions $X_l(x)$ and $T_m(t)$ with $l = 1, \dots, N$ and $m = 1, \dots, T$ that satisfies:

$$h_{ij} = h(x_i, t_j) = \sum_{l=1}^N X_l(x_i) \cdot T_l(t_j) \quad (3.5)$$

Where $l = 1, \dots, N$ is the number of functions $(X_l(x), T_l(t))$ used in the analysis. As it can be seen it is a similar procedure to the Fourier series but without imposing beforehand those function to be sinusoidal. In this case, is the method itself that defines the shape of such functions depending on the variability of the studied dataset, h_{ij} . This flexibility allows the EOF method to be applied to study different variables within the coastal environment, such depths in cross-shore profiles, shoreline positions or volumetric changes.

If there exist a structure or trend within the data, which mean they are not completely random, then, most of its variability will be explained by just a reduced number of functions. In such case the required number of functions N will be much smaller to the theoretical N used in (eq. 3.5) leading to the appearance of a residual error, ε , due to the neglected terms of the series. This error can be written as follows:

$\varepsilon_{ij} = h_{ij}(\text{measured}) - h_{ij}(\text{estimated})$, that using equation (3.5) results:

$$\varepsilon_{ij} = h_{ij}(\text{measured}) - \sum_{l=1}^N X_l(x_i) \cdot T_l(t_j) \quad (3.6)$$

Two choices can be considered at this stage, both are developed here for clarity.

Option A: Let $X(x)$ be the vector basis and $T(t)$ its coefficients. In order to obtain the value of such coefficients the conditions of minimising the error ε is imposed. Such conditions is applied by minimising the mean squared error between the measurements and the estimations as follow:

$$\sum_{i=1}^{n_x} \varepsilon_{ij}^2 = \sum_{i=1}^{n_x} \left(h_{ij} - \sum_{l=1}^N X_l(x_i) \cdot T_l(t_j) \right)^2 \quad j = 1, \dots, n_t \quad (3.7)$$

To minimise Eq. (3.7), the equation is derived with respect T_l and equating to 0:

$$\sum_{i=1}^{n_x} \left(h_{ij} X_l(x_i) - \sum_{m=1}^N X_m(x_i) \cdot T_m(t_j) \cdot X_l(x_i) \right) = 0 \quad (3.8)$$

If eigenvectors $X_l(x)$ are also required to be orthonormal $X_l(x)X_m(x) = \delta_{lm}$ and then, the second summatory in (3.8) cancel all its terms except for the case where $m=l$, in which case using the orthonormality condition $X_l(x_i) \cdot X_l(x_i) = 1$ and therefore

$$\sum_{m=1}^N X_m(x_i) \cdot T_m(t_j) \cdot X_l(x_i) = T_l(t_j) \quad (3.9)$$

Using this result in eq. (3.8):

$$\sum_{i=1}^{n_x} [h_{ij} X_l(x_i) - T_l(t_j)] = 0 \quad l = 1, \dots, N \quad (3.10)$$

Clearing T_l ,

$$T_l(t_j) = \sum_{i=1}^{n_x} h_{ij} X_l(x_i) \quad l = 1, \dots, N \quad (3.11)$$

Option B: Similarly $T(t)$ could be taken as the basic vector resulting in:

$$\sum_{j=1}^{n_t} \varepsilon_{ij}^2 = \sum_{j=1}^{n_t} \left(h_{ij} - \sum_{l=1}^N X_l(x_i) \cdot T_l(t_j) \right)^2 \quad i = 1, \dots, n_x \quad (3.12)$$

To minimise (3.7), the equation is derivate respect X_l and equating to 0:

$$\sum_{j=1}^{n_t} \left(h_{ij} T_l(t_j) - \sum_{m=1}^N X_m(x_i) \cdot T_m(t_j) \cdot T_l(t_j) \right) = 0 \quad (3.13)$$

If eigenvectors $T_l(t)$ are also required to be orthonormal:

$$X_l(x_i) = \sum_{j=1}^{n_t} h_{ij} T_l(t_j); \quad l = 1, \dots, N \quad (3.14)$$

From (3.11) and (3.14) can be concluded that obtaining one of the series ($X_l(x_i)$ or $T_l(t_j)$) the other can be calculated by multiplying by the dataset h_{ij} . In order to find out those first functions data variability will be studied. If the mean has been removed from the data set, data variability matches the covariance. Provided that is the case, it will be designated by σ^2 . Then:

$$\sigma^2 = \frac{1}{n_x n_t} \sum_{i=1}^{n_x} \sum_{j=1}^{n_t} h(\text{measured})^2(x_i, t_j) \quad (3.15)$$

Replacing $h(\text{measured})$ by $h(\text{estimated})$ and using the orthogonality condition imposed to the eigenvectors as defined in (3.5)

$$\sigma^2 = \frac{1}{n_x n_t} \sum_{i=1}^{n_x} \sum_{j=1}^{n_t} \left[\sum_{l=1}^N X_l(x_i) \cdot T(t_j) \right]^2 \quad (3.15)$$

$$\sigma^2 = \frac{1}{n_x n_t} \sum_{j=1}^{n_t} \sum_{l=1}^N T^2(t_j) \quad (3.16)$$

To obtain the functions $X_l(x)$ the contribution to the data variance is maximise. To avoid arbitrarily large coefficients, the dimensions of such functions are limited to the unit. Moreover, as it is intended to condition the maximization problem, Lagrange multipliers are used. In such case, the expression to maximise is:

$$\sum_{j=1}^{n_t} T_l^2(t_j) - \lambda_l \left[\sum_{i=1}^{n_x} X_l^2(x_i) - 1 \right] \text{ where } l = 1, \dots, N \quad (3.17)$$

Replacing T_l for its expression in (3.11)

$$\sum_{j=1}^{n_t} \left[\sum_{i=1}^{n_x} h_{ij} \cdot X_l(x_i) \right]^2 - \lambda_l \left[\sum_{i=1}^{n_x} X_l^2(x_i) - 1 \right] \quad l = 1, \dots, N \quad (3.18)$$

Differentiating respect X_l and equating to zero:

$$\sum_{j=1}^{n_t} \left[\sum_{i=1}^{n_x} h_{ij} \cdot X_l(x_i) \right] \left[\sum_{i=1}^{n_x} h_{ij} \right] - \lambda_l \sum_{i=1}^{n_x} X_l(x_i) = 0 \quad (3.19)$$

$$\sum_{j=1}^{n_t} \left[\sum_{i=1}^{n_x} X_l(x_i) \cdot \sum_{s=1}^{n_x} h_{ij} h_{sh} \right] = \lambda_l \sum_{i=1}^{n_x} X_l(x_i) \quad (3.20)$$

$$\sum_{i=1}^{n_x} X_l(x_i) \cdot \sum_{j=1}^{n_t} \sum_{s=1}^{n_x} (h_{sj} h_{sj}) = \lambda_l \sum_{i=1}^{n_x} X_l(x_i) \quad (3.21)$$

Assuming that the matrix $A = H \cdot H^T$ can be formed multiplying the matrix containing the field data $H = h_{ij}$ by its transpose, the eq. (3.16) can also be written as:

$$X_l(x_i) \cdot A = X_l(x_i) \cdot \lambda_l \quad (3.22)$$

expression which is identical to:

$$[A - \lambda I]X_l = 0 \quad (3.23)$$

Eq. (3.23) is similar to the classical eigenvectors problem shown in (3.2) and therefore λ and X_l are the eigenvalues and eigenvectors of A respectively. Also, as $H = \{h_{ij}\}$ is a matrix of n_x rows and n_t columns, $H^T = \{h_{ij}\}$ will have n_t rows and n_x columns, and therefore $A = H \cdot H^T$ is a squared matrix $n_x \cdot n_x$ where:

$$a_{ij} = h_{i1} \cdot h_{j1} + h_{i2} \cdot h_{j2} + \dots + h_{int} \cdot h_{jnt} \quad (3.24)$$

$$a_{ji} = h_{j1} \cdot h_{i1} + h_{j2} \cdot h_{i2} + \dots + h_{jnt} \cdot h_{int} \quad (3.25)$$

Consequently, $a_{ij} = a_{ji}$, A is symmetric. Also, eq. (3.15) can be differentiated respect $T_l(t)$ resulting in $T_l(x) \cdot B = T_l(t) \cdot \lambda_l$, where $B = H^T \cdot H$ is an squared matrix with dimensions $n_t \cdot n_t$

According to eqs. (3.11) and (3.12), once X_l is known the others functions T_l can be calculated, or vice-versa.

$$h_{ij} = h(x_i, t_j) = \sum_{l=1}^N X_l(x_i) T_l(t_j) \quad (3.5)$$

Generally, before performing the EOF analysis, the mean is often removed. When such operation is done, the EOF components represent variations over the mean value. This approach is commonly employed in studying steady processes or changes around an equilibrium scenario. However, in this study changes from an initially flat beach are studied. In this situation, the mean value does not represent an equilibrium situation as the beach continuously evolves during the experiment. For these cases, it has been proposed to remove the initial profile, in order to study changes related to the

initial situation. This is for instance useful when studying the effects of a singular storm on the shoreline (Muñoz-Perez, 2001). For the present study, the later approach is chosen and the initial volumetric changes are subtracted from the original data set. Initial volumetric changes are zero, and therefore the first EOF component will correspond to the mean value. In other studies where the focus is set on steady states rather than on a quickly evolving situation removing the mean instead of the original value could be a more suitable approach.

3.3 DYNAMIC EOF METHOD

As the standard EOF method provides information describing the variability of a data set within the measurement period, extrapolating the EOF components for predictions can be done in principle, but is limited for a short period due to the components representing the average variations of the given parameter over the measurement period, as seen in the studies of Reeve (2008) and Horillo-Caraballo Horillo-Caraballo et al. (2014). Theoretically, the temporal information is kept in the EOF temporal components only. These components have been extrapolated in order to predict results beyond the measurement period, but using the spatial components obtained for the measurement period. Nevertheless, the spatial component calculated for a particular period of time, T , might not be adequate to describe changes beyond such period. The hypothesis of this thesis is that EOF spatial components should also be extrapolated beyond the period T in order to obtain better results when forecasting. However, EOF spatial components, by definition, do not keep information of the temporal evolution of the system, and therefore they cannot be directly extrapolated.

The methodology proposed in this chapter approach this issue by describing the temporal evolution of the EOF spatial components. This temporal evolution can be used to extrapolate the spatial components beyond the measurements period. Figure 3.2 shows a schematic description of the EOF method (top panel), the current extrapolation methodology (middle panel) and the proposed EOF extrapolation methodology (top panel).

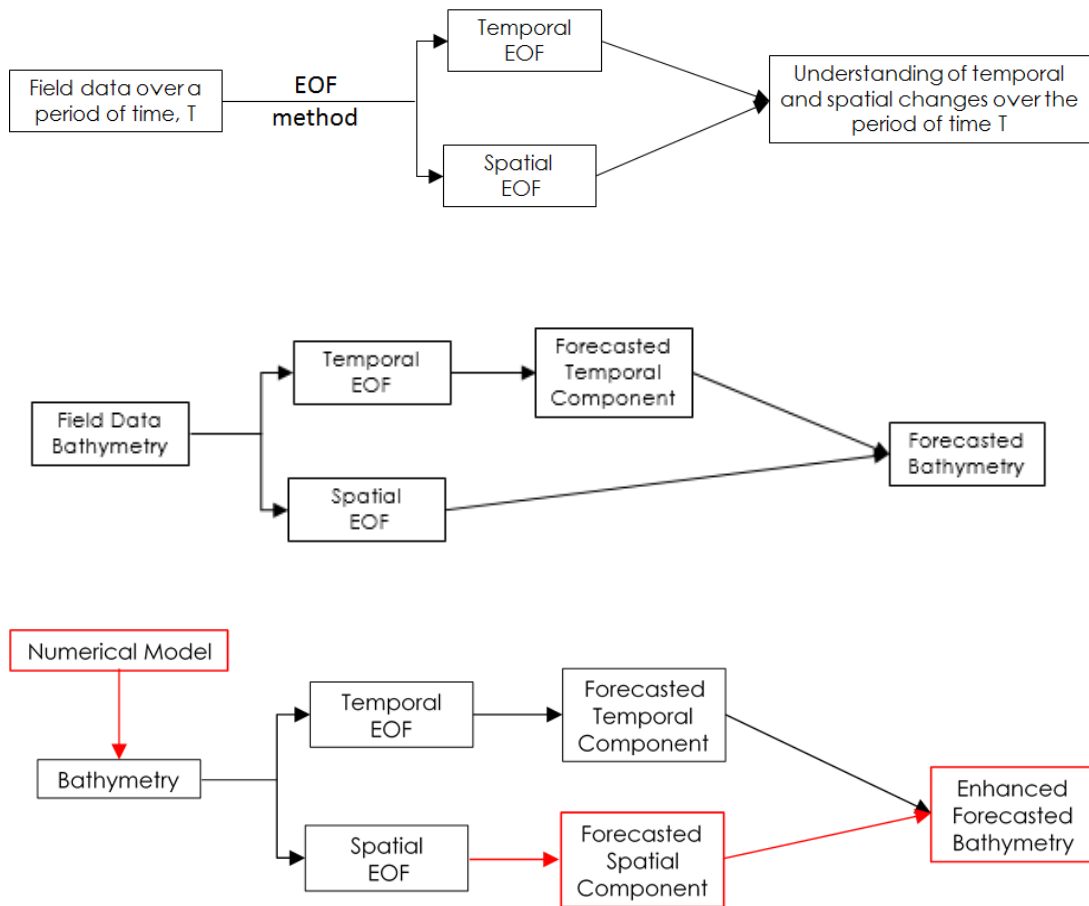


Figure 3.2. Schematic diagram of the dynamic EOF approach (c) in comparison with the method of Horrillo-Caraballo et al. (2014) (b) and standard EOF method (a).

To enable to extrapolate the EOF spatial components, the dynamic EOF method performs the standard EOF method to a number of subintervals within the training period. The information obtained from this analysis enables to describe the temporal evolution of the EOF spatial components and also to increase the accuracy of the EOF temporal component extrapolation when compared to traditional methods.

3.3.1 EOF Spatial Component extrapolation

To enable the interpolation of the spatial EOF components accurately, it becomes necessary to examine the temporal variation of these components. The proposed methodology is to study sub-intervals within the period of study T, studying for each spatial location the value of the spatial component for the different sub-intervals. Then, the temporal evolution of the EOF spatial component can be studied and parameterized for each location. In order to illustrate this idea Figure 3.3 is shown:

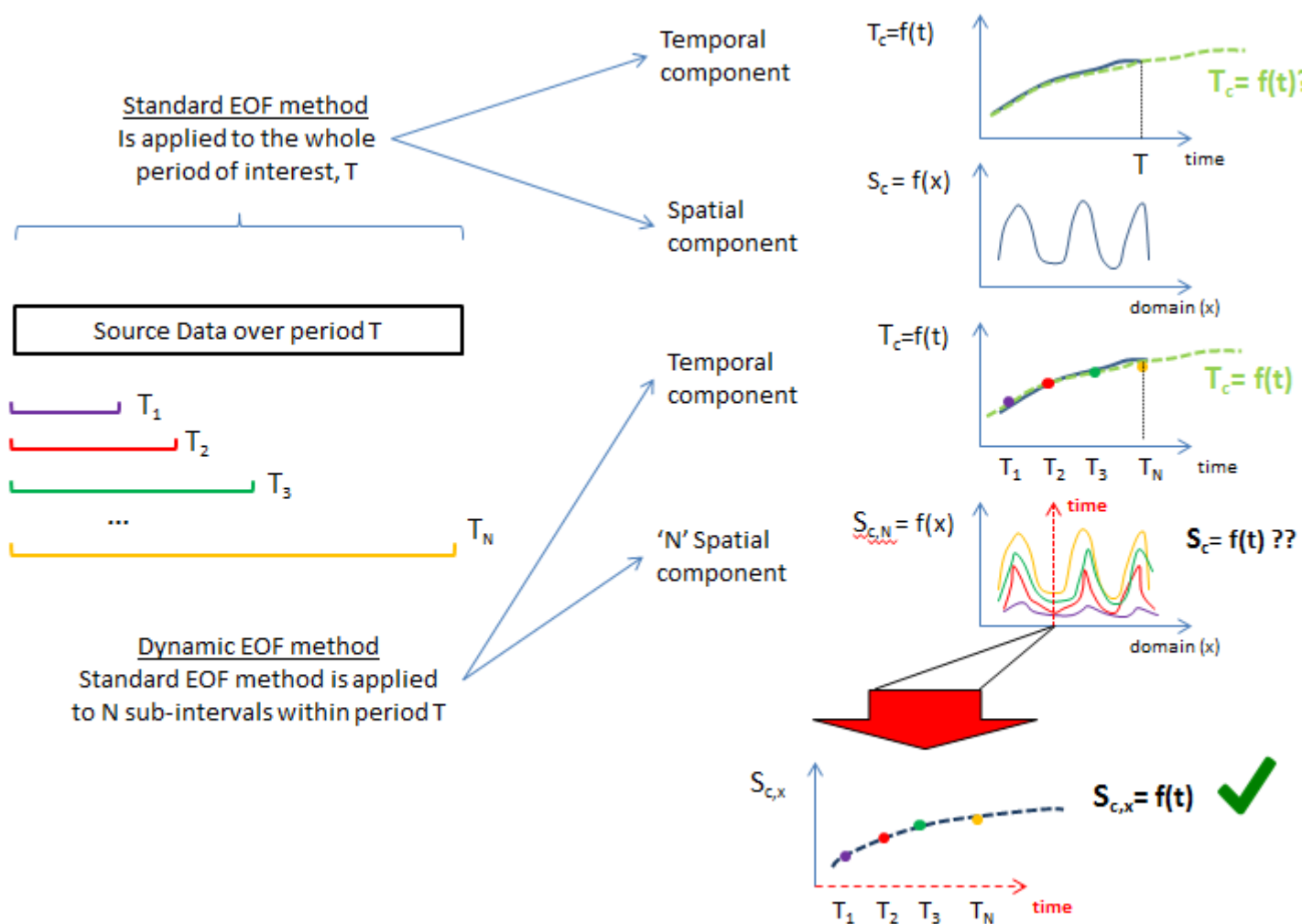


Figure 3.3. Dynamic EOF component extrapolation concept.

As described in Figure 3.3 the standard EOF method applied to the period T , will only provide one set of 1st EOF spatial and temporal component, 1 set of 2nd EOF spatial and temporal components and so on. The dynamic EOF method applies the standard EOF method to N sub-intervals within the period T . This methodology produces N sets of 1st EOF spatial and temporal components, N sets of 2nd EOF spatial and temporal components and so on. Therefore, for each particular location of the domain, i , the N values obtained for the 1st EOF spatial component for different sub-intervals, represent the temporal evolution of such EOF spatial component at that particular location.

A function for each location, i , a function f_i can be defined that fits the N values obtained for the EOF spatial component. Functions f_i can be then used to forecast the value of the EOF spatial component, beyond the training period T . The same methodology can be applied to each point within the spatial domain, defining a function f_i for each of the points. Then the EOF spatial component can be forecasted for the whole domain. This process is schematized in Figure 3.4.

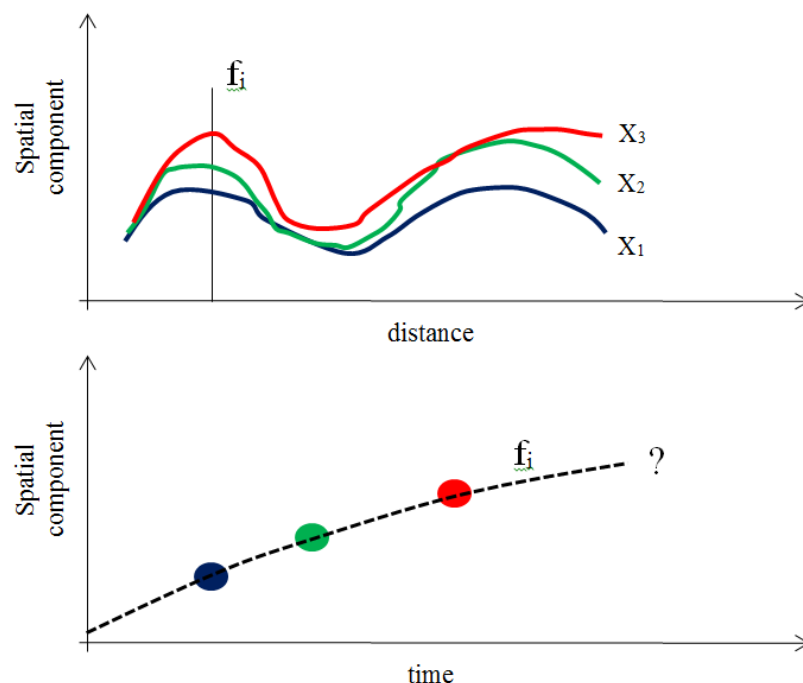


Figure 3.4. Example of EOF spatial component extrapolation.

Therefore, the problem of extrapolating the EOF spatial component is reduced to the problem of fitting a given dataset.

3.3.2 EOF Temporal Component extrapolation

As seen previously the EOF temporal component extrapolation has already been experimented by some authors (Reeve et al. 2008; Horrillo-Caraballo et al. 2014; Alvarez and Pan 2014). In those cases, regardless of the method used to calculate the function for extrapolation, the EOF temporal component behaviour was directly extrapolated extending the behaviour of such component beyond the period of study, T . This procedure is based on the idea that the EOF temporal component keeps the temporal information of the data variation in the system. Therefore in order to extrapolate results beyond the period, T the EOF temporal component should be extrapolated or extended beyond T . This procedure implies that if the EOF method is performed in sub-intervals within the sampled period, T , the obtained EOF temporal components for those sub-intervals should overlap, representing smaller portions within the full-length EOF temporal component. If that is the case, the procedure followed in the literature review should be correct and a direct extrapolation is adequate. The following figure represents the idea developed above.

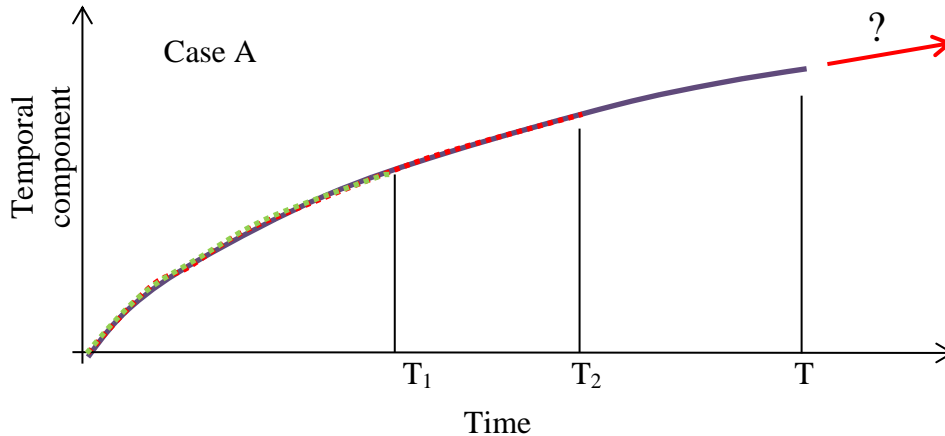


Figure 3.5. Example of standard EOF temporal extrapolation.

Figure 3.5 represents a conceptual example of the EOF temporal component extrapolation. It can be seen that for smaller subintervals of T , named T_1 and T_2 , the obtained EOF temporal components overlap with the EOF temporal component for the longer sub-interval. For instance, the EOF temporal component for subinterval T_2 , is the same than for the subinterval T_1 plus the extension from T_1 to T_2 . Identically, the

EOF component for interval T is the same than for the subinterval T_2 plus the extension from T_2 to T . Following this idea, if EOF temporal component is to be extrapolated beyond T , the extrapolated component should be the same than for period T plus the extension from T to T^+ .

However, the usage of data derived from a numerical model providing high-quality data in both temporal and spatial domain suggests that this approach might not be necessarily correct. Results suggest that for a longer period, the new EOF component is not necessarily an extension of the calculated for that shorter period, and therefore direct extrapolation would not be valid. Although results will be discussed in depth in Chapter 6, some idealised scenarios are shown here for better interpretation. Despite of the advantages of using data from a numerical model this approach should be treated with caution due to the inherent limitations of numerical models themselves that will translate to the dataset generated. Therefore the Dynamic EOF method should be applied to a set of field data when possible.

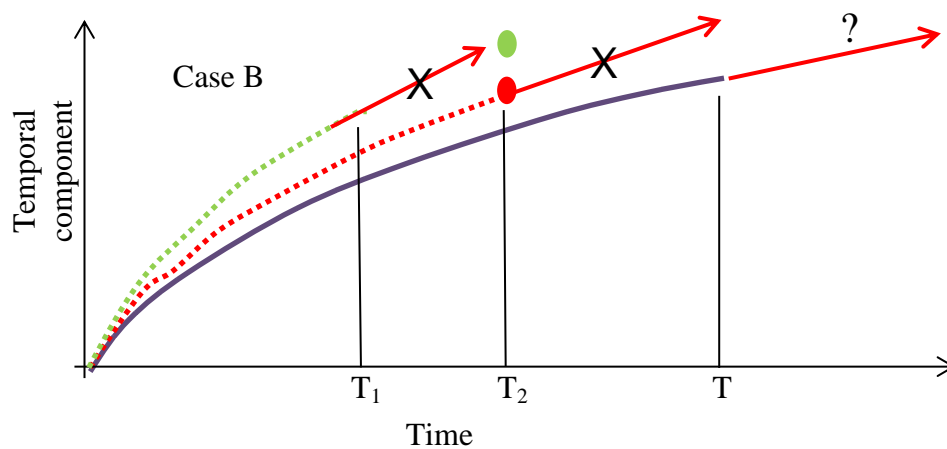


Figure 3.6. Example of inadequate EOF temporal extrapolation.

According to these results, extrapolation should not be done directly using the original EOF temporal component but a more in-depth analysis should be done where possible. In Figure 3.6, it can be seen that for the smaller periods the extension of the component does not necessarily represent the value of the temporal component for the longer period. For instance, when directly extrapolating the component obtained for

the period T_1 up to T_2 , the extrapolated value (green dot) will differ for that obtained applying the EOF method directly to the period T_2 (red dot).

The proposed methodology is to analyse just the final values for the EOF temporal component obtained for each sub-interval and fit those points into a function that will be extrapolated, rather than directly extrapolating the EOF component for the period T . Figure 3.7 shows the proposed methodology for EOF temporal extrapolation. Following this idea, given the sample period T , a direct extrapolation of the temporal obtained for period T will not always represent the values for times beyond T .

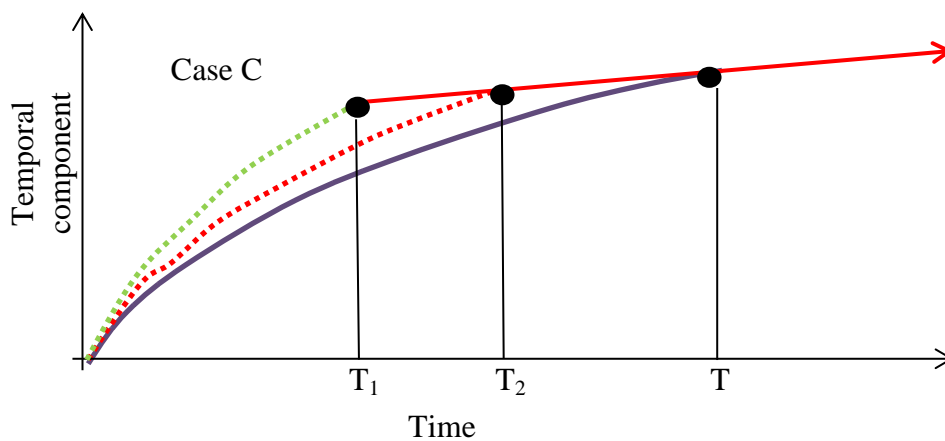


Figure 3.7. Example of Dynamic EOF temporal extrapolation.

In order to assess the validity of this hypothesis, both approaches will be followed. EOF temporal components will be extrapolated as suggested by previous work extending the behaviour of the component (Case A) and also the new methodology will be used (case C). A detailed discussion of the results is shown in Chapter 6: Dynamic EOF Analysis

3.4 SUMMARY

The details the standard EOF method and mathematical background are presented, and the advantages and limitations of the EOF method are explored and discussed regarding its application to predictions. The results from a number of studies show that EOF components can be successfully extrapolated beyond the training period in order

to forecast results. However, previous studies only extrapolated the EOF temporal components, assuming the EOF spatial component remains invariant over time.

A novel methodology, the Dynamic EOF method, to extrapolate EOF components is proposed and explained in detail. This methodology suggests that the EOF spatial components should also be extrapolated beyond the training period in order to obtain more accurate predictions of these components. The new methodology also suggests a different procedure for EOF temporal component extrapolation.

4 PROCESS-BASED MODEL

4.1 INTRODUCTION

In order to provide sufficient data for the dynamic EOF analysis with well controlled forcing conditions, it is decided that the process-based COAST2D (Pan et al. 2005; Du et al. 2010; Du et al. 2012); (Pan et al. 2013) is used in this study. The COAST2D model has been well developed and validated in the previous studies. Before the COAST2D model is used for the provision of the data required, a further validation is also carried out. This chapter describes the details of COAST2D as well as the re-validation study.

4.2 MODEL DESCRIPTION

COAST2D is a 2D depth-averaged coastal area model consisting in different interactive modules accounting for wave propagation processes, currents and morphodynamics. The model consists of a number of fully interactive modules, including: a wave module to determine wave-period averaged wave energy or wave height and wave direction for the wave transformation from offshore to nearshore; and a current module to compute the depth-integrated current velocity and water surface elevation under both tide and wave actions; and a morphological module to compute the sediment transport rates using equilibrium formulae, as well as the resulting bed level changes. The model also includes full wave-current and hydrodynamic-morphological interactions. While the further information can be found elsewhere, only principal governing equations are briefly given in this report in the following sections to the aspects of currents, waves and sediment transport.

A 2D depth-averaged model, by definition, neglects some of the processes happening in the vertical dimension such under-toe currents. These currents can have an impact on the morphodynamics surrounding coastal structures, in particular shore-parallel breakwaters. Therefore, the results provided by the model should be analysed with caution.

4.2.1 Currents

The water surface elevation is calculated using the following two-dimensional continuity equation:

$$\frac{\partial z}{\partial t} + \frac{\partial}{\partial x}(dU) + \frac{\partial}{\partial y}(dV) = 0 \quad (4.1)$$

where z is the surface elevation; U , V are the horizontal depth-integrated velocity components; and d is the water depth.

The horizontal velocity components U and V are calculated by the depth-average momentum equations as:

$$\begin{aligned} \frac{\partial dU}{\partial t} + \frac{\partial dUU}{\partial x} + \frac{\partial dUV}{\partial y} - \frac{\partial}{\partial x} \left(\nu \frac{\partial dU}{\partial x} \right) - \frac{\partial}{\partial y} \left(\nu \frac{\partial dU}{\partial y} \right) + \\ gd \frac{\partial z}{\partial x} + C_x U \sqrt{U^2 + V^2} + fdV - \frac{1}{\rho} \left(\frac{\partial S_{xx}}{\partial x} + \frac{\partial S_{xy}}{\partial y} \right) + \tau_{wx} = 0 \end{aligned} \quad (4.2)$$

$$\begin{aligned} \frac{\partial dV}{\partial t} + \frac{\partial dVU}{\partial x} + \frac{\partial dVV}{\partial y} - \frac{\partial}{\partial x} \left(\nu \frac{\partial dV}{\partial x} \right) - \frac{\partial}{\partial y} \left(\nu \frac{\partial dV}{\partial y} \right) + \\ gd \frac{\partial z}{\partial y} + C_y V \sqrt{U^2 + V^2} - fdU + \frac{1}{\rho} \left(\frac{\partial S_{xy}}{\partial x} + \frac{\partial S_{yy}}{\partial y} \right) + \tau_{wy} = 0 \end{aligned} \quad (4.3)$$

where C_x and C_y are the frictional coefficients in x and y directions for U and V respectively; ν is the turbulent eddy viscosity; f is the Coriolis force coefficient; S_{xx} , S_{xy} , S_{yy} is the wave radiation stresses if wave computation is coupled (detailed later); τ_{wx} , τ_{wy} is wind shear stresses on the surface. If the bed form effects are not considered, the bed friction is calculated by $C_x = C_y = 0.016(\Delta/d)^{1/3}$, where: Δ is the roughness height, which can be related to the sediment size as $\Delta \approx 2.5D_{50}$; D_{50} is the medium grain size.

4.2.2 Waves

The two equations describing the wave vectors are derived from the kinematic conservation equation (Phillips, 1977):

$$\frac{\partial K_i}{\partial t} + \frac{\partial \omega}{\partial x_i} = 0 \quad (4.4)$$

where K_i is the wave number vector ($\{i=1,2\}$); t is the time; ω is the apparent wave frequency; and x_i is the horizontal coordinate vector. To include the effect of currents, it is assumed that the waves are propagating on a medium moving with velocity U_i . The apparent frequency is then given by the Doppler equation: $\omega = \sigma + K_j U_j$, where σ is the intrinsic wave frequency. Assuming small amplitude wave theory being applied, the intrinsic wave frequency can be described by the linear dispersion equation: $\sigma^2 = gk \tanh(kd)$, where k is the wave separation factor. It should be stressed that since diffraction effects will be accounted for the separation factor is not equivalent to the wave number.

Taking account for the wave diffraction based on the approach proposed by Battjes & Janssen (1978), which is the effect of wave amplitude on the kinematics of small-amplitude waves, therefore, the wave number vectors can be calculated using:

$$K_j K_j = k^2 + \frac{1}{A} \nabla^2 A \quad (4.5)$$

where A is the wave amplitude. Differentiating Eq. (4.5) leads to the following equations for wave directions in both x and y directions respectively:

$$\frac{\partial P}{\partial t} + \left[C_g \frac{P}{k} + U \right] \frac{\partial P}{\partial x} + \left[C_g \frac{Q}{k} + V \right] \frac{\partial P}{\partial y} + \frac{\sigma G}{2d} \frac{\partial d}{\partial x} - \frac{C_g}{2k} \frac{\partial \Phi}{\partial x} + P \frac{\partial U}{\partial x} + Q \frac{\partial V}{\partial x} = 0 \quad (4.6)$$

$$\frac{\partial Q}{\partial t} + \left[C_g \frac{P}{k} + U \right] \frac{\partial Q}{\partial x} + \left[C_g \frac{Q}{k} + V \right] \frac{\partial Q}{\partial y} + \frac{\sigma G}{2d} \frac{\partial d}{\partial y} - \frac{C_g}{2k} \frac{\partial \Phi}{\partial y} + P \frac{\partial U}{\partial y} + Q \frac{\partial V}{\partial y} = 0 \quad (4.7)$$

where P and Q are the wave number vectors in x and y directions and $\Phi = \frac{1}{A} \nabla^2 A$;

$$C_g = \frac{\sigma}{2k} (1+G); \text{ and } G = \frac{2kd}{\sinh(2kd)}.$$

The equation for wave amplitude is derived from the energy conservation equation for small-amplitude and linear waves in a moving medium (Phillips, 1977):

$$\frac{\partial E}{\partial t} + \frac{\partial}{\partial x_i} (EU_i + F_i) + S_{ij} \frac{\partial U_j}{\partial x_i} + \tilde{D} = 0 \quad (4.8)$$

where E is the total wave energy; F_i is the wave flux vector; S_{ij} is the radiation stress tensor $\{i=1,2\}$; and \tilde{D} is the energy dissipation due to the wave breaking and the bottom friction. Considering the relation between wave amplitude and wave energy gives the following equation:

$$\begin{aligned} \frac{\partial A}{\partial t} + \frac{1}{2A} \left\{ \frac{\partial}{\partial x} \left[A^2 \left(\frac{C_g}{k} P + U \right) \right] + \frac{\partial}{\partial y} \left[A^2 \left(\frac{C_g}{k} Q + V \right) \right] \right\} \\ + \frac{1}{\rho g A} \left[S_{xx} \frac{\partial U}{\partial x} + S_{xy} \left(\frac{\partial U}{\partial y} + \frac{\partial V}{\partial x} \right) + S_{yy} \frac{\partial V}{\partial y} \right] + C_a A = 0 \end{aligned} \quad (4.9)$$

where C_a is the dissipation coefficient due to the wave breaking and the bottom friction; and S_{xx} , S_{xy} , S_{yy} are the wave radiation stresses given by:

$$S_{ij} = \frac{1}{2} \left[(1 + G) \frac{K_i K_j}{k^2} + G \delta_{ij} \right] E \quad (4.10)$$

Wave breaking is considered in the model. For random waves, it is based on the approach proposed by Battjes and Janssen (1978). The probability of wave breaking

Q_b that at a given point is assumed as: $\tilde{D} = \frac{\alpha \pi}{2T} Q_b H_m^2$, and H_m = the maximum possible wave height.

4.2.3 Sediment transport

The total sediment transport without distinction of the bed load and suspended sediment transport suggested by Soulsby (1998) formula is used for combined waves and current, as well as for asymmetrical waves, which is given as:

$$q_t = A_s U \left[\left(U^2 + \frac{0.018}{C_D} U_{rms}^2 \right)^{1/2} - U_{cr} \right]^{2.4} (1 - 1.6 \tan \beta) \quad (4.11)$$

Where,

$$A_{sb} = \frac{0.005h(d_{50}/h)^{1.2}}{[(s-1)gd_{50}]^{1.2}}$$

$$A_{ss} = \frac{0.012d_{50}D_*^{-0.6}}{[(s-1)gd_{50}]^{1.2}}$$

$$A_s = A_{sb} + A_{ss}$$

$$C_D = \left[\frac{0.40}{\ln(h/z_0) - 1} \right]^2$$

where q_t is the volumetric transport rate; D_* is the dimensionless grain diameter; C_D is the drag coefficient due to current alone; β is the slope of bed in stream wise direction, positive if flow runs uphill; \bar{U} is the depth-averaged current velocity; U_{rms} is the root-mean-square wave orbital velocity; and z_0 is the roughness height. For rippled bed, z_0 is set to 6 mm.

All governing equations described above are discretised and solved using explicit finite difference methods with appropriate boundary conditions specified. All modules are fully and dynamically interacting between both hydrodynamics and morphodynamics.

4.3 MODEL RE-VALIDATION

To ensure the satisfactory performance of the COAST2D model for the long period simulations required in this study, a further model validation is carried out at the Aveiro coast Portugal, where good quality field measurements are available (Alvarez et al. 2016 to be submitted).

4.3.1 Study Area

The validation site is located in the Aveiro region, northern Portugal. This site was particularly chosen because of the complex hydro-morphodynamics due to the presence of the coastal structures as well as the availability of the field data. Extensive bathymetrical and topographical measurements at this site were taken by the University of Aveiro from the 9th October 2013 and the 1st February 2014, along the

stretch of coast between towns of Vagueira and Praia de Mira, as shown in (left) In this study, the computational covers 9km in the alongshore direction and 2.5 km in the cross-shore direction, as shown in Figure 4.1 (left), including, two groynes at Aeroa and Poço da Cruz. Both groynes are in a slightly curved configuration against the predominant incoming wave direction as shown in Figure 4.1 (right).

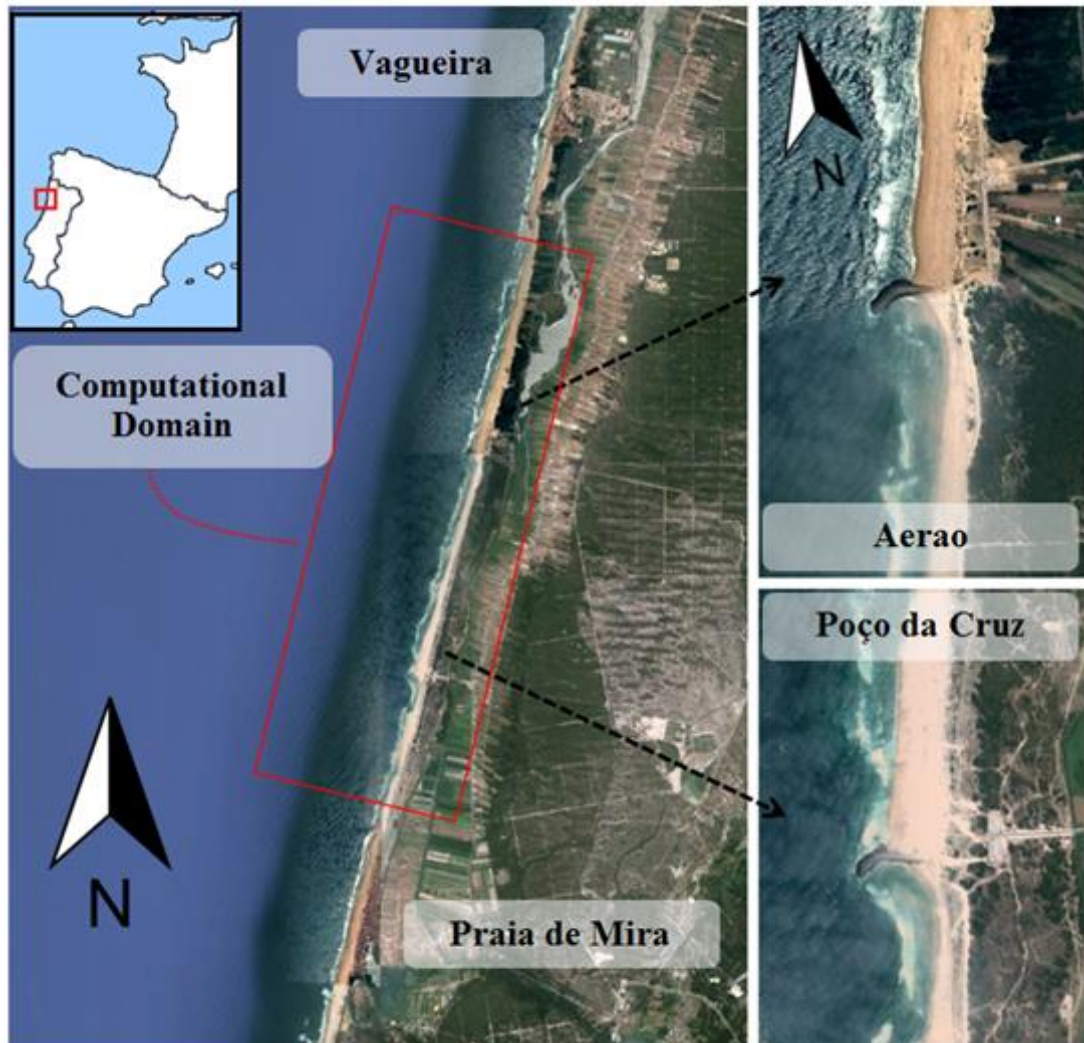


Figure 4.1. Validation study area.

There were a number of bathymetric surveys at this site, including those surveyed on 09 Oct and 01 Feb 2014. Sediment size along the Aveiro coastline was also extensively measured in this area (Silva et al. 2009), showing a high temporal and spatial variability. Within the present study area, d_{50} ranges from 0.35 mm to 0.52 mm.

4.3.2 Model Setup

The COAST2D model is set to cover an area of 9025 m by 2580 m in the longshore and cross-shore directions respectively in the central part of the coast between Vagueira and Praia de Mira to include two groynes as shown in Figure 4.2. The computational grid consists of 361x172 node points with grid sizes of 25m in the longshore direction and 15m in the cross-shore direction. A finer grid size is used in the cross-shore direction to increase the resolution in order to better capture the hydrodynamic and morphodynamics variations and to better present the curvature of the groynes. Bathymetry data surveyed on 9 October 2013 is interpolated into the grid and used as the initial bathymetry for the model. The water depth along the offshore (open) boundary is approximately 14 m.

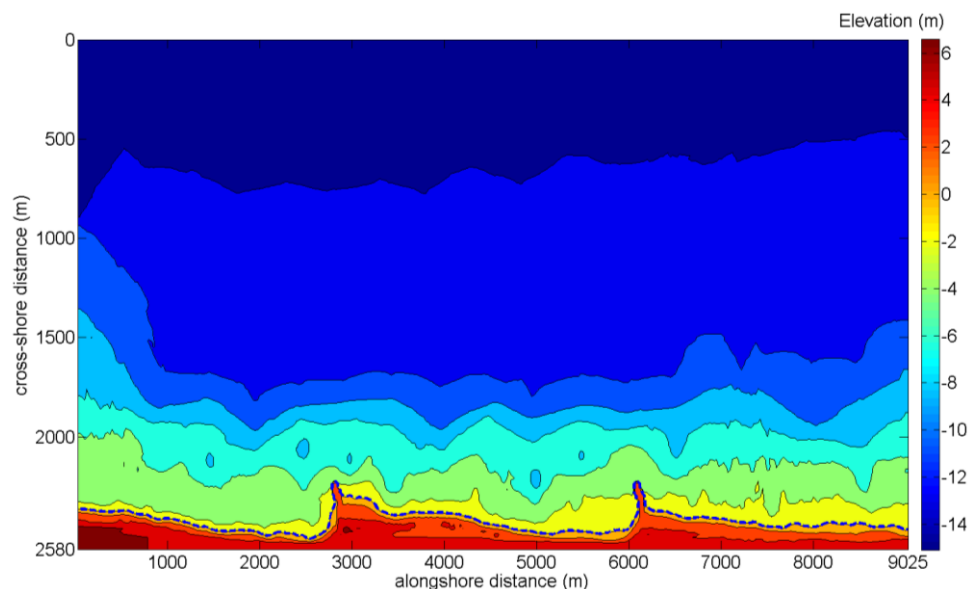


Figure 4.2. Initial computational domain for the model COAST2D. Initial shoreline position is indicated in blue.

The model is forced by the wave and tide conditions based on the field measurements which are described in detail in as follows. According to the work of Baptista (2014), the tides in the area are semidiurnal, with the average spring and neap tidal ranges being 2.8 m and 1.2 m respectively. Wave data for the period of simulations is provided from a wave station at Leixoes, some 80km north of Aveiro. During this period, two major storms with the significant wave height up to 7m being measured. The time series of the significant wave height measured at Leixoes station are shown in Figure 4.3 over the period from Oct 2013 to March 2014. Red dots represent the start and the end of the simulation.

Wave directions are shown in Figure 4.4. At this study site, waves are mainly north-westerly. This characteristic produces a net alongshore sediment transport from north to south.

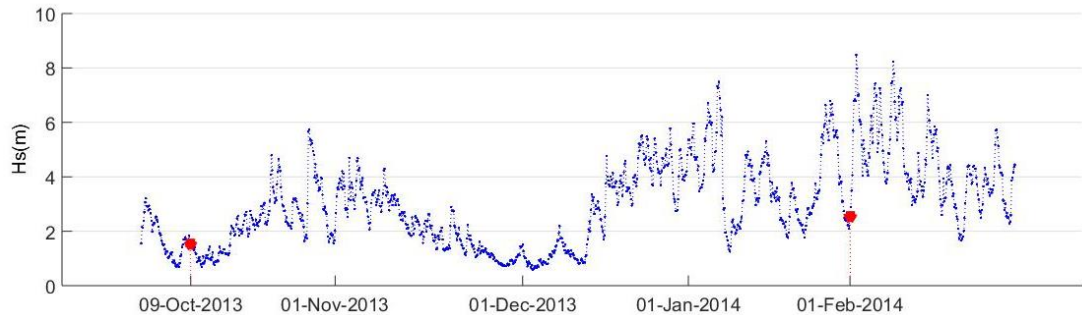


Figure 4.3. Offshore significant wave height at Leixoes station.

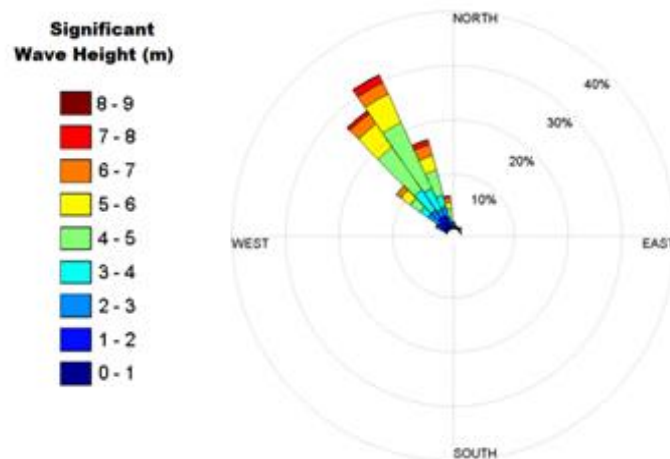


Figure 4.4. Wave direction rose at Leixoes station.

The wave periods from the measurements are shown in Figure 4.5, ranging from 5 seconds to 15 seconds showing a linear correlation with the wave height.

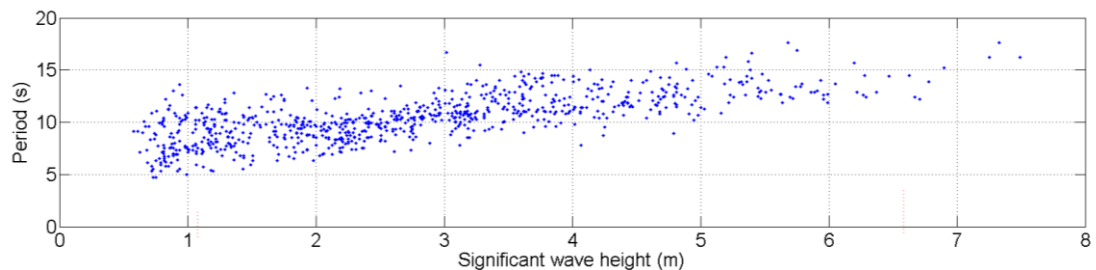


Figure 4.5. Significant wave height VS wave period at Leixoes station.

Along the offshore boundary, time varying wave conditions (wave height, period and direction) are also specified in 0.5 hourly intervals, based on the measurements

obtained at the Leixoes Station. Although the measuring station is further away from the open boundary of the computational domain, it is assumed that the changes of wave conditions from the station to the open boundary to be insignificant as waves propagate mainly in the deep water area (>15 m in the current study). In this study, an M2 semidiurnal tide with a 2 m tidal range is used along the offshore boundary of the computational domain as the representative tides at the study site. Despite the high temporal and spatial variability of the sediment size presented by Silva et al (2009), sediment with d50 of 0.45 mm is used for the entire domain. Groynes are treated as bathymetry with increased roughness, but non-erodible, although sediment deposition on groynes is allowed. The crest level of the groynes is set to 4 m and their curvature is approximated well within the computational grid.

A 4-month simulation is carried out using COAST2D with the wave conditions in the period from the 9th October 2013 to 1st February 2014. Bathymetric data is available for the study period and will be used to assess the performance of the model. Currents velocity data is not available and therefore a direct comparison between modelled and measured velocities cannot be performed. The predicted waves, currents and sediment transport rates under calm and storm conditions from the model are examined as described in the following section.

4.3.3 Results and Discussion

Figure 4.6 shows the wave height distribution on the 11th October 2013, which represents a calm condition with the offshore wave height, is around 0.82m. For these conditions, it can be seen how the groyne effectively offer shelter to a region approximately 100m downstream reducing the wave height.

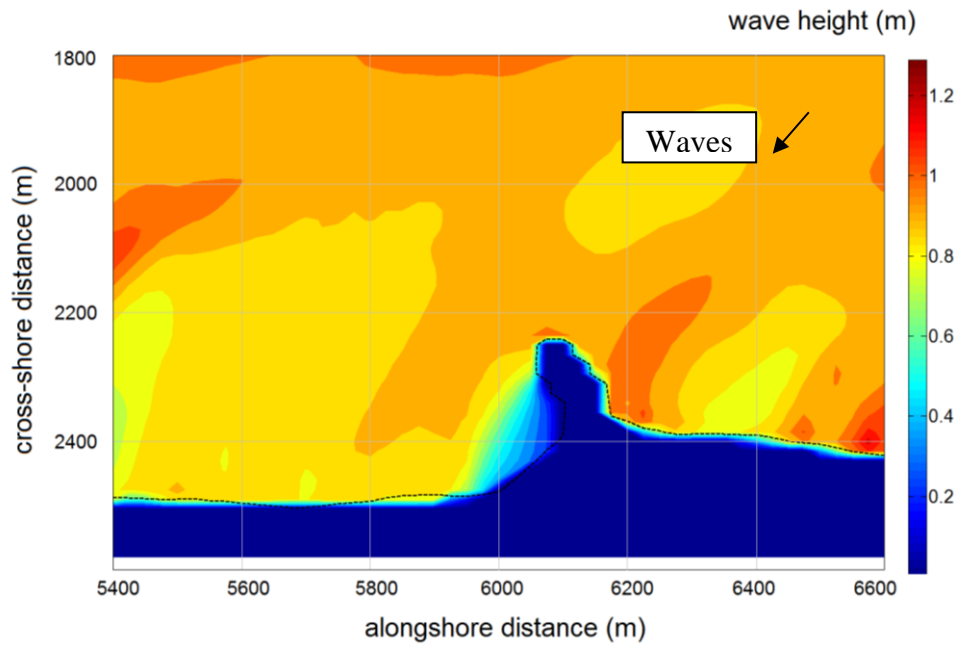


Figure 4.6. Significant wave height at the Aerao Groyne on the 11th October 2013 with offshore significant wave height 0.82m during high tide (calm conditions).

Figure 4.7 shows the corresponding combined tide and wave-induced currents .Re-circulation can be found in the exposed side of the groyne. Currents bypass the groyne although it can be seen that current values are smaller on the area protected by the groyne around 5900m to 6100m.

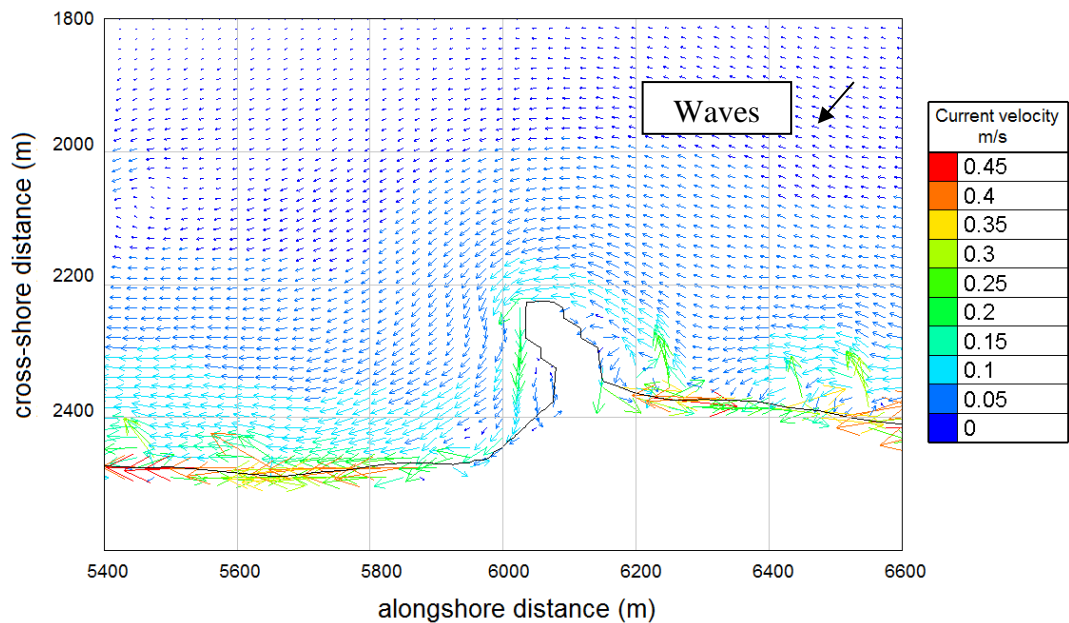


Figure 4.7. Currents at the Aerao Groyne on the 11th October 2013 with offshore significant wave height 0.82m during high tide (calm conditions).

Figure 4.8 shows the sediment transport rates in the study area. It can be seen that the sediments are mobilized towards the groyne in a very limited area close to shore line where some erosion can be expected. However, waves do not have enough energy to move the sediments around the groyne and therefore accretion is expected to happen in the near up-drift area of the groyne. On the other hand, the down-drift area of the groyne is affected by the waves but sediment transport remains blocked by the groynes. Therefore, erosion is expected to occur in the immediate lee side of the groyne. This is the general response expected from a shoreline affected by a groyne and oblique waves.

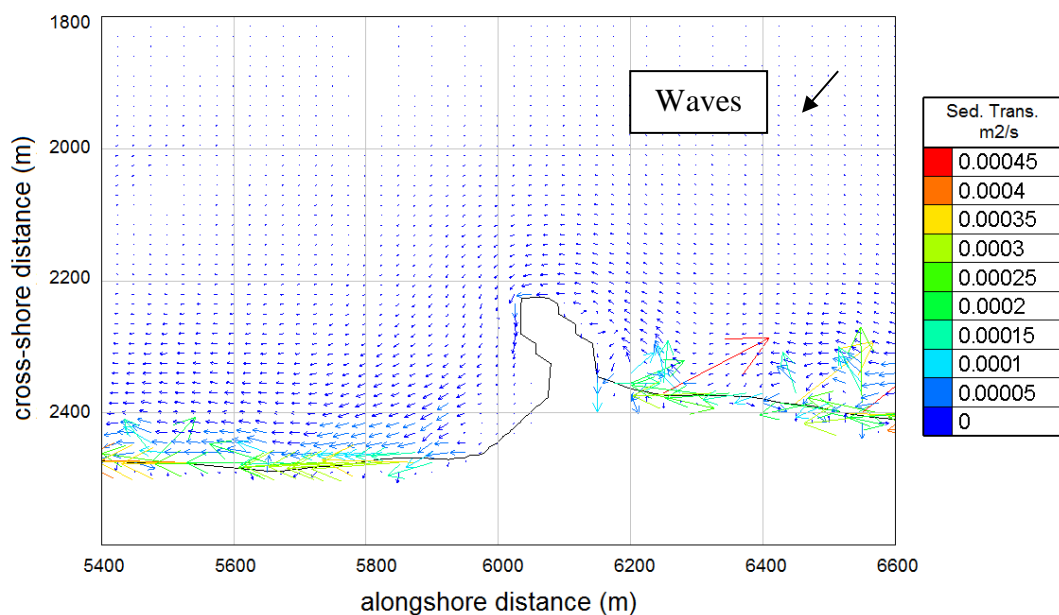


Figure 4.8. Sediment transport rates at the Aerao Groyne on the 11th October 2013 with offshore significant wave height 0.82m during high tide (calm conditions).

Figure 4.9 shows the wave height distribution around the Aerao Groyne during the first storm on 26th October 2013 during a high tide with offshore significant wave height of 5.3 m. Figure 4.10 shows the combined tide and wave-induced currents for the same storm conditions. It can be seen that there is a large band with high velocity current from 2000m to 2400m in the cross-shore direction. Recirculation can be found especially in the protected side of the groyne from 5600m to 6100m.

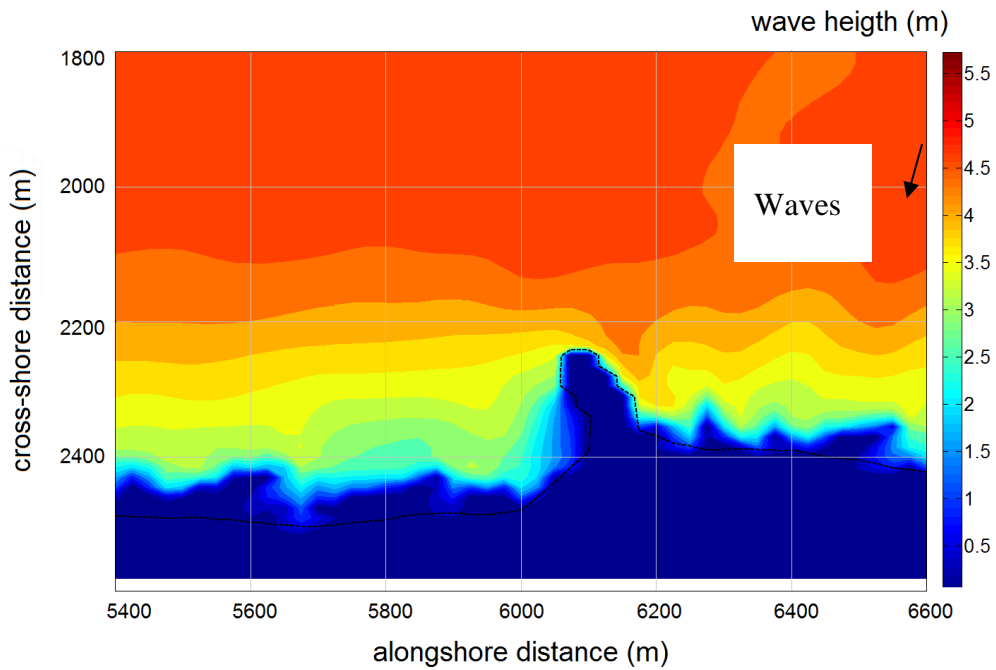


Figure 4.9. Significant wave height at the Aerao Groyne on the 26th October 2013 with offshore significant wave height 5.3m during high tide (storm conditions).

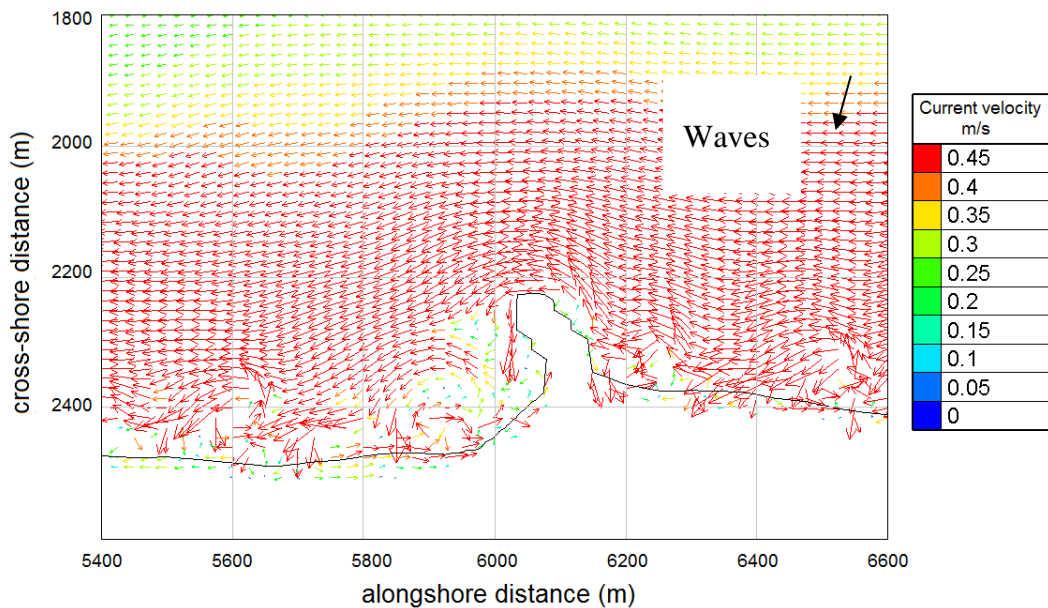


Figure 4.10. Currents at the Aerao Groyne on the 26th October 2013 with offshore significant wave height 5.3m during high tide (storm conditions).

Figure 4.11 shows the sediment transport rates around the Aerao Groyne for the same storm conditions. It can be seen that during the high tides affected by the energetic nearshore waves (shown in Figure 4.7), the sediments are transported in the large area (a strip of approximately 200 m in width) near the shoreline, bringing a large amount of sediment around the groyne which causes erosion in the up-drift of the structure and

deposition in the down-drift. This behaviour is significantly different from that seen for the calm conditions. Although Figures 4.10 and 4.11 correspond to the same storm conditions Figure 4.10 shows high tide conditions and Figure 4.11 low tide conditions.

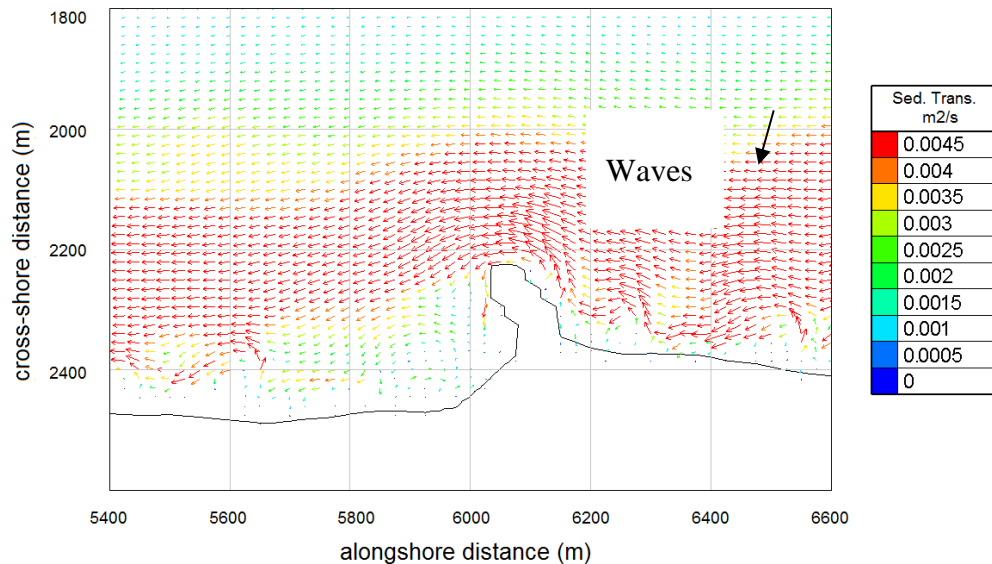


Figure 4.11. Sediment transport rates at the Aerao Groyne on the 26th October 2013 with offshore significant wave height 5.3m during high tide (storm conditions).

As seen in Figure 4.3, the waves climate measured in the period of study is compounded by two big storms with a very short period of calm period (around 1st December 2013) between them. Therefore, it can be expected the overall behaviour of the shoreline during the studied period will follow the behaviour under storms conditions described in Figure 4.9, Figure 4.10 and Figure 4.11.

The final shoreline predicted by COAST2D is shown in Figure 4.12, together with both the initial shoreline position and the final shoreline position from the survey on 1st February, 2014. It can be seen that final shoreline positions from both the model and survey match reasonably well in general. According to Figure 4.12 the model accurately represents the areas that present erosion or accretion. Overall erosion is found in the exposed face of the groyne whereas deposition occurs at the lee of the groyne.

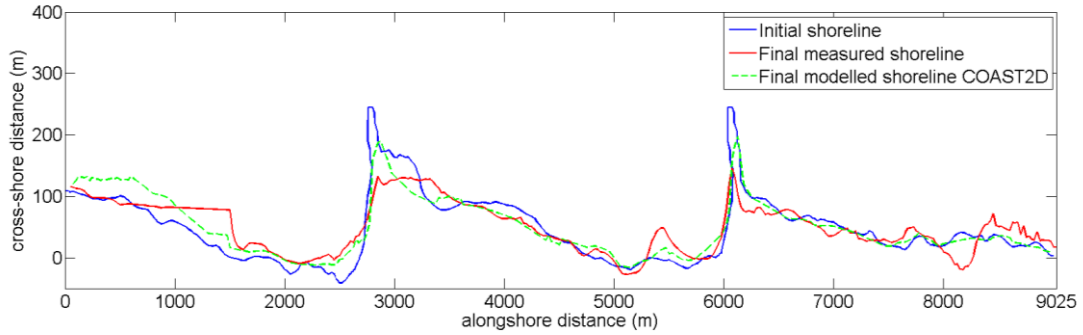


Figure 4.12. Initial (blue) and final (red) measured shoreline and final modelled shoreline (green).

Figure 4.13 shows the net advance or recess of the measured (top panel) and the modelled shorelines (bottom panel), where the positions of two groynes are indicated by two red lines. The net advance/recess is calculated at each alongshore computational section every 25 m. Three areas are defined. Area 1 corresponds to the southern part of the scheme. Area 2 corresponds to the stretch of coast between the two groynes. Area 3 is the northern area. From Figure 4.13, it can be argued that the general advance and recess patterns from the model and measurements agree well. In Area 1, the shoreline presents an advance trend. In Area 2, erosion of the shoreline occurs in the updrift area and advance in the down-drift area of each groyne. In Area 3, the shoreline is mostly eroded.

The results are within the expectation, as the predominant storm waves are north-westerly, which likely cause the erosion in the up-drift of each groyne and accretion in their down-drift. In Area 2, accretion is expected to likely occur immediately down-drift of the right groyne (Aerao) and erosion is expected in the area up-drift of the left groyne (Poço da Cruz). Both the model results and measurements have confirmed the erosion and accretion patterns. The model slightly under-predicts the erosion and accretion magnitudes in Areas 3 and 1. The discrepancies in those two areas (Areas 3 and 1) are likely to be affected by the ends of the computational domain, where the local equilibrium sediment transport rates are assumed. However, the predicted erosion and accretion in Area 2 agree well with measurements.

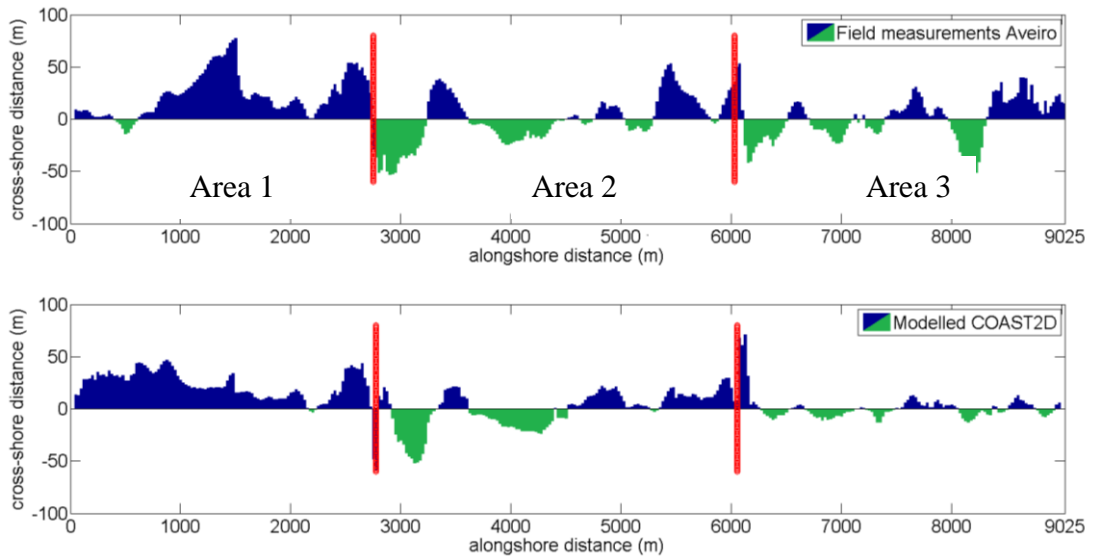


Figure 4.13. Net measured (top panel) and modelled (bottom panel) advance-recess of the shoreline.

The maximum erosion of the shoreline in this area of approximately 50 m is confirmed by the measurements, although the maximum advance of the shoreline predicted by the model is 25 m, smaller in comparison of the measurements. The averaged shoreline advanced/recess is similar for both measured and modelled results as shown in Figure 4.14. Given the fact that in Area 2, the model simulation is less affected by the boundary condition, the results demonstrate the accuracy and capability of the COAST2D model in representing the complex hydrodynamics and morphodynamics in this case.

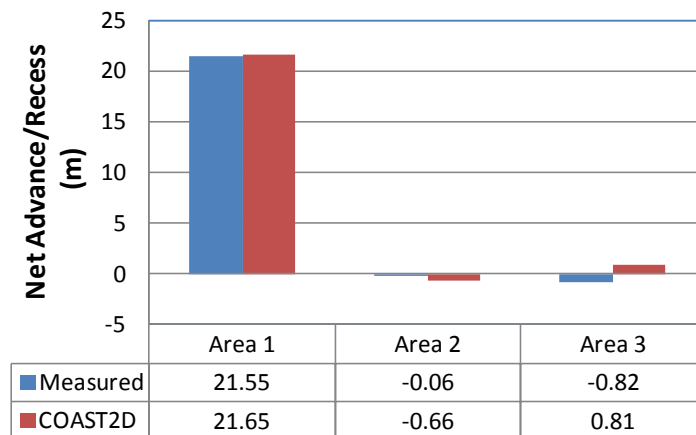


Figure 4.14. Net shoreline advance/recess values (m) for each area.

A process-based numerical model, COAST2D, has been used to model the shoreline changes over a 4-month period under the combined wave and tide conditions with the

presence of two groynes along the coast in Aveiro, north Portugal. During the 4-month simulation period, there were a number of storms including some highly energetic ones, mainly from the North West. During the storms, large erosion are found on the updrift side of the groynes in the exposed area updrift the groynes with a slight deposition right at the groynes base. Deposition is also found in the area directly protected by the groynes. According to the model results, this behaviour is caused by the storms as the opposite behaviour is found during calm periods.

The final shoreline from the COAST2D model agrees reasonably well with the measured shoreline, particularly in the areas of groynes , Modelled results show a good agreement with the field data and shoreline changes are overall well modelled especially in the area surrounding the groynes. These results show the ability of the used software COAST2D to successfully represent shoreline changes under storm conditions. In order to improve model results sediment size variability should be included in the model, as the area presents a high temporal and spatial variability that may play an important role in the morphodynamics.

The results also highlight the morphological dynamics of this stretch of coast that experienced shoreline advances and recesses of tens of meters in just a 4-month storm period. This case is a clear example of the issues coastal erosion represents and the importance for coastal engineers and managers to accurately describe the morphodynamics and hydrodynamics of the study area in order to better assess the effectiveness of future coastal defence schemes.

4.3.4 Summary

This chapter describes the background and details of a process-based numerical model, COAST2D. This model will be used to generate high quality data to perform the EOF method analysis and to assess the validity of the proposed methodology, Dynamic EOF method. A re-validation case study has been performed in the coast of Aveiro, Portugal, to confirm the validity of the model for larger spatial and temporal domains. Results confirm the model is able to successfully represent the coastal hydrodynamics and morphodynamics for a 4-month period and 9km long stretch of coast. These results increase the range of proven applicability of COAST2D.

5 DATA GENERATION

5.1 INTRODUCTION

To illustrate the concept of the Dynamic EOF analysis as proposed previously for studying the morphological changes at the coast with presence of a breakwater scheme, the well calibrated process-based numerical model – COAST2D is to be set up over an idealised breakwater scheme to provide the required data. Bed level change is chosen as the main variable of study as it is the more direct approach to study morphological changes.

5.2 IDEALISED STUDY DOMAIN

The COAST2D model is setup over an idealised domain containing four shore-parallel breakwaters, as shown in Figure 5.1. The breakwater scheme present in the domain, which is similar to that at Sea Palling, UK, consists of four shore-parallel breakwaters, located approximately 200 m from the initial shoreline. Each breakwater is 200 m long with a gap of 250 m between them. The crest of the breakwaters is set to be 3 m above the mean sea level, as the surface piercing structures in all cases. The sediment size of the bed material is assumed to be $250\mu\text{m}$ and is constant within the domain. Different breakwater schemes were tested in early stages in order to find a configuration providing salients or tombolos depending on the wave conditions.

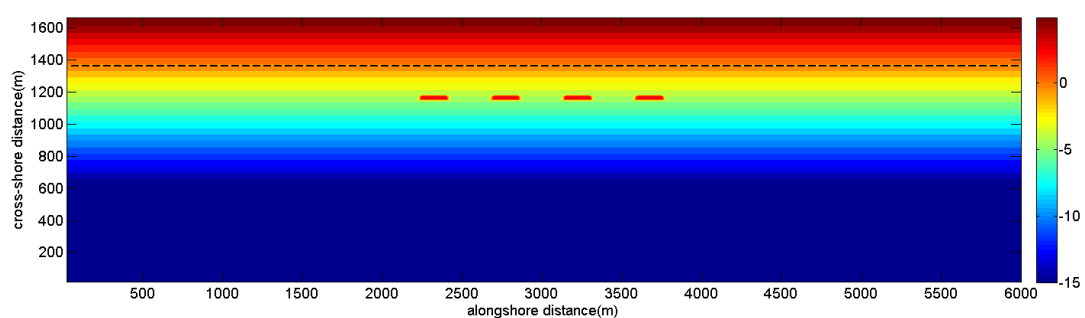


Figure 5.1. Model domain. Shoreline ($z=0$) represented by black dashed line.

In order to study the effect of a group of breakwaters four breakwaters are chosen, rather than individual structures. As the first and last breakwater of the scheme can be considered to have particular effects on the morphological changes, at least three should be considered to define a group. In order to have an embayment not directly

influenced by the first and last breakwater, at least four are required. Also, as discussed in the literature review, the first scheme built in the Sea Palling consisted of four breakwaters making this study more interesting as it can be compared to those at Sea Palling. Some definitions are provided that will be used during this text. Breakwaters are numbered from 1 to 4 from left to right. Embayments are also numbered from left to right. As waves approach the structures from left to right with a 30 degrees angle, the left area of the domain is referred as up-stream area and the right area of the domain is referred as down-stream area.

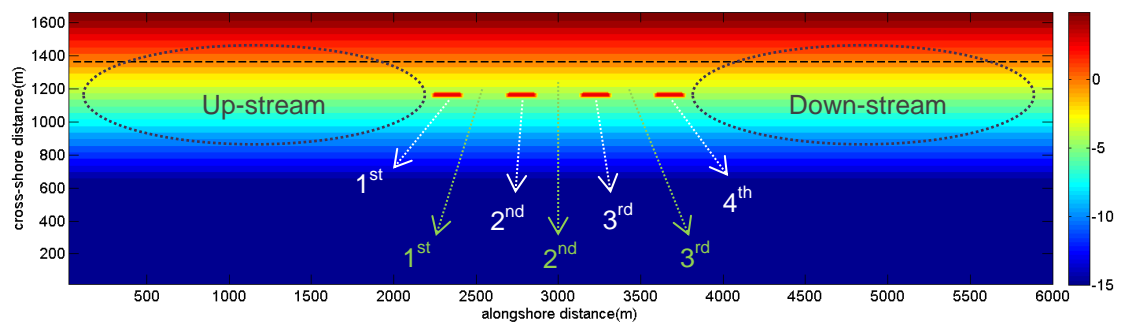


Figure 5.2. Model domain definitions.

The model is defined by a mesh articulated by 241x111 nodes, with grid size of 25 m by 15 m in alongshore and cross-shore directions respectively. These dimensions allow simulating a domain large enough to include the four breakwaters far from the boundaries with enough resolution to represent the structures and without increasing the computational cost excessively. It covers an area of 6025m alongshore and 1665m cross-shore. The offshore water depth is set to 15 m. The selected depth is considered deep enough to not affect the incoming waves while approaching to the shoreline. The initial beach slope is set to 1:50.

In order to reduce the computational cost of applying EOF method several times to the 2D domain, the EOF analysis is limited to a sub-set of mesh with 142x72 nodes or 3550m by 1080m within the computational domain and centred in the breakwaters area as showed in the box shown in Fig. 5.3.

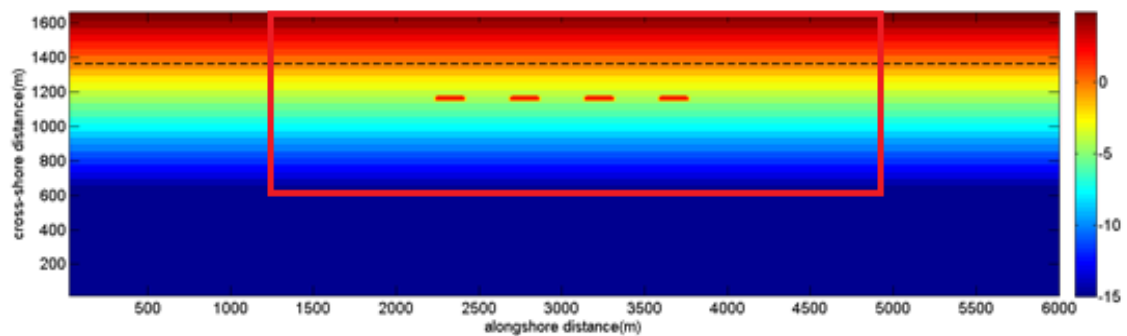


Figure 5.3. Computational domain and reduced domain for EOF analysis (red square).

5.2.1 Boundary Conditions

Different scenarios for wave height and direction have been simulated

Table 2. Incident waves parameters

Case	H	Dir	T
S101	2	30	6
S102	2	15	6
S103	2	5	6
S104	0.5	30	6
S105	0.5	15	6
S106	0.5	5	6

Stationary M2 tides with a range of 3m are used during the simulations. These values for the hydrodynamics conditions are similar to those used in (Environment agency, 2010). The simulations are run for 1500h and data is output hourly. The first 750h are considered as the training period and will be used to apply the Dynamic EOF method. The values obtained at the end of the simulation, for $t=1500h$, will be used to assess the performance of the Dynamic EOF method.

Other parameters required by COAST2D are specified as follow:

Table 3. Parameters used for COAST2D

Parameter	Value
Water density (kg/m ³)	1025
Sand density (kg/m ³)	2650
Temperature (deg)	8
Hydrodynamic time step (s)	0.6
Increment for solution output	6000
Starting time step for morphological computation (h)	6

5.2.2 Model Results

The model provides outputs for different variables. The variables analysed during this work have been, sediment transport rates and bed level changes. Also, derived from bed level changes, shoreline position was studied as the cells with elevation equal to zero. Sediment transport rates are provided for both directions, alongshore and cross-shore independently. Bed level changes are defined as the change in elevation of each computational cell regarded the original bed level of such computational cell, and therefore is measured in meters. Multiplying the area of the cell by the corresponding bed level changes, it is possible to obtain the volume changes in the corresponding computational cell.

Results are provided with a temporal resolution of 1h at all the nodes within the domain. These high temporal and spatial resolutions allow for post-processing the data and rearranging it according to the needs of the study.

COAST2D provides a range of variables that can be analysed. The current version of the model provides hydrodynamic information such as free surface, velocities U and V, wave direction or water depth. Morphodynamics information is also provided such as bathymetry, sediment transport rates and d_{50} .

Figure 5.4 shows the wave distribution for cases S101, S102 and S103. These three cases model the same wave height, $H=2\text{m}$, but using different wave incident angle. It can be seen how the more oblique is the wave incident angle the more oblique is the shadow area protected by the breakwaters. Also, the more perpendicular is the wave incident angle the higher become the wave before breaking. Case S101 is used as a reference case for the Dynamic EOF method analysis as it provides well developed salients and tombolos during the 1500h of simulation.

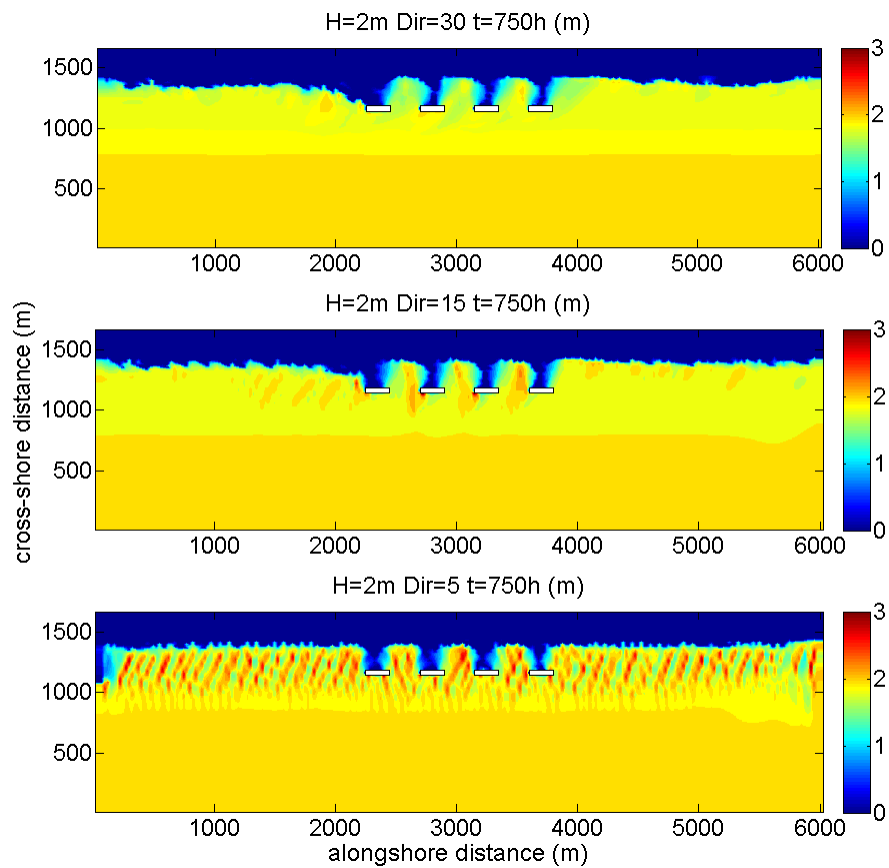


Figure 5.4. Wave height distribution for the cases S101 (top), S102 (middle) and S103 (bottom).

Figure 5.5 shows the wave height distribution for the three calm cases with $H=0.5\text{m}$. It can be seen that the darker area behind the breakwaters (smaller waves) is reduced when compared to the $H=2\text{m}$ cases. This means that sediment transport rates will be less affected during these conditions, as expected.

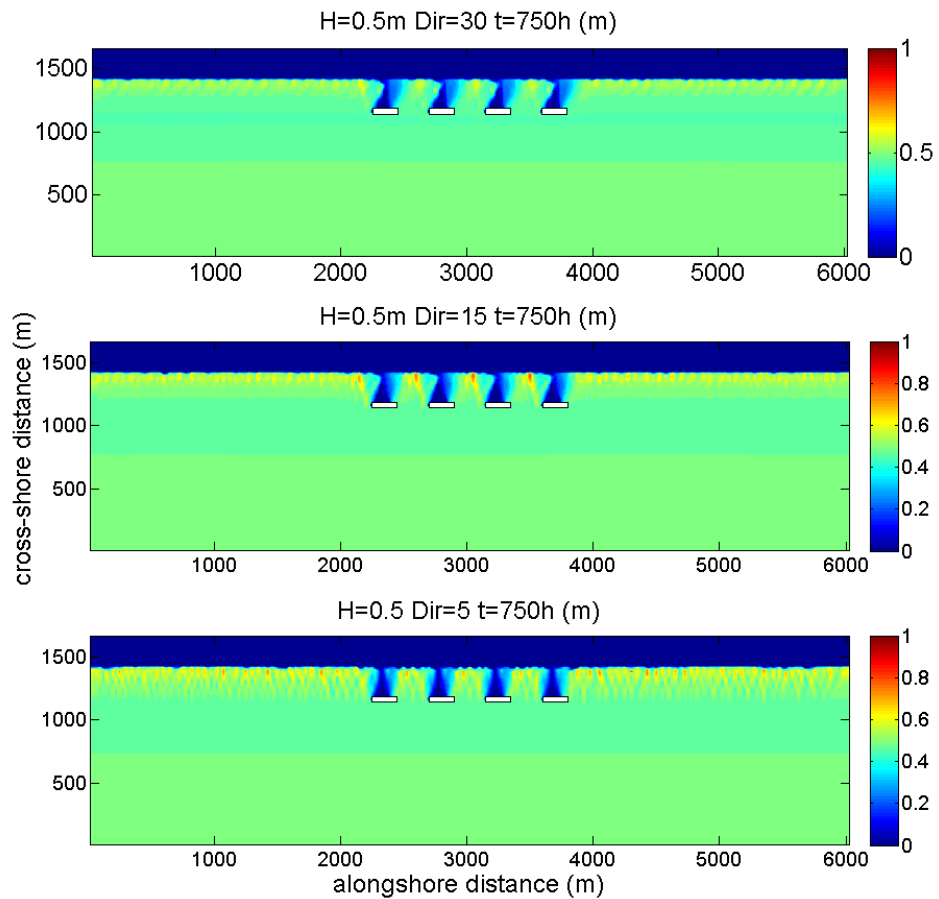


Figure 5.5. Wave height distribution for cases S104 (top), S105 (middle) and S106 (bottom).

Figure 5.6 represents the bathymetric changes after 750h of simulations for caess S101, S102 and S103. It can be observed that the higher the wave incident angle, the more asymmetry can be found between the upstream and downstream areas. Also, the higher the wave incidence angle the more curved are the tombolos formed, presenting a clear horn-shape for the case S101. For the nearly-perpendicular waves of case S103, the tombolos present lower extension as well as the erosion at the embayments.

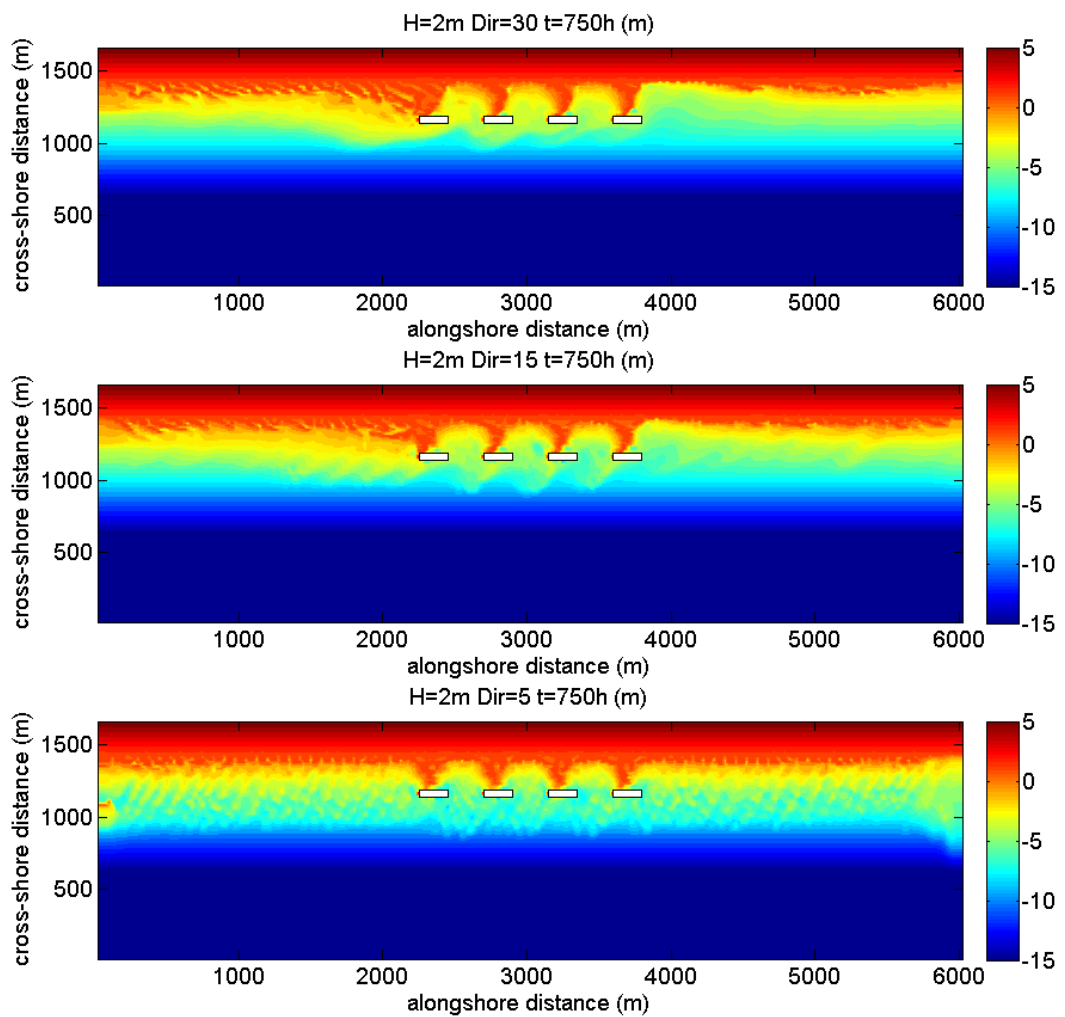


Figure 5.6. Bathymetric changes after 750h for cases S101 (top), S102 (middle) and S103 (bottom).

For the calm cases, Figure 5.7 represents the bathymetric changes for the different wave incidence angle. It can be see that the effect on the morphology is much smaller for $H=0.5\text{m}$ than for $H=2\text{m}$ as expected. S104 and S105 present some small salients at the lee of the breakwaters without forming full tombolos. For S106 the effect on the shoreline is limited, presenting only slight accretion right behind of each breakwater.

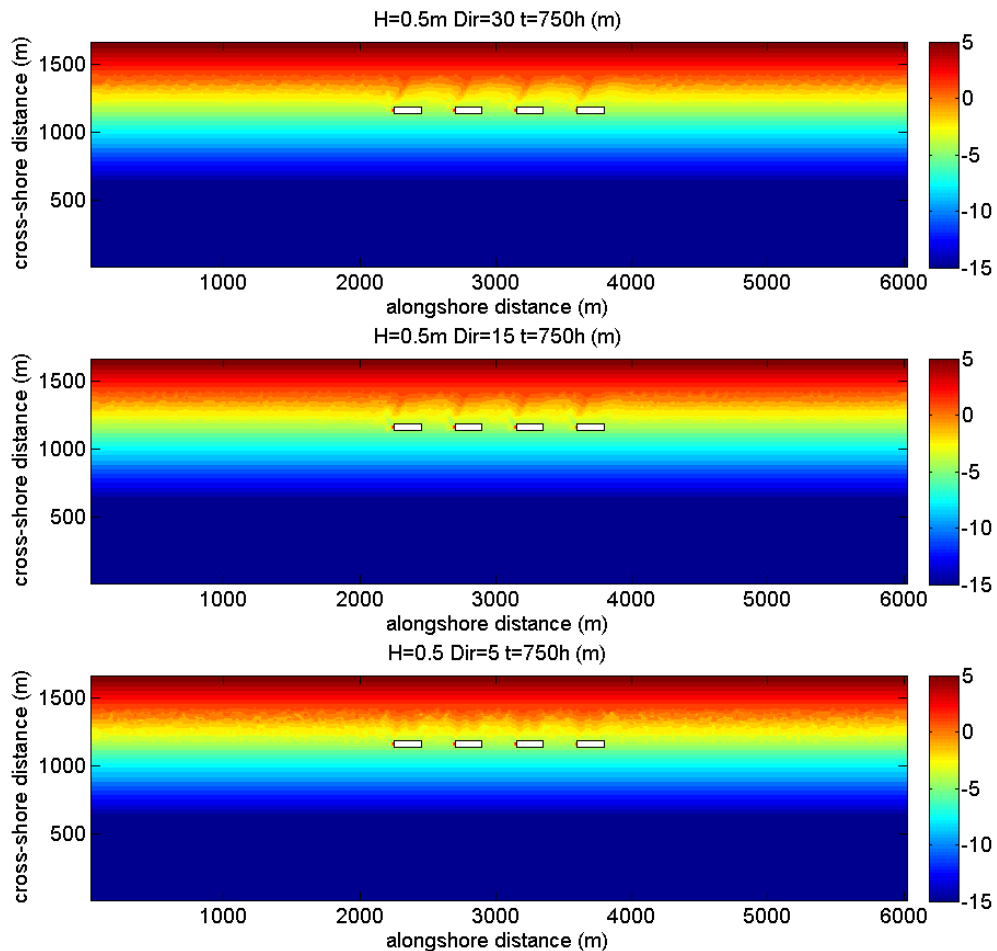


Figure 5.7. Bathymetric changes after 750h for cases S104 (top), S105 (middle) and S106 (bottom).

The rest of the figures shown in this document are based on the simulation S101 as is the one producing more significant changes in the domain and therefore are based on storm conditions under constant wave incidence angle.

Figure 5.8 represents the wave height at the start of the simulation and after 750h. This figure provides an idea on how the domain dynamically changes over time as the bathymetry changes.

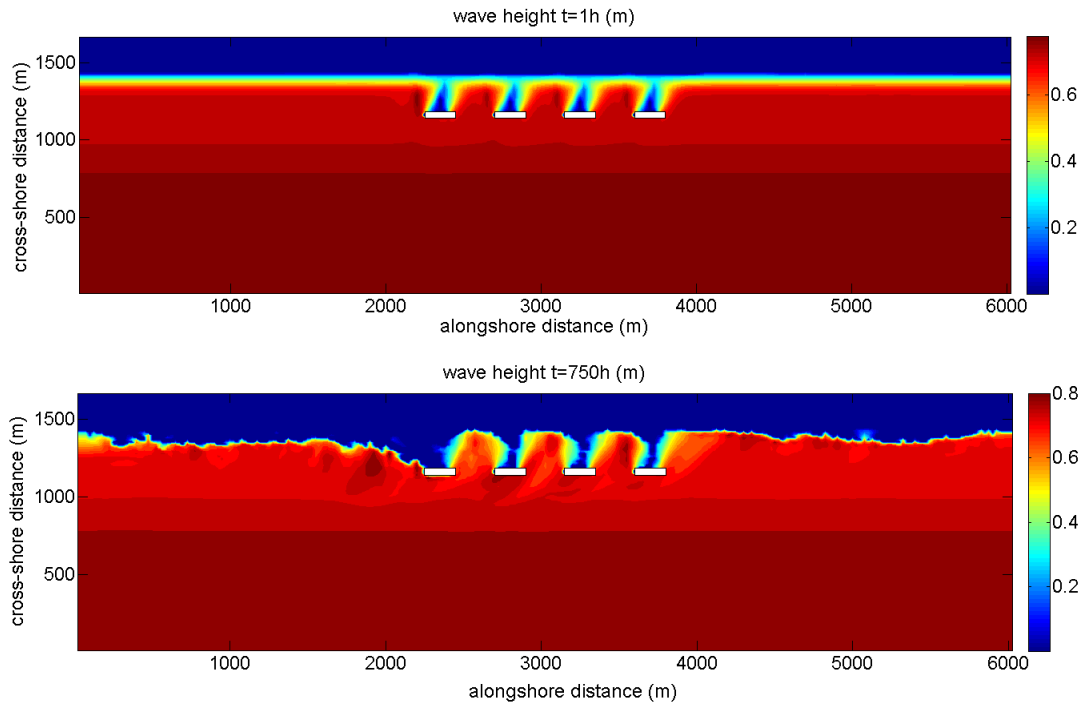


Figure 5.8. Wave height for $t=1h$ (top panel) and $t=750h$ (bottom panel).

Wave height is setup to 2m in the boundaries. It can be seen how the model successfully represent the effect of the breakwaters on the incoming waves, reducing their wave height behind them and therefore reducing the energy reaching the coastline. This disruption of the wave energy induces a disruption on the alongshore sediment transport rates. Figure 5.9 shows the alongshore sediment transport rates after 100h of simulation.

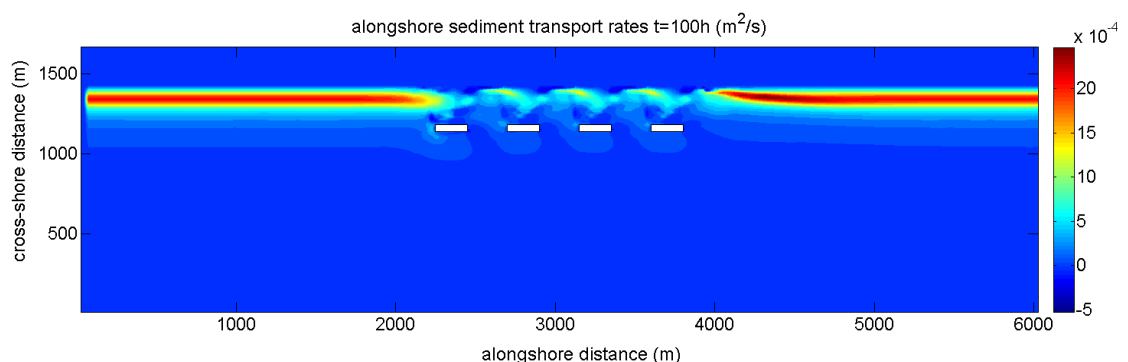


Figure 5.9. Alongshore sediment transport for $t=100h$.

Red values represent a high positive transport rate (left to right). It can be seen how on the left of the image, in the area unaffected by the breakwaters, the transport rate is constantly moving sediment towards the right of the domain. However, the wave height reduction induced by the breakwaters also reduces the sediment transport rates

behind those. It can be seen sediment transport rates are low right behind the breakwaters. This will cause sediment to settle and shoreline to advance towards the breakwaters forming salients or eventually tombolos. Also, it can be seen in the embayments some dark blue colour indicating sediment are travelling in the opposite direction (right to left). This is due the eddies formed in the embayment that cause the erosion in those areas. It is also remarkable that the higher values (dark red) is found at the right of the domain, after the last breakwater. This indicates that this area will be the most eroded one. These changes in the wave distribution and sediment transport rates, produces the bathymetry to change accordingly.

Figure 5.10 shows the bathymetry for $t=1h$ and $t=750h$. For $t=1h$ (top panel) it can be seen how the beach presents a perfectly even slope throughout the domain. After 750h (bottom panel) the beach morphology has changed significantly. Tombolos have developed behind the breakwaters due to the reduction on the sediment transport rates. Also, following the last breakwater, at the right of the domain, a large erosion area has developed, as indicated by the high sediment transport rate shown in Figure 5.9.

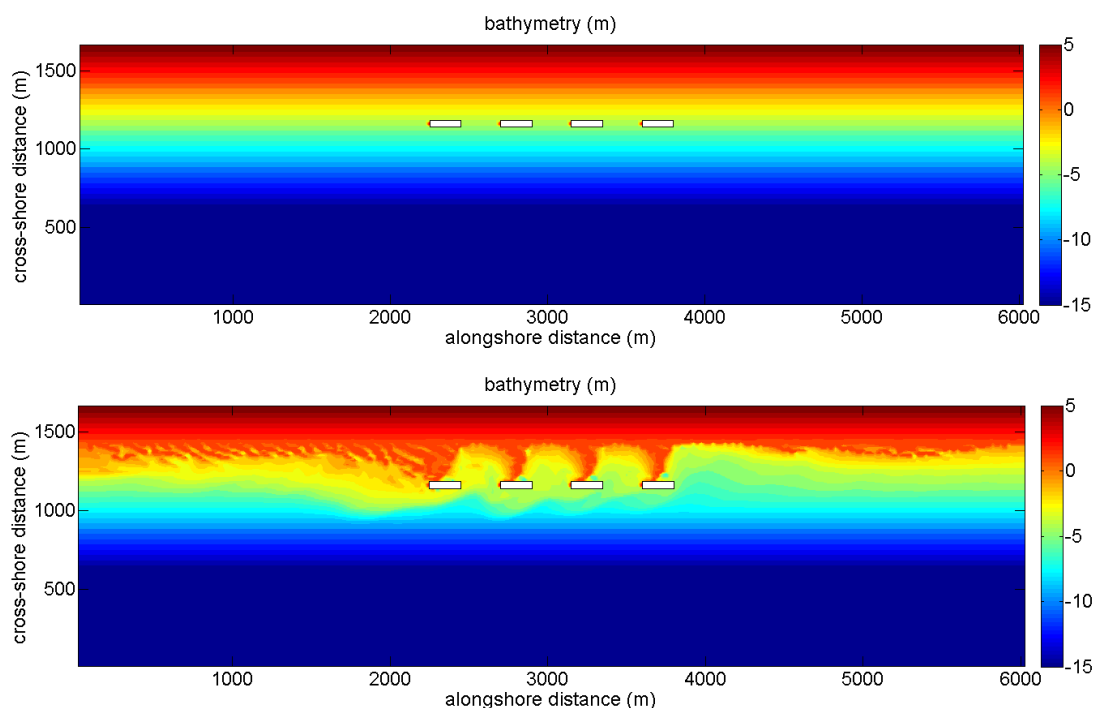


Figure 5.10. Bathymetry for $t=1h$ (top panel) and $t=750h$ (bottom panel).

Although COAST2D does not provide shoreline position directly, this can be extracted from the bathymetric changes. If shoreline is defined as the isoline with elevation

equal to 0m, shoreline can be extracted at any given time from the bathymetry results regardless what is the tide level, as coordinate z reference does not vary on time. For instance, shoreline extracted for the model for $t=750h$ is shown in Figure 5.11. Vertical axis has been referred to the initial flat shoreline to better understand the magnitude of the erosion and accretion.

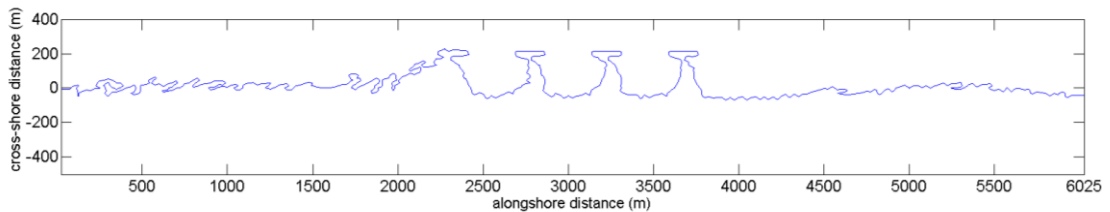


Figure 5.11. Shoreline for $t=750h$.

It can be seen that four tombolos have completely developed behind the breakwaters. Also, the first (left) tombolo is blocking the sediments creating a large accretion area. This feature was seen also at the Sea Palling scheme. This sand accumulation in the first tombolo is starving the rest of the domain generating the large erosion area following the last (left) breakwater.

Bathymetry changes can be also expressed as bed level changes. This variable measures the change in elevation (m) for each computational cell. Figure 5.12 represents the bed level changes for $t=750h$. Positive values (warm colours) represent accretion while negative (cold colours) represent erosion. It can be seen that bed level changes provides the possibility to directly assess whether the domain has suffered erosion or accretion.

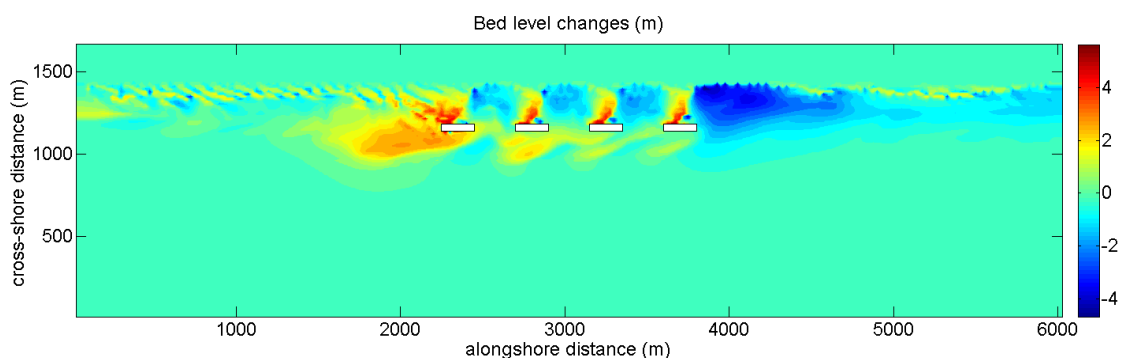


Figure 5.12. Bed level changes for $t=750h$.

5.3 DATA PREPARATION

To perform the EOF analysis in this study, data is obtained from the results of simulations carried out using a process-based numerical model. This provides not just high temporal and spatial resolution but also the possibility of studying different variables within the domain. As shown in the previous section, the temporal resolution available from the model is 1h interval and the spatial resolution is that provided by the grid, 25m alongshore and 15m cross-shore. This procedure overcomes one of the issues of EOF which is the data availability. Also, the possibility of controlling the hydrodynamic inputs allows studying with more precision the effect of the geometrical characteristics of the breakwater scheme. Each pair of spatial and temporal EOF component represents a certain percentage of the data variability. In this work the first four pairs of EOF components are enough to explain over the 99% of the total data variability. This value is higher to those seen in previous work as discussed in the Literature Review chapter (Fairley et al., 2009; Muñoz-Perez et al., 2001). This situation is expected due to the constant wave and tide conditions used in the model.

Different variables are studied in order to assess which one provides better results when applying the EOF method in order to identify the effects of shore-parallel breakwaters on the surrounding area of the schemes.

In order to study morphological changes in coastal areas by using the EOF method different approaches have been taken in the past. Some authors studied shoreline changes (Miller and Dean 2007a; Munoz-Perez et al. 2001; Fairley et al. 2009). In these cases the advance or recess of the shoreline is measured at different locations alongshore for different times. In such cases, rows in the F matrix represent the shoreline position for different times, from the first survey (row) to the last survey (row). In other cases, bed level changes were studied for a particular cross-section. In those cases, rows in matrix F represent the bed levels along the cross-shore profile for the initial time (first row) to the last survey (last row). Bed level changes, or volumetric changes have been used both in 1D (Losada et al. 1991) and 2D (Reeve et al. 2001; Reeve and Karunaratna 2011). Also, sediment transport rates could be potentially analysed via EOF method and the results can be used to describe morphological changes in the future. In this work, the three approaches were initially

considered. In this section a discussion of the proposed approach to study each variable and the difficulties as well as main findings are exposed.

5.3.1 Shoreline Changes

Shoreline position is an adequate indicator to study the effect that shore-parallel breakwaters have on the nearshore. As discussed in the literature review, the main purpose of these structures is to reduce the incoming wave-energy in order to produce a net advance of the shoreline, or an increase in the beach surface behind the breakwaters. Therefore, shoreline changes are a way to directly measure the impact of such structures. Although it is assumed that some erosion will appear on the embayments, the objective of breakwater schemes is to increase beach size behind the breakwater while limiting the erosion in the embayments and the edges of the scheme. Shoreline position provides direct information about that advance/recess of the beach face and therefore it is studied in this thesis. Shoreline variations have been studied via EOF method previously, both in open beaches (Munoz-Perez et al. 2001) and behind a shore-parallel breakwater scheme (Fairley et al. 2009). Nevertheless the increased temporal and spatial resolution provided by the model together with the possibility of controlling the hydrodynamics conditions are considered enough reason to justify this study.

Shoreline positions defined as lines with elevation $z = 0$ have been extracted from the model. EOF method requires the variable analysed to be bijective, $f(x_i)=y_i$ meaning that at each location x_i there is just un single value, y_i . When studying shoreline changes around coastal structures, sand spits are often formed. This fact represents an issue as sand spits represent a non-bijective value for the shoreline function. On the other hand, depending on the wave climate, salient might come close to a horn-shape form, colliding with the bijectivity condition. Finally, due to the complex currents pattern induced by the structures on the nearshore, small islands or sand formations can arise in front of the shoreline. When the shoreline reaches these islands the shape of the shoreline suddenly changes affecting the EOF results interpretation. Figure 5.13 shows an these issues schematically. They also can be seen in a modelled bathymetry data as shown in Figure 5.11.

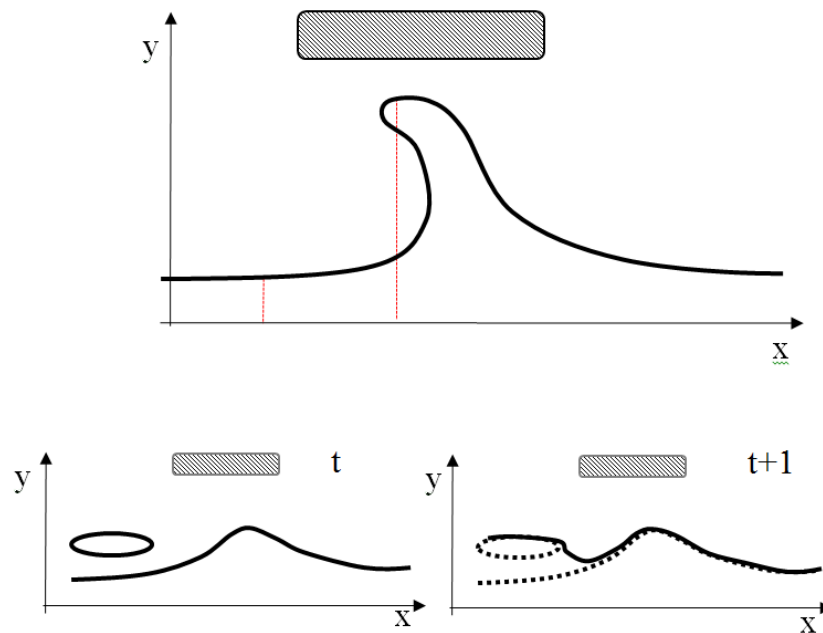


Figure 5.13. 1D shoreline changes issues. Horn-shaped salients (top panel). Shoreline discontinuous jumps.

The proposed methodology is intended to provide a general solution to different scenarios, regardless the wave conditions or the specific conditions for each study case. Solutions to these issues were looked for. However, they often rely in excessive simplification of the morphological changes adding imprecision to the whole analysis. Therefore, although shoreline changes remain the main variable that this thesis tries to identify, its direct analysis does seem to not be adequate for the above explained reasons.

5.3.2 Volumetric changes – alongshore sections

Cross-shore volume changes can be related to shoreline advance or recess using the one-line model concept as discussed in the literature review chapter. According to (Dean and Dalrymple, 2004) the movement of the shoreline position Δy can be described as:

$$\Delta y = \frac{\Delta V}{\Delta x} \frac{1}{B + d^*} \quad (5.1)$$

where B is the berm height and d^* the depth of closure previously defined. This equation can be simplified when Δx is equal to 1m and therefore $\Delta V(m^3)$ becomes

$\Delta S(m^2)$ per alongshore unit. Therefore at for particular section i the movement of the shoreline can be related to the surface change in that cross-section:

$$\Delta y_i = \frac{\Delta S_i}{B_i + d_i^*} \quad (5.2)$$

The numerical model provides bed level changes (unit volumetric changes) at each point of the domain for every time during the simulations. In the model, unit volumetric changes represent the change in elevation for each particular cell compared to the initial value and therefore is measured in meters. Multiplying the area of each cell (m^2) by the unit bed level changes (m) provides volumetric changes (m^3). For each time t the model provides a matrix named BLC with dimensions $BLC^t = [m \times n]$ containing a value for the unit volumetric changes. In order to analyse this data using a 1D EOF analysis while being able to use the equation mentioned before to reconstruct shoreline advance and recess the following procedure is followed.

At each time t , the values for the unit volumetric changes at each particular alongshore cross-section m are sum providing a single value, in meters, for each alongshore section m .

$$V_m^t = \sum_{n=1:L_y} BLC_{m,n}^t \quad (5.3)$$

Figure 5.12 showed the bed level changes map for $t=750h$. Such map, for example, would represent $BLC_{m,n}^{t=750h}$. When adding all the values per section, $V_m^{t=750h}$ is obtained. This is represented in Figure 5.14. It can be seen that the cumulative bed level changes gives an idea on when the domain is suffering erosion or accretion in each cross-section. The four peaks reaching between 40 and 60m represent the areas behind the four breakwaters, where sand is accumulated forming the tombolos. Following section 150 (following the last breakwater) a large erosion area is seen. This feature was suggested by Figure 5.9 and Figure 5.10 (bottom panel). However, it is more evident when looking at the cumulative bed level changes.

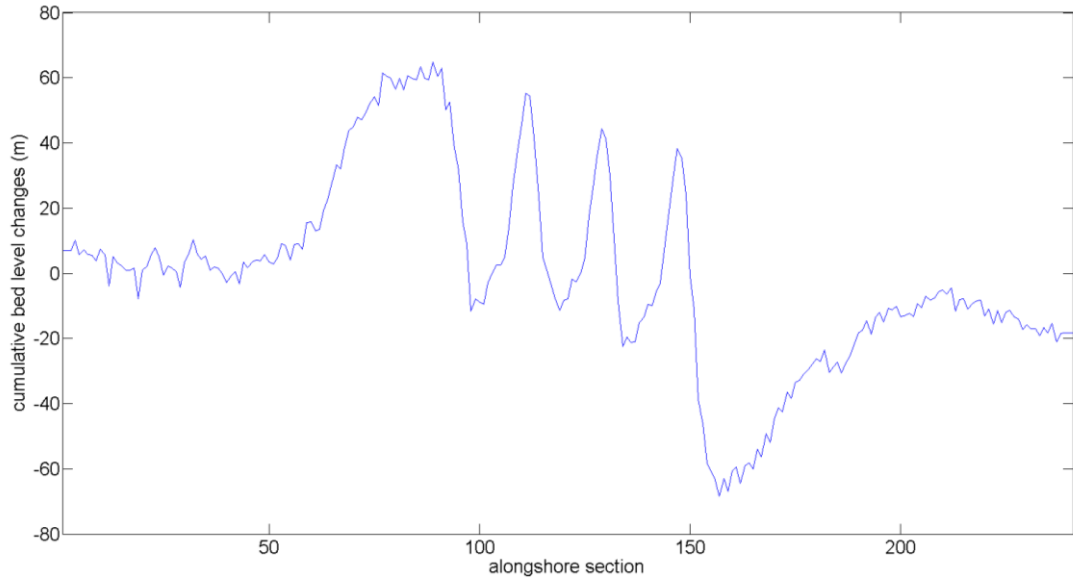


Figure 5.14. Cumulative bed levels per section for $t=750h$ at each section.

This process allows compressing a 2D variable, BLC , into a 1D variable, V being the sum of cross-sectional changes alongshore. Therefore, at each temporal step, a vector with dimensions $[1 \times n_x]$ is obtained. When repeating the process for all the considered outputs, T , a matrix F is conform with dimensions $F = [n_x \times T]$

$$F(m, t) = V_{m=1:dx:L_x}^{t=1:dt:T}$$

F is the matrix to be analysed by the EOF method. It has to be noted that the matrix F contains values for unit volumetric changes in meters. Matrix F is conformed by 241 columns, corresponding to each of the 241 alongshore sections, and 66 rows corresponding to each of the 66 time steps or surveys considered in this analysis. The standard EOF method is then applied to matrix F . The pairs of EOF components obtained (spatial and temporal) explain different amounts of variability as explained in Table 4.

Table 4. Percentage of variance explained by each component for the 1D unit volumetric changes 750h period analysis.

EOF analysis for 750h period	
component	(%)
1st	96.3
2nd	3
3rd	0.3
4th	0.1

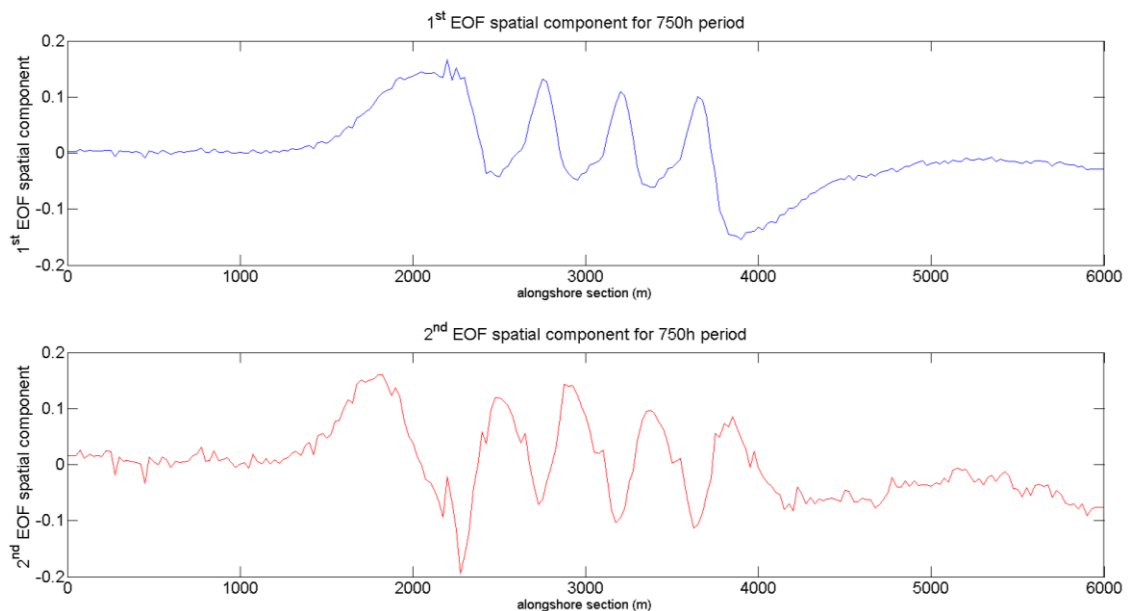


Figure 5.15. 1st and 2nd EOF spatial components for the 750h period analysis.

Figure 5.15 shows the first and second spatial components for the 750h analysis using the 1D unit volumetric changes. It can be seen how the first spatial component is similar to the shoreline changes that could be expected behind a set of shore-parallel breakwaters. For instance, at $x=2000\text{m}$, the spatial component present high values that correspond to the large accretion area that forms upstream the first breakwater. Similarly, around $x=4000\text{m}$ the low values of the 1st spatial component seem to indicate an erosion area downstream the last breakwaters.

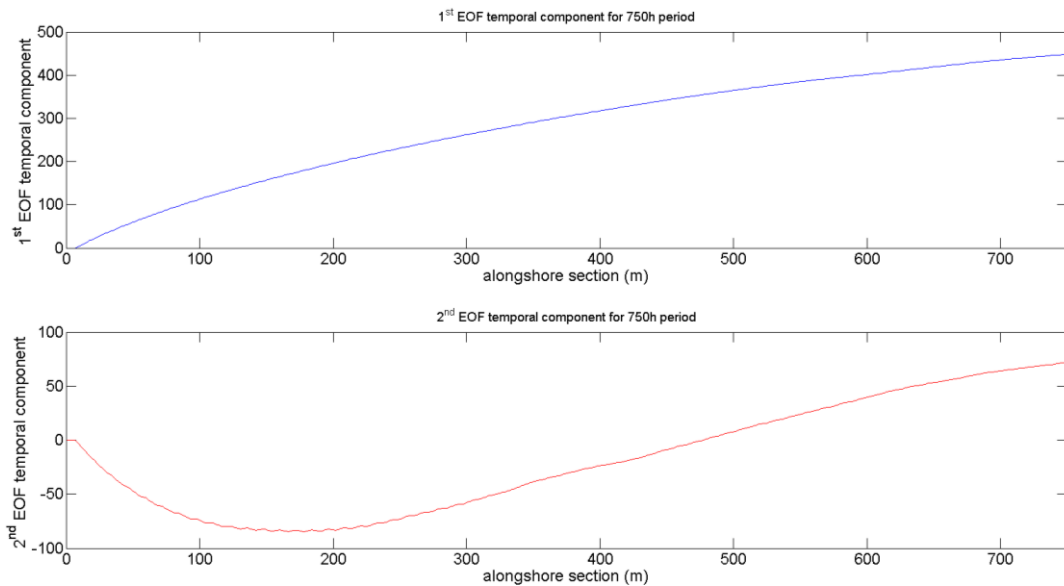


Figure 5.16. 1st and 2nd EOF temporal components for the 750h period analysis.

To understand the second spatial component, the second temporal component has to be assessed in conjunction. First and second EOF temporal components are shown in Figure 5.16. It can be seen that the second EOF temporal component (red) takes negative values initially and then changes to positive values. Considering this, the second EOF spatial component value around $x=1750\text{m}$ can be understood as a correction in the morphological pattern shown by the first component. Initially, the second spatial component is delaying the growth of the accretion area to add more accretion by the end of the simulation. This matches the observed behaviour as the first tombolo has to be completely developed before the mentioned accretion area starts increasing its size significantly. Similarly, the negative values for the second spatial component from $x=4000\text{m}$ to $x=6000\text{m}$ are negative only when the second temporal component becomes positive. This means that initially, the second component is not increasing the erosion in this area. Erosion increases only when the second temporal component becomes positive. This can also be related to the behaviour observed in the field, large erosion downstream the scheme will not start until the tombolos block most of the alongshore sediment transport.

When studying the bed level changes as a 1D variable all the cross-section information is compressed into a single variable and therefore this approach is not suitable to study changes within the cross-section itself. Section 5.3.3 describes the 2D approach which provides more details on changes across both alongshore and cross-shore dimensions.

In this study different values for the depth of closure are considered as the breakwaters modify the nearshore hydrodynamics and d_i^* cannot be supposed constant for the whole domain. Therefore, three different values are considered, 1) for the open sea areas, where the hydrodynamics are not affected by the presence of the breakwaters, 2) behind the breakwaters, where these represent a physical limitation to the shoreline advance and 3) in the embayments, where the currents generated in between the breakwaters affect the sediments movement. These three values are obtained from the model.

Table 5. Depth of closure values.

depth of closure (m)	
open coast	15
behind breakwaters	2.5
embayments	4.5

5.3.3 Volumetric changes – computational cells

In previous sections along this chapter different variables have been considered in order to assess the effects that shore-parallel breakwater produce in the nearshore. However, all of them were a simplified approach as they were trying to address a 2D process (morphological changes in a 2D domain) using 1D variables. In this case, bed level changes (volumetric changes) are studied as a 2D variable.

The numerical model provides bed level changes (unit volumetric changes) at each point of the domain for every time during the simulations. In the model, unit volumetric changes represent the change in elevation for each particular node compared to the initial value and therefore is measured in meters. For each time t the model provides a matrix with dimensions $BLC^t = [m \times n]$ containing a value for the unit volumetric changes. Therefore, if T surveys are considered to perform the EOF analysis, the matrix to be analysed would have dimensions $F = [n_x \times n_y \times T]$. In such case, F is a 3-dimensional matrix. In order to analyse this 2D variable by using the 1D EOF method procedure a dimension reduction is done as that proposed by Reeve et al.

(2008) so the 3-dimensional matrix $F_{nx,ny}^t$ becomes a 2-dimensional matrix $F_{nx \times ny}^t$. As a reminder, the domain is structured by nx nodes alongshore and ny nodes in the cross-shore direction.

$$\text{Therefore, } F_{nx,ny}^t = \left(\begin{array}{cccc} BLC_{1,1}^t & BLC_{1,2}^t & \cdots & BLC_{1,ny}^t \\ BLC_{2,1}^t & BLC_{2,2}^t & \cdots & BLC_{2,ny}^t \\ \vdots & \vdots & \ddots & \vdots \\ BLC_{nx,1}^t & BLC_{nx,2}^t & \cdots & BLC_{nx,ny}^t \end{array} \right)^{t=1:T} \quad \text{can be reduced as follows:}$$

$$F_{nx \times ny}^t = \left(\begin{array}{ccccccccc} BLC_{1,1}^1 & BLC_{1,2}^1 & \cdots & BLC_{1,ny}^1 & BLC_{2,1}^1 & \cdots & BLC_{2,ny}^1 & BLC_{nx,1}^1 & \cdots & BLC_{nx,ny}^1 \\ BLC_{1,1}^2 & BLC_{1,2}^2 & \cdots & BLC_{1,ny}^2 & BLC_{2,1}^2 & \cdots & BLC_{2,ny}^2 & BLC_{nx,1}^2 & \cdots & BLC_{nx,ny}^2 \\ \vdots & \vdots & \ddots & \vdots & \vdots & \ddots & \vdots & \vdots & \ddots & \vdots \\ BLC_{1,1}^T & BLC_{1,2}^T & \cdots & BLC_{1,ny}^T & BLC_{2,1}^T & \cdots & BLC_{2,ny}^T & BLC_{nx,1}^T & \cdots & BLC_{nx,ny}^T \end{array} \right)$$

The methodology explained above is illustrated with the following example. Figure 5.12 showed the bed level changes for $t=750h$ throughout the domain. That dataset can be expressed as a matrix 241×141 corresponding to time $t=750h$. The same data can be rearranged to a 1×26751 vector containing the same information for each cell. The final matrix, $F_{nx \times ny}^t$, will be formed by the equivalent vector for all the time steps considered.

The new matrix $F_{nx \times ny}^t$ can be analysed using the standard 1D EOF method described in Chapter 3. The EOF method will provide temporal components with dimensions $[1 \times T]$ and spatial components with dimensions $[1 \times nx * ny]$. Those spatial components are difficult to interpret in such form due to the transformation done performing the dimension reduction. In order to interpret the spatial components appropriately the inverse process can be done, converting those 1D spatial components into 2D spatial components.

Table 6. Percentage of variance explained by each component for the 2D unit volumetric changes 750h period analysis.

EOF analysis for 750h period	
component	(%)
1st	91.1
2nd	5.3
3rd	1.4
4th	0.7

Figure 5.17 and Figure 5.18 show the first and second spatial EOF component and temporal EOF components respectively.

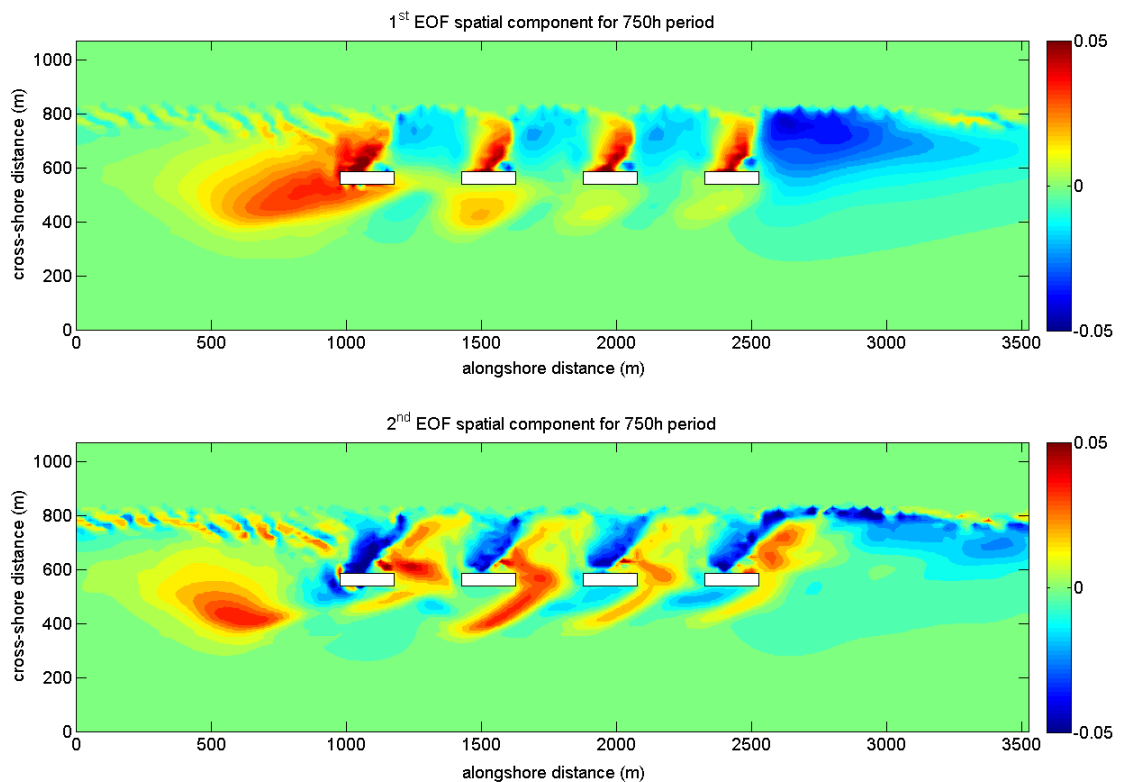


Figure 5.17. 1st and 2nd EOF spatial components for the 750h period analysis.

Figure 5.17 shows the first and second spatial EOF components for the 2D case for a 750h analysis. The behaviour shown in Figure 5.17 can be explained in the same way it was explained for the 1D case in Figure 5.15. However it can be seen comparing both figures how, the 2D nature of this case allows for a more detailed description. It can be

seen that for the 1D case a positive or negative value of the spatial EOF component was shown for the whole section while the 2D case shows that the same section can take both negative and positive values depending on the cross-shore location.

The first and second EOF temporal components shown in Figure 5.18 show a similar behaviour to that observed for the 1D case in Figure 5.16.

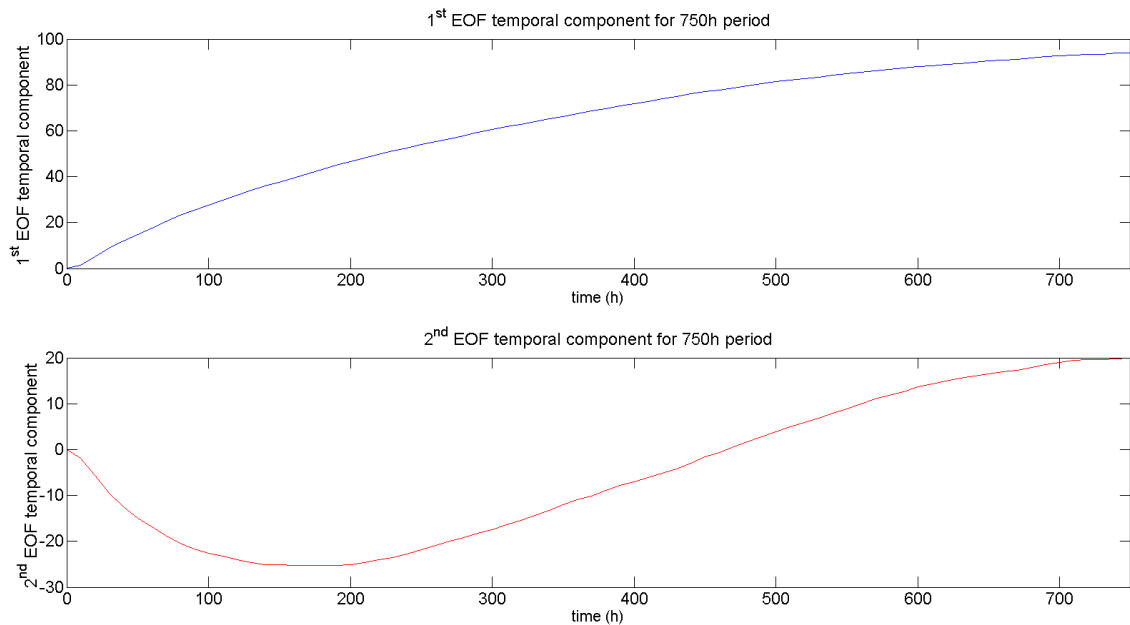


Figure 5.18. 1st and 2nd EOF temporal components for the 750h period analysis.

5.4 SUMMARY

COAST2D has been used to simulate morphological changes in an idealised domain containing a set of shore-parallel breakwaters under different wave conditions. Results show that COAST2D successfully represents the hydrodynamics and morphodynamics in these conditions. Results obtained from the model have been prepared in order to apply the EOF method which were shown to be more suitable to perform the EOF method. Volumetric changes have been selected as the more suitable variable to perform the Dynamic EOF method, both as a 1D and 2D variables. It has been seen that the 1D case is easy and quick to apply although some features can be overlooked when compressing the cross-shore variability into a single value. The 2D unit volumetric changes analysis offers the possibility to study in great detail the morphological changes surrounding these structures. It has also been shown how the EOF components can be successfully related to morphological features.

It has been seen that EOF components suggest that major changes in the system occur in the area directly behind the breakwaters. These results agree with the general overview in breakwater design where those structures are built to protect that region and therefore maximum considerations is paid to such region. However, a more detailed unit volumetric changes 2D analysis suggests that major changes both in the main mode (first component) and second mode (second component) actually occur at the edges of the breakwaters, as far as 1km down stream in this case. These results suggest that these areas should be considered to be as important as the area behind the breakwater itself.

6 DYNAMIC EOF ANALYSIS

6.1 INTRODUCTION

With the data generated from the COAST2D model, it is now possible to apply the newly developed dynamic EOF analysis. Tests were carried out in determining the most suitable variable to be used in the dynamic EOF analysis. It was found that the bed level changes provide the better representation of coastal morphological changes. Two approaches: (i) 1D and (ii) 2D are considered and explained in this section.

As described in the previous chapter, the simulation period is 1500h in total. It is decided that the data generated in the first 750h is used for the dynamic EOF analysis, and the results at the 1500h are used to validate the performance of the proposed approach. Extrapolated EOF components for $t=1500h$ are then used to reconstruct the bathymetric changes at that time. Reconstructed values are compared to modelled values in order to assess the validity and performance of the proposed methodology. In order to study the effect of extrapolating the spatial component, two different reconstructions for $t=1500h$ are done. One of them follows the same approach as that of other authors (Reeve et al. 2008; Horrillo-Caraballo et al. 2014) where only temporal component is extrapolated. The other applies the methodology explained in this chapter extrapolating both the spatial component and temporal EOF components. Then the new methodology can be assessed compared to modelled results and to extrapolated results using the current method. Given the percentages of variability explained by the EOF components both for the 1D and 2D approaches as shown in Table 4 and Table 6, only the 1st EOF components will be used to apply the Dynamic EOF method. However, the methodology could be extended to as many components as required.

6.2 1D APPROACH

For the 1D case, the dynamic EOF analysis is carried on the unit volumetric changes at each alongshore section in the sampling area, following the procedure described in Section 5.2.3. The training period consists on a total 750h with hourly outputs. Integrating the unit volumetric changes along the cross-direction gives the unit volumetric change at each alongshore section at 25 m spatial intervals and at hourly

output of the model results. The results provide a 241x750 data matrix for EOF analysis. However, in order to reduce the computation expenses and also to remove the uncertainty associated with the data at the early stage of the simulations, the data used for actual dynamic EOF analysis is a reduced data set: extending from the 100th hour to 750th hour at 10 h intervals. This constitutes a matrix of 241x66 data, which is consequently used to carry out the EOF analysis progressively. As a result, 66 sets of the EOF components can be obtained and the variations of the EOF components can be examined.

In total, this generates 241 data points in the alongshore direction. In the spatial domain, data is output at each alongshore section, accounting for a total of 241 sections every 25m intervals as described in Chapter 4. Section 5.2.3 applies the standard EOF method to this data set, analysing therefore a matrix with dimensions 241x750.

According to the methodology proposed in Chapter 3, EOF analysis has to be performed for a number of subsets within the training period. For this case 66 intervals are considered with a temporal gap of 10h between sub-intervals. Therefore the 1st subinterval considered covers 100h, the 2nd subinterval 110h, and so on until the 66th sub-interval covers 750h. The first interval is defined as 100h and no less to allow the system to accommodate the rapid morphological changes occurring during the first 100h of simulation.

For each of the 66 sub-intervals, the dimensions of the matrix to be analysed via EOF method varies from [100x241] for the 1st sub-interval to [750x241] for the 66th sub-interval. For each matrix the EOF method is applied as described in Chapter 3.

The methodology provides sets of spatial components for each sub-interval. In this case, the method provides 66 1st spatial EOF components, 66 2nd EOF spatial components and so on. Figure 6.1 shows a selection of the 1st spatial EOF components from the analysis at 100th, 200th, 300th, 400th, 500th, 600th and 700th hour for the sake of clarity.

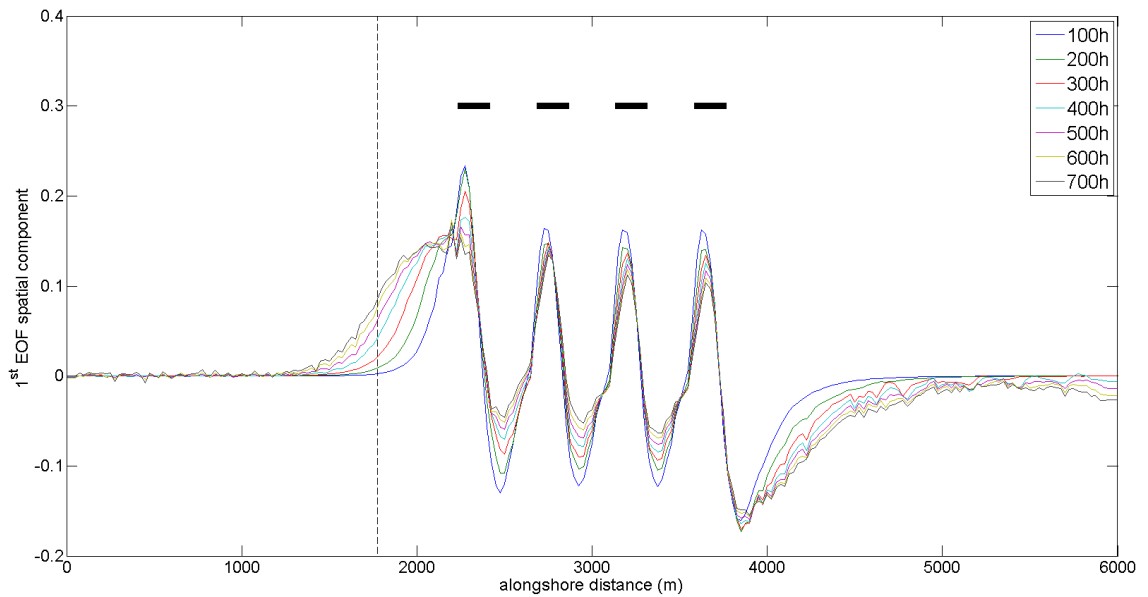


Figure 6.1. Samples of the 1st spatial EOF components for 66 analysis, 1D case.

The standard EOF method would produce one 1st EOF spatial components only and therefore temporal evolution of such component cannot be defined. The dynamic EOF method provides 66 1st EOF spatial components. This feature allows for defining the temporal evolution of the spatial components at each location of the domain. The black dashed line represents the alongshore Section 71 ($x=1775\text{m}$), the results at which will be discussed in detail.

Figure 6.2 shows the 66 values for the 1st EOF spatial component at section 71. This figure shows time in the x-axis and the EOF spatial component values in the y-axis. Therefore the evolution of the 1st EOF temporal component at section 71 can be now described.

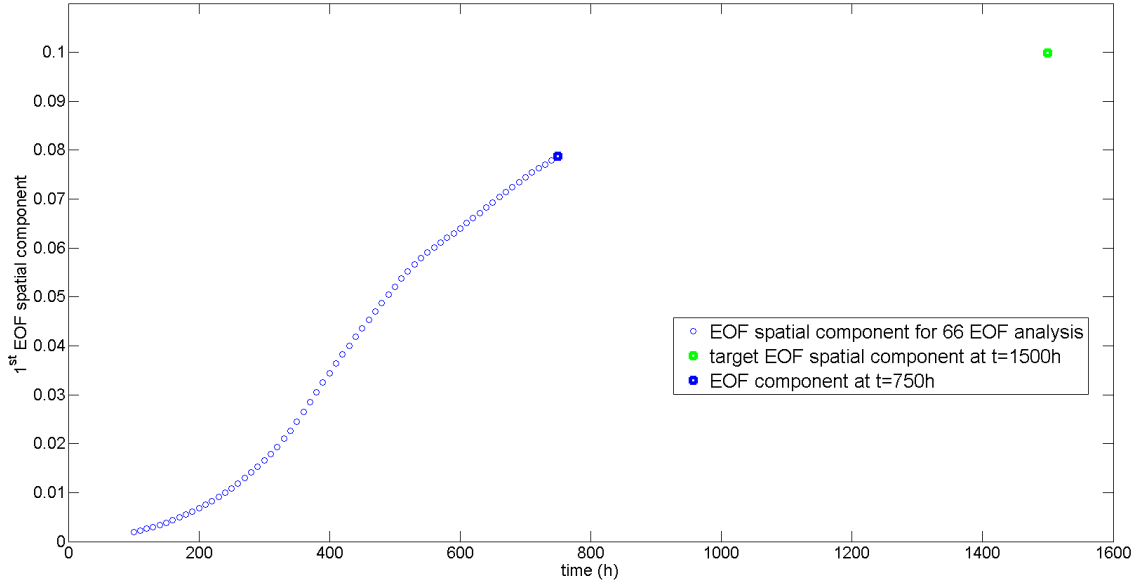


Figure 6.2. Temporal evolution of the first spatial EOF component at location $x=1775\text{m}$.

According to the proposed methodology a function $f_{i,p}$ can be found to fit the temporal evolution of the p spatial component for the section i . For the unit volumetric changes concerned in this case, it is expected that under the constant wave and tide conditions, the unit volumetric changes would trend to reach an equilibrium state. It can be supposed that the further from the equilibrium the system is, the faster it will evolve towards the equilibrium following an exponential behaviour. Therefore, mathematically, this function can be reasonably assumed to be exponential.

$$f(t) = \alpha_1 (e^{-\alpha_2 t} - 1)$$

Where function $f(t)$ represents the value of the spatial component at any given time t . Coefficients α_1 and α_2 are calculated for each section i and component p . Fitting is done using a non-linear least square solver supplied by MATLAB (version 2015b) which finds the coefficients $x = (\alpha_1, \alpha_2)$ by minimising the overall error:

$$\min \sum_h (f(x, xdata_h) - ydata_h)^2.$$

The numerical model provided hourly data for 750h. The Dynamic EOF method has been applied to the first 100h of results and to increasing intervals of 10h resulting on a total of 66 sub-intervals. Therefore a set of values out of the 66 points has to be selected in order to calculate the fitting coefficients α_1 and α_2 . A decision has to be

taken whether considering the 66 values or a reduced subset of those. In this case a subset of the last 40 values out of the 66 is considered. The reason to not choose the 66 values is that the initial values are changing quickly providing a worse fitting. Therefore just the last 40 points are considered for extrapolation.

Once the coefficients are found for each location independently, EOF components can be extrapolated beyond the training period $T=750h$, to the validation period $T_v=1500h$. An example of such extrapolation corresponding to Section 71 ($x=1775m$) is shown in Figure 6.3.

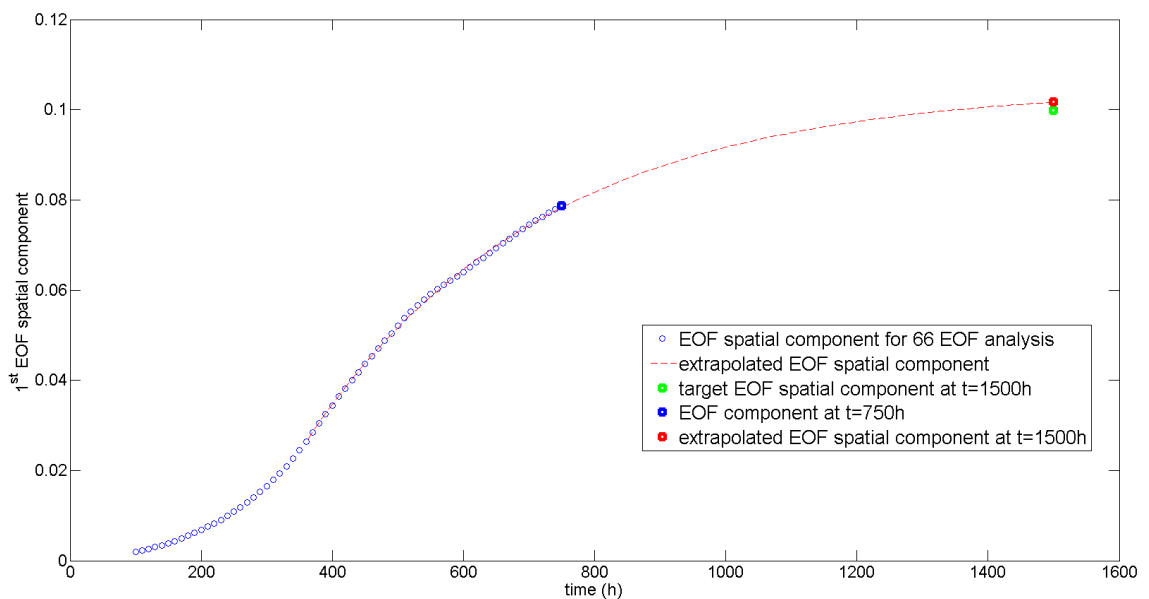


Figure 6.3. 1D extrapolation for section 71, $x=1775m$.

As seen in the Literature Review, EOF extrapolation techniques used to date extrapolate EOF temporal components only. In the example shown in Figure 6.3 standard EOF extrapolation techniques would consider the EOF spatial component value obtained for the training period $t=750h$, with a value of $X_{750}=0.07872$ represented by the bold blue circle. However, it can be seen that the actual calculated EOF spatial component at $t=1500h$ takes a value of $X_{1500}^{measured}=0.09984$ as represented by the green square. Therefore, if no extrapolation is performed for the EOF spatial component the error assumed would be a 22%. When EOF spatial component is extrapolated using the dynamic EOF method, a value of $X_{1500}^{extrapolated}=0.1017$ is obtained as represented by the red square, reducing the error to 1.8%. The same

methodology is applied to each of the 241 alongshore section and EOF spatial component can be then reconstructed for the whole domain at $t=1500h$. Figure 6.4 shows the 1st EOF spatial component for $t=750h$ (blue line), and the measured (green line) and extrapolated (red line) 1st EOF components for $t=1500h$.

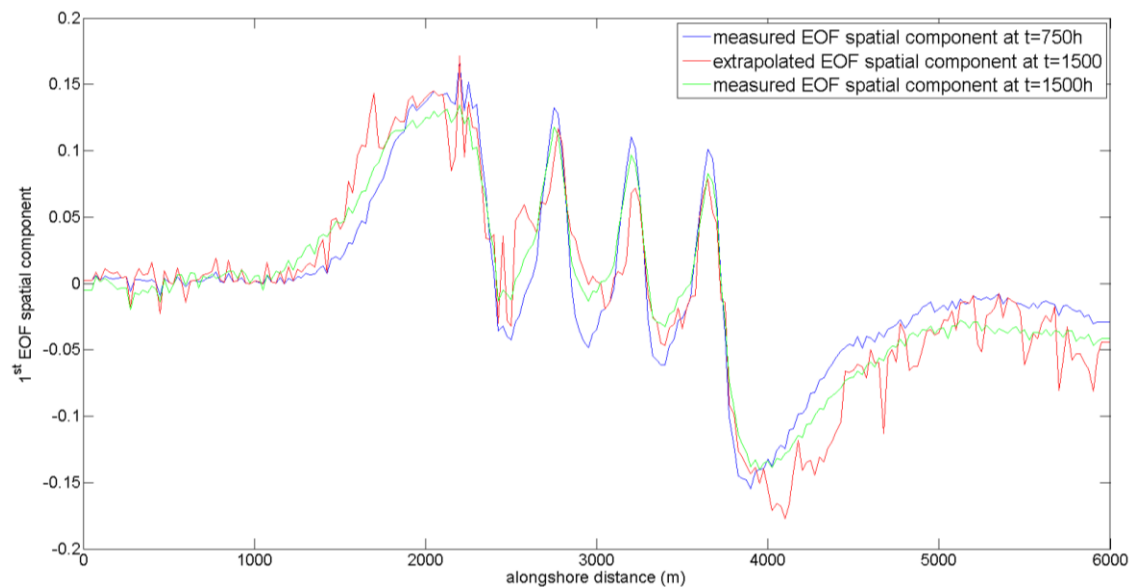


Figure 6.4. 1st EOF spatial component extrapolation using the Dynamic EOF method.

The measured evolution of the EOF spatial component is represented by the differences between the blue and the green lines. From $x=1000m$ to $x=2000m$ it can be observed an increase in the EOF spatial value. This area corresponds to the upstream area. For the surrounding areas to $x=2500m$, $x=2900$ and $x=3300m$ corresponding to the three embayments, the EOF spatial component values have also increased from $t=750h$ and $t=1500h$. Finally, in the last section, from $x=4000m$ to $x=6000m$ the EOF spatial component has reduced its value. It can be seen, that the extrapolated EOF component for $t=1500h$ (red line) shows the same behaviour than the measured EOF component at $t=1500h$, which in turn, shall provide a better reconstruction of the variable in study. If no spatial extrapolation is performed, the above mention changes will not be accurately represented by the reconstructions. It can be seen in Figure 6.4 that the results provided by the Dynamic EOF method on this variable are noisy. A smoothing technique could be applied. However, results are shown without any filtering to highlight the issues with the 1D approach and its limitations on the extrapolation techniques used. This method has been greatly improved in Section 6.3 for the 2D analysis and this figure can be used as a comparison.

As discussed in Section 3.3.2 the EOF temporal extrapolation has been classically performed by directly extrapolating the EOF temporal component obtained for the training period. Figure 6.5 shows the 1st EOF temporal component obtained for different subintervals within the training period.

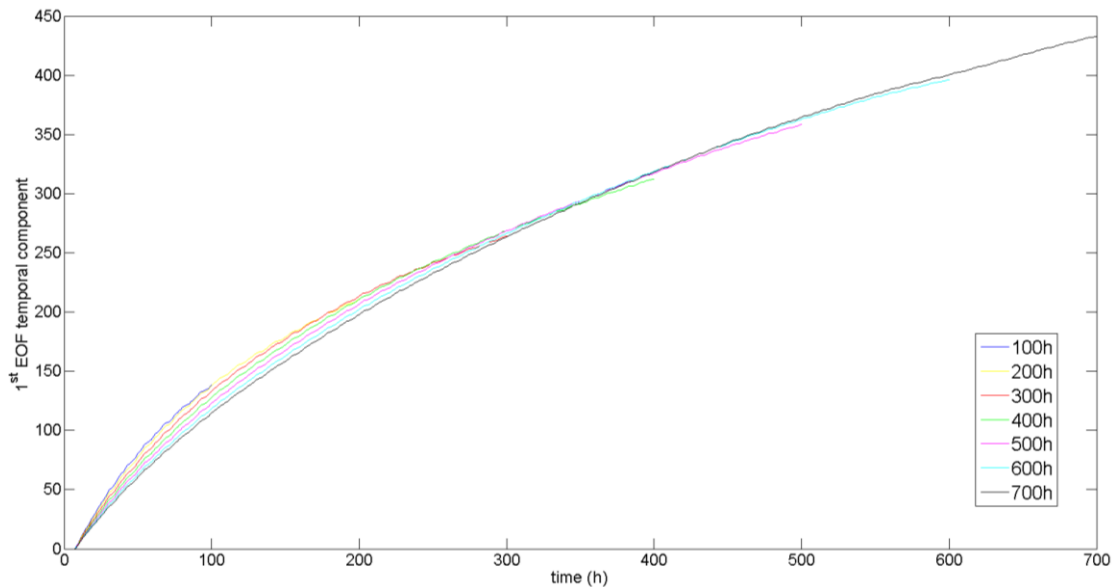


Figure 6.5. 1st EOF temporal component for different sub-intervals.

Figure 6.6 shows the EOF temporal extrapolation performed using the standard method (top panel) vs the EOF temporal component extrapolation using the dynamic EOF method. For the classic extrapolation, the EOF temporal component obtained for the whole training period, 750h, is directly extrapolated. For the dynamic EOF method, the last value of the EOF temporal component obtained for each subinterval within the training period are used for extrapolation.

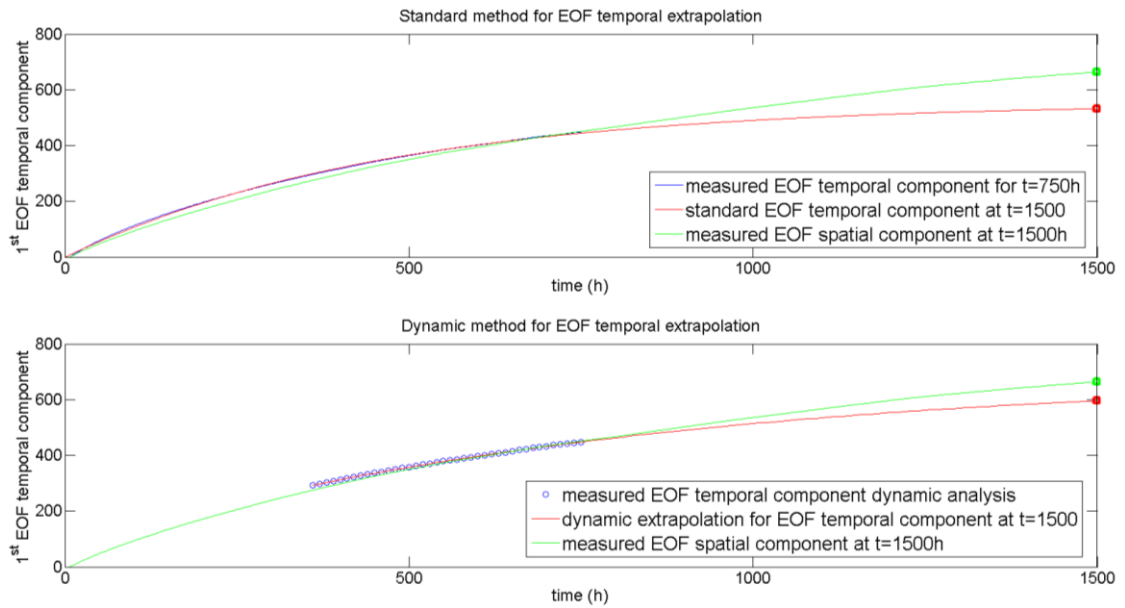


Figure 6.6, 1st EOF temporal component extrapolation. Standard method (top panel). Dynamic EOF method (bottom panel).

Table 7 summarised the key numbers shown in Figure 6.6. The measured temporal component at $t=1500\text{h}$ takes the value 664.5, this is the target value for the extrapolation techniques. The standard extrapolation techniques provides a value of 532.5 at $t=1500\text{h}$ which represents an error of 20%. The dynamic EOF extrapolation method provides a value 596.6 representing an error of 10.3%.

Table 7. 1st EOF temporal component values for 1D unit volumetric changes.

1st EOF temporal component at $t=1500\text{h}$	Value	Error (%)
Measured	664.5	
Standard extrapolation	532.5	20
Dynamic EOF extrapolation	596.6	10.3
Measured at $t=750\text{h}$	448.2	32.5

It can be seen that the dynamic EOF method yields better results for temporal extrapolation obtained a value closer to measurements for $t=1500\text{h}$. Once both temporal and spatial components are extrapolated to $t=1500\text{h}$, unit volumetric changes values can be reconstructed at that time.

In order to compare results, reconstructions are done following the standard EOF extrapolation method and the dynamic EOF method. Numerical model simulations are

carried out up to 1500h, so reconstruction can be compared with the actual modelled results.

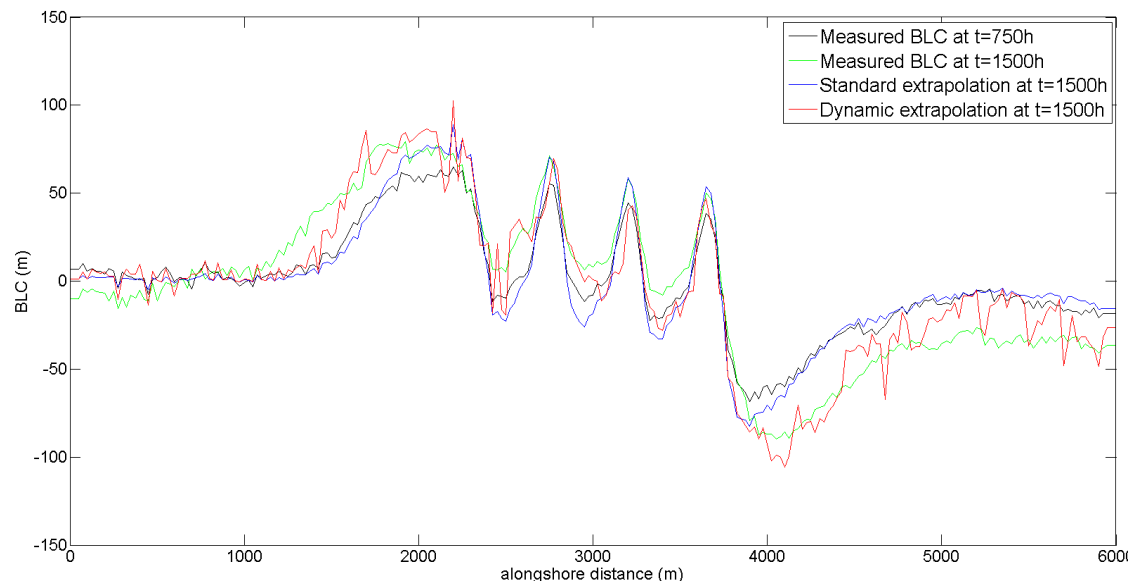


Figure 6.7. 1D unit volumetric changes extrapolation using standard method (blue line) and dynamic EOF extrapolation (red line).

Figure 6.7 shows the measured unit volumetric changes at $t=750h$, $t=1500h$ and extrapolated at $t=1500h$ using the standard and the Dynamic EOF method. It can be seen how the Dynamic EOF method extrapolation (red line) is closer to the measured unit volumetric changes (green values) especially in the upstream area, the downstream area and also in the embayments. The standard extrapolation technique fails to represent the larger erosion area produce between $t=750h$ and $t=1500h$ in the downstream area. However, the Dynamic EOF method is able to cope with these features representing them accurately.

It can be seen in Figure 6.7 that the Dynamic EOF method show, in some areas, error of up to 20%. This error can be magnified when reconstructing the shoreline position. As discussed before, this is another sign of the limitations, not of the Dynamic EOF method per-se but of the simplistic extrapolation techniques used in the 1D approach. These techniques have been refined for the 2D approach showing better results.

Unit volumetric changes can be used to define shoreline changes as defined in Section 5.3.2. Figure 6.8 shows the measured shoreline at $t=1500h$ and the reconstruction shoreline at $t=1500h$ using the extrapolated EOF components for unit volumetric

changes. Prediction fits reasonably well especially in the upstream and downstream areas. Fitting is worse than that seen in Figure 6.7 for unit volumetric changes, especially at the embayments. This can be explained by some of the unit volumetric changes in the embayment section happening further offshore and not actually contributing to the advance of the shoreline.

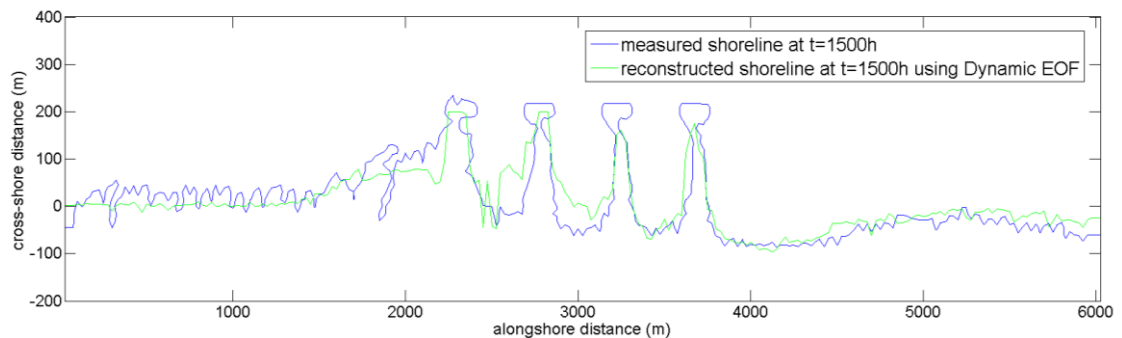


Figure 6.8. Measured vs reconstructed shoreline at $t=1500h$ using extrapolated EOF components.

These results show one of the limitations of applying the 1-line formulation for the complex case of shore-parallel breakwaters. Defining the depth of closure for a shore-parallel breakwater system is not trivial. A simple approximation was done in this study with only 3 different values. However further investigation should be carried out in order to explore in detail the depth of closure for a scheme of shore-parallel breakwaters. Definition of the depth of closure behind shore-parallel breakwater is complex and is beyond the scope of the thesis.

The 1D methodology described in this section was presented in the International Conference on Coastal Engineering, 2014 (Alvarez et al., 2014). In such case the training period was 1000h and results were extrapolated up to 2000h. Also the number of sub-intervals considered was different. In the presented section, the same methodology has been followed although the number of sub-intervals as well as the training period has been changed in order to make it consistent with the study carried out for the 2D case and presented in the next section.

The approach considered in this section, follows the core idea of the proposed methodology although it has some limitations when finding the extrapolation functions and coefficients. For instance, just exponential function has been considered. Although in an open beach under constant wave conditions the beach will evolve towards and

equilibrium position following an exponential behaviour, this might not be the case for each alongshore section when studying morphological evolution behind a set of shore-parallel breakwaters. Therefore other functions might be considered. Also, a constant number of surveys were used to find the fitting coefficients (40). That value is considered by the user based on the individual study of some particular sections but does not respond to a systematic analysis on what number of surveys should be considered. Nevertheless, this approach has proven to be computationally fast, easy to apply and to interpret.

6.3 2D APPROACH

In this section the proposed methodology for EOF components extrapolation is applied to a 2D variable. The variable in study represents bathymetric changes at each node in a 2D domain as explained in chapter 4. In order to conduct the EOF analysis for the 2D variable, a dimension reduction is applied (Reeve et al., 2004), the reader is referred to Chapter 4 for further details. The purpose of this analysis is not just to study the results on a 2D variable but to improve the methodology application presented in the previous section by tackling some of the limitations there exposed.

In order to produce consistent results, the number of surveys considered and the gap between surveys are similar to those used in the 1D case explained in the previous section. However, as explained in Chapter 4, for the 2D variable study not the whole domain (241 by 111) is studied and a reduced domain only (142 by 72) is analysed via EOF method.

The number of matrices to be studied is therefore equal to 66 and dimensions vary for each sub-interval. Due the dimension reduction, from 2D to 1D, data for every time step consisting in a 142 by 72 matrix will be transformed to a 1 by 10224 vector. Therefore the dimensions of each sub-interval vary being [100×10224] for the 1st sub-interval and [750×10224] for the 66th sub-interval. These matrices are considerably larger than those for the 1D case. For instance the larger matrix for the 1D contains $750 \times 241 = 180750$ elements whereas the largest matrix for the 2D case contains $750 \times 10224 = 7668000$ elements. Nevertheless, a regular desktop can solve the 66

EOF analysis on these matrices in a reduced amount of time (hours), and therefore the computational cost is not a limitation as it could be discussed.

The methodology provides a set of 66 spatial components. In order to be able to understand and interpret the spatial components provided by the method, the dimension reduction has to be reversed. The EOF components are transformed from the 1D form provided by the EOF method to the 2D shape, revering the changed done before performing the EOF method. As a result, EOF spatial component are no longer a 1D variable along one axis, but a 2D field as shown below:

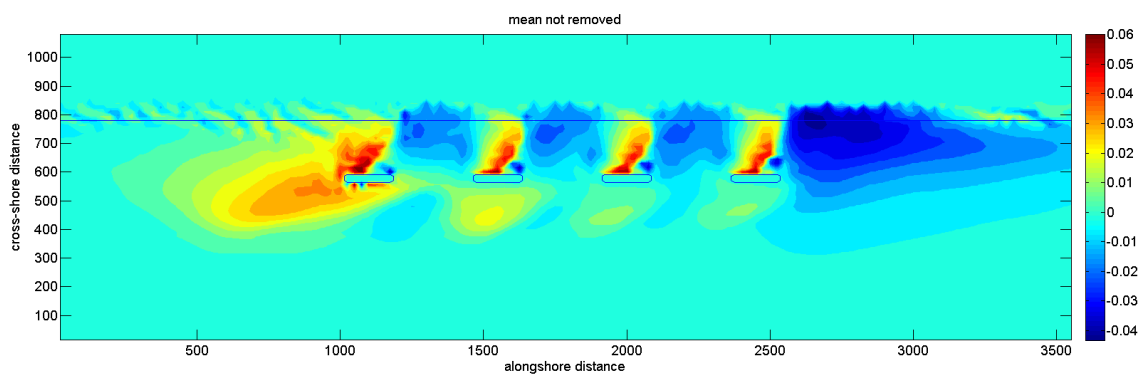


Figure 6.9. First EOF component as 2D for the 750h period analysis.

Therefore, for each location of the 2D domain the value for the spatial component has been calculated for 66 different sub-intervals and thus its temporal evolution can be studied in detail. Figure 6.10 provides an example of such evolution for a specific location.

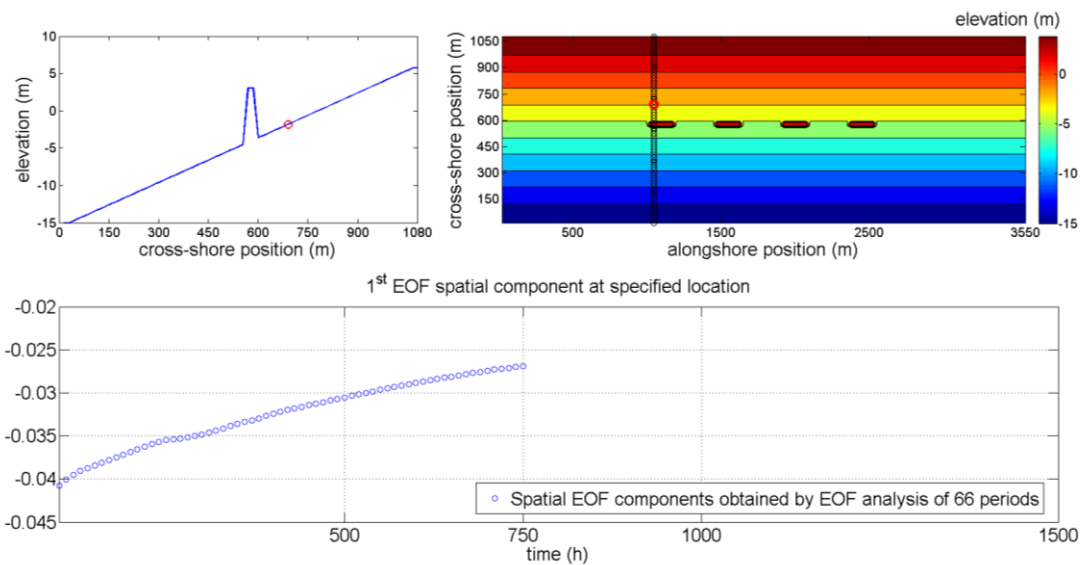


Figure 6.10. 1st EOF components for 66 analyses at one particular location.

Figure 6.10 shows a clear trend in the EOF spatial component value. The problem to be solved is to fit such evolution into a function. In the 1D case, exponential function only was considered according to the equilibrium profile concept. While the equilibrium profile concept can be applied to the evolution of a whole cross-shore section, it might not be a valid hypothesis when studying individual locations in a 2D spatial domain governed by shore-parallel breakwaters.

The location within the 2D domain used to plot Figure 6.10 differs from that used in Figure 6.1 for the 1D domain. The reason is that Figure 6.10, showing an exponential behaviour is intended to be compared with Figure 6.12 that shows a clearly linear behaviour. Also an specific location of the 2D domain cannot be directly compared with any of the cross-section of the 1D case, as the locations in the 1D case represent the whole cross-section and not individual values within the cross-section.

It should be noted that there are 10224 points within the domain and finding a unique fitting system that suits every point is a complex task. For such reason, in this case, linear behaviour is also considered as it was done previously in Reeve et al., Reeve et al. (2008). According to the EOF method, the temporal and spatial components are independent. This assumption implies spatial change is independent from temporal changes. The functions considered in this section to fit the temporal evolution of the spatial components are:

$$f^1(t) = \alpha_1^1 (e^{-\alpha_2^1 t} - 1) \text{ and } f^2(t) = \alpha_1^2 \cdot t + \alpha_2^2$$

where functions f^1 and f^2 are the exponential and linear functions chosen to fit the spatial component, $\alpha_1^1, \alpha_2^1, \alpha_1^2, \alpha_2^2$ are the coefficients to be found and t represents the time

Fitting for f^1 is done using a non-linear least square solver supplied by MATLAB (Matlab R2015b) which finds the coefficients $x = (\alpha_1^1, \alpha_2^1)$ that minimise

$$\min \sum_h (f(x, xdata_h) - ydata_h)^2$$

Fitting for f^2 is done using a polynomial curve fitting supplied by MATLAB (Matlab R2015b) that also uses a least squares method to find the coefficients $x = (\alpha_1^2, \alpha_2^2)$. As it was discussed in the 1D section, a set of values has to be selected in order to calculate the fitting coefficients. In the 1D case, a fixed subset of the last 40 points was considered for every location. This procedure was recognised as one of the limitations of the 1D approach presented before. In order to overcome such limitation, four different subsets are considered, including the last 60, 50, 40, 30 and 20 points of the 66 possible. This decision tries to tackle the issue posed by the high spatial variability observed in the 2D domain.

This approach yields to a total of eight possible functions for each location:

$$f_{20}^1, f_{30}^1, f_{40}^1, f_{50}^1, f_{60}^1, f_{20}^2, f_{30}^2, f_{40}^2, f_{50}^2, f_{60}^2$$

In order to choose the most suitable fitting, correlation coefficient between each of those fittings and the corresponding data are calculated. The function providing the best correlation coefficient is then chosen to extrapolate the EOF spatial components beyond the training period $T=750h$. This approach not only finds the best possible fitting but also help us understanding the behaviour of the system. It can be plotted which fitting has been chosen for each location, which help understanding which areas

follow an exponential or linear behaviour but also, depending on the number of points selected, which areas are more stable than others.

Figure 6.11 shows an example where f_{50}^1 was chosen to extrapolate the 1st EOF spatial component. It can be seen that the EOF spatial component value for the training period is $X_{750}^{measured} = -0.02686$. The EOF spatial component value for validation period is $X_{1500}^{measured} = -0.0224$ (red square). Therefore, if spatial extrapolation is not performed, the error at this location would be 19.9%. The extrapolated EOF spatial component value is $X_{1500}^{extrapolated} = -0.02391$ (black square) representing an error of 6.7%. Therefore, for this particular location, using the extrapolated EOF spatial component will produce a closer value to the actual component for the same time.

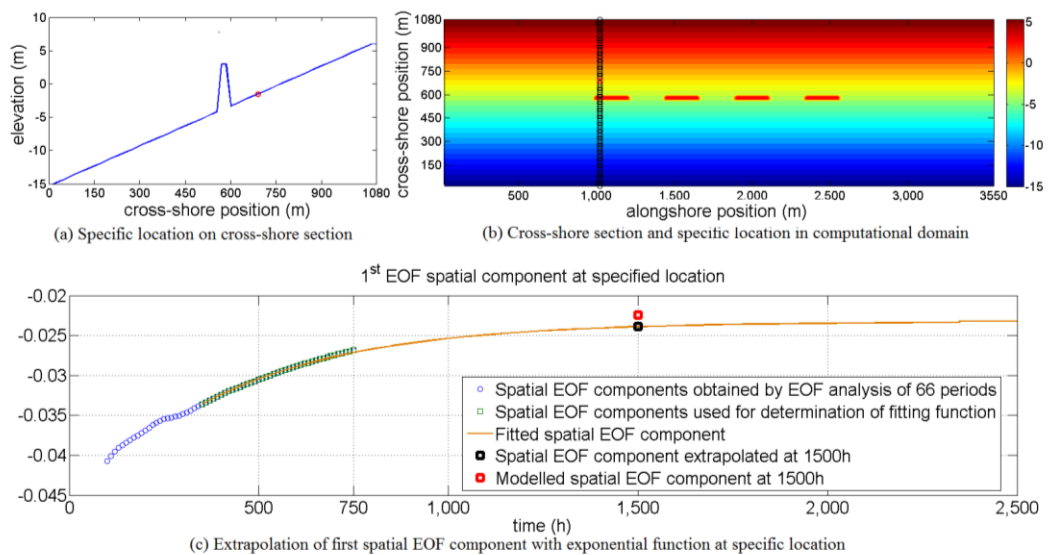


Figure 6.11. Example of exponential extrapolation with 50 points.

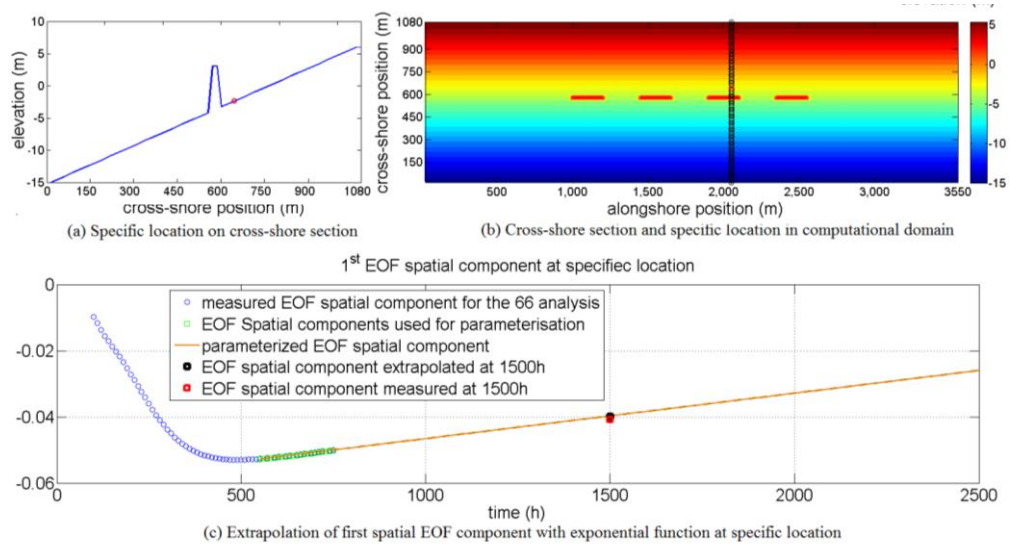


Figure 6.12. Example of linear extrapolation with 20 points.

Figure 6.12 shows an example of linear extrapolation using 20 points only, f_{20}^2 . The extrapolated value (black square) is $X_{1500}^{extrapolated} = -0.03989$ almost identical to the target value (red square) $X_{1500}^{measured} = -0.04086$ producing an error of 2.4%. In this case, the no extrapolation method would be assuming an error of 22.7% as $X_{750}^{measured} = -0.05014$.

The proposed methodology is applied individually to each of the 10244 points within the domain. Once the coefficients providing the highest correlation coefficients are found for each location, if such coefficients are higher than the correlation threshold, R_t , components can be extrapolated beyond the training period T , to the validation period $T_v = 1500h$. Figure 6.13 shows the 1st EOF temporal component for the 750h training period (top panel), the measured 1st EOF component for the validation 1500h period (middle panel) and the extrapolated 1st EOF component at $t=1500h$.

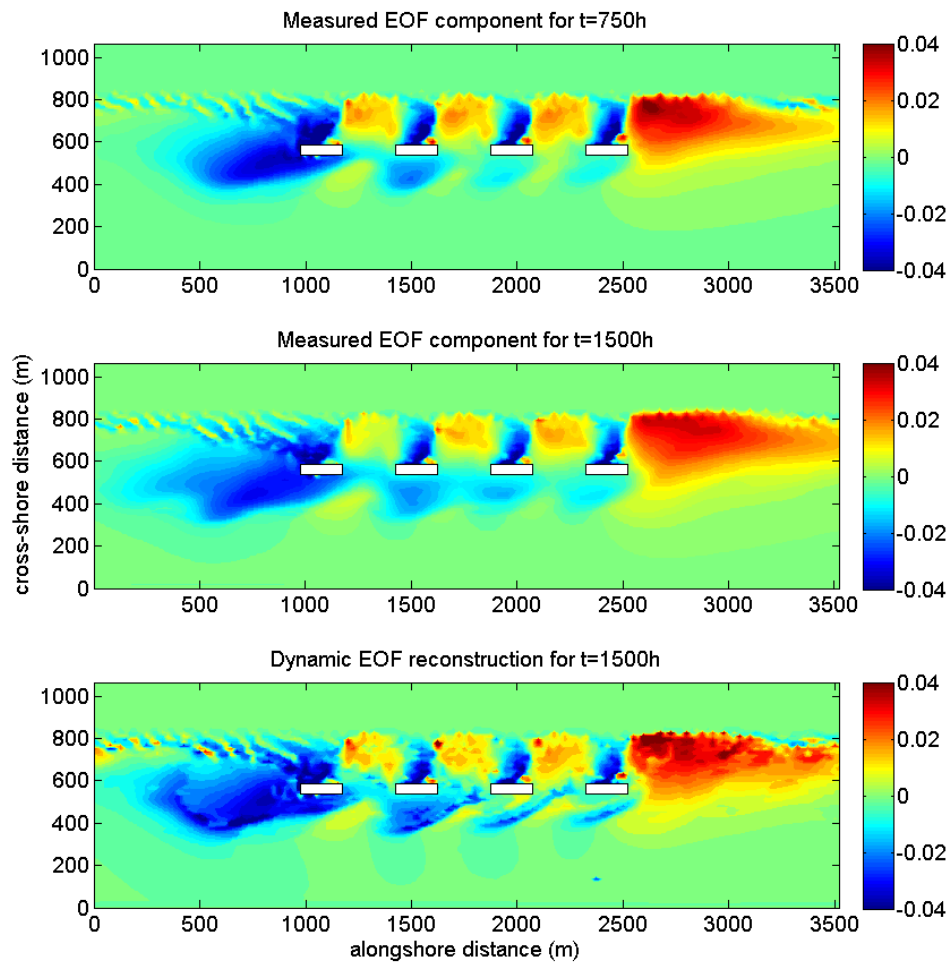


Figure 6.13. Dynamic EOF extrapolation for the 1st EOF spatial component in 2D.

From top to middle panel it can be seen that the 1st EOF component has evolved. The low values area in the upstream zone has extended further offshore and further to the left. The high values area in the downdrift zone has also extended further to the right. The low values just offshore the breakwaters have expanded almost connecting together. All these changes will not be reflected in the reconstruction using the standard EOF extrapolation method where the EOF spatial component obtained for $t=750h$ is used for reconstruction at $t=1500$.

However, the bottom panel shows the extrapolated EOF component at $t=1500h$ using the Dynamic EOF method. It can be seen that it is closer to the obtained EOF spatial component at $t=1500h$ representing all the features mentioned in the previous paragraph. To clearly assess to what extent the extrapolated EOF spatial component at $t=1500h$ is closer to the actual EOF component measured at $t=1500h$ than the measured EOF component at $t=750h$ some statistics are calculated.

Figure 6.14 represents the error (%) between the extrapolated and measured EOF spatial component at $t=1500h$ (top panel) vs the measured at $t=750h$ and measured at $t=1500h$.

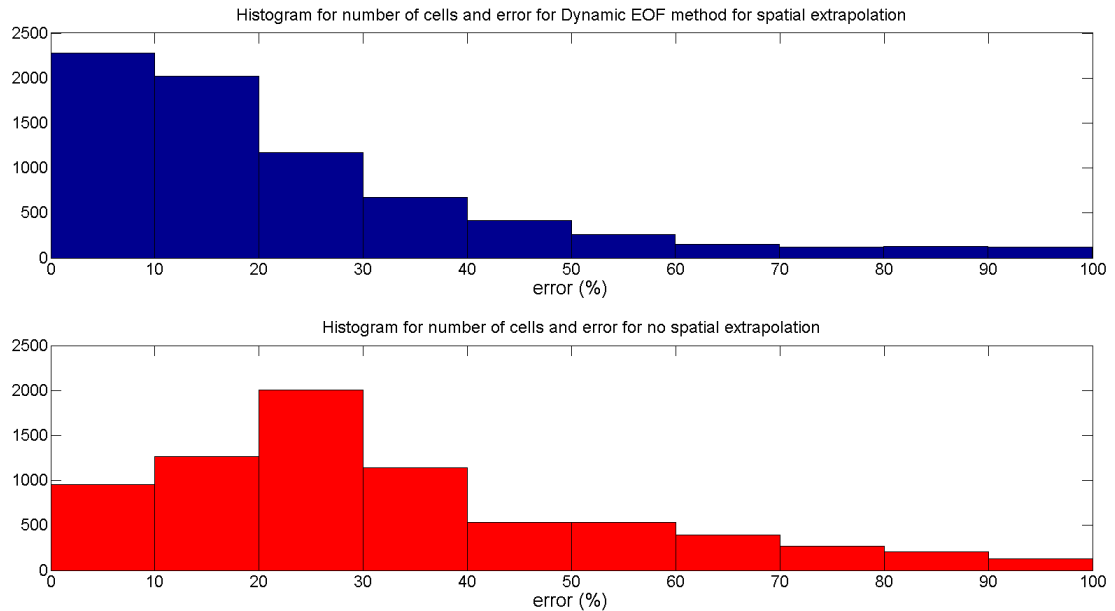


Figure 6.14. Percentage of error histogram for the extrapolated 1st EOF component using the Dynamic EOF extrapolation method vs no extrapolation method.

The vertical axis represents the number of cells that have a difference with the target value of 0-10%, 10-20% and so on. It can be seen how the dynamic EOF extrapolation method (blue) obtains many more cells with a closer value to the actual target value at $t=1500h$ when compared to the no-extrapolation case (red). This improved accuracy in the EOF spatial component will translate in a more accurate reconstruction of the unit volumetric changes values at $t=1500h$.

The dynamic EOF method also provides the opportunity to analyse how the domain is behaving, showing where linear extrapolation is chosen over exponential extrapolation or where 60 points are chosen over 20 points. This information can provide further details on how the system is behaving.

Figure 6.15 shows the areas where linear extrapolation was chosen over exponential extrapolation. It can be seen how the areas with little change (offshore) are better represented by linear extrapolation. Also, the connection of the salient with the shoreline uses linear extrapolation. The reason is that these areas also suffer little changes during the simulation.

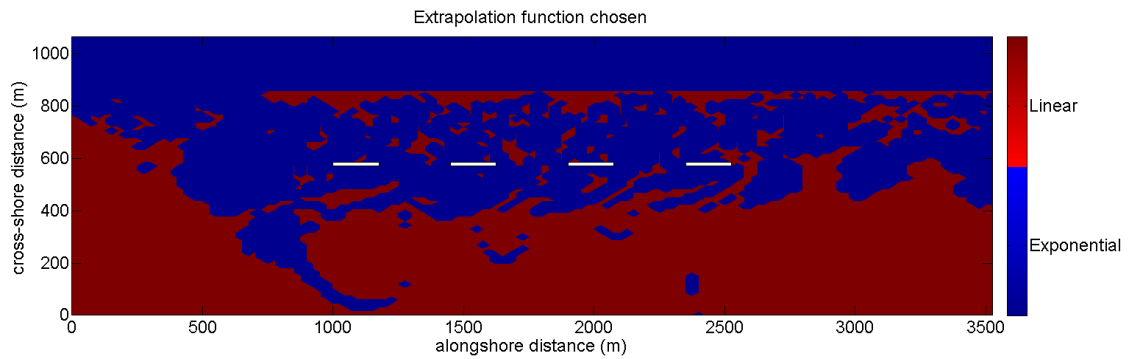


Figure 6.15. Extrapolation type selected by the Dynamic EOF method.

Figure 6.16 shows the number of points selected for each computational cell. This map shows how stable the changes are the system is suffering from. For instance when 60 points are selected, it means the system is following a continuous trend during 600 hours. Other areas however, may suffer more rapid changes being more difficult to adjust during a longer time and therefore only 20 points were selected. According to this explanation it can be seen that the upstream accretion area and downdrift erosion areas are the main areas using 60 points meaning that these processes are constantly acting during the whole training period and extending to the target period.

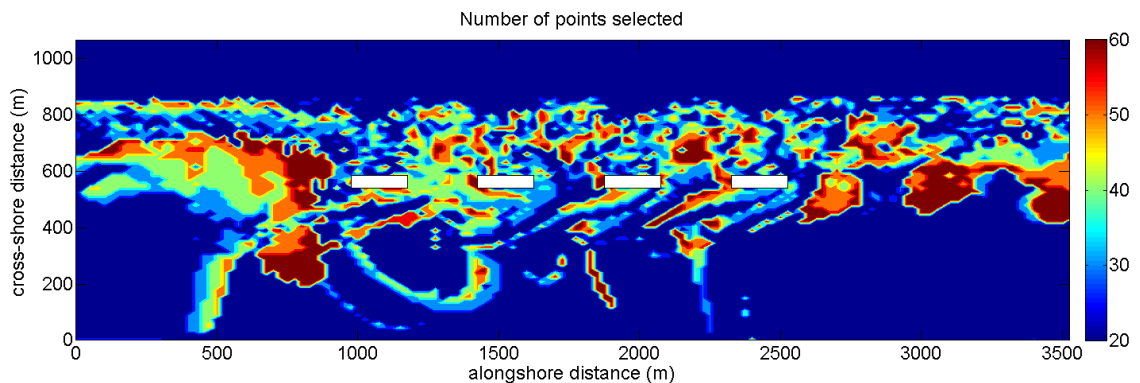


Figure 6.16. Number of points selected by the Dynamic EOF method.

Fitting a function might not be always possible due to the high variability of the variable in study, sometimes with random or chaotic behaviour. In order to acknowledge that possibility and include it on the methodology, a system to control the extrapolation process is included. A correlation threshold is defined as R_t . If for one specific location, none of the eight correlation coefficients is higher than the specified correlation threshold R_t , no extrapolation is done for that particular location. This situation means that the spatial component obtained for the training period (750h)

is used for forecasting results at 1500h. This feature avoids obtaining non-sense extrapolated values and guaranteeing that the extrapolation provided by the methodology is at least as good as using the standard methodology of extrapolating the EOF temporal component only. Also, this addition helps interpreting the system as it can be easily plot which areas in the 2D domain cannot be extrapolated, indicating a complex behaviour in such areas that might require special attention.

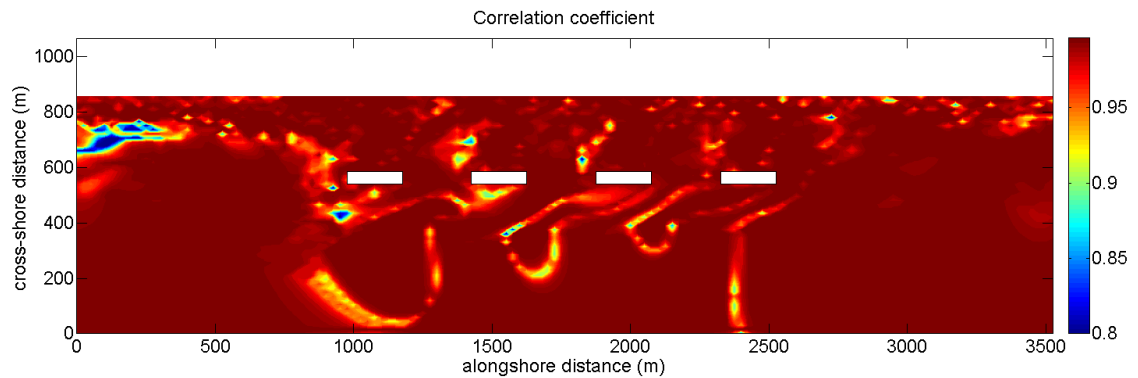


Figure 6.17. Correlation coefficient for each cell using the Dynamic EOF method.

Figure 6.17 shows the correlation coefficient of the fitting chosen for each point. Overall correlation coefficients are high but there are a few areas where it is lower or even 0.8 or smaller. The blue area represent points where no extrapolation was done because the maximum correlation coefficient obtained was not in any case larger than 0.8. It is also interesting the 3 U-shaped features offshore of the breakwaters gaps. These features could also be intuited in Figure 6.16 although being more evident in Figure 6.17. Although the final bathymetric changes do not show big changes in these regions it looks that there is a clear pattern that could be representing some morphological feature related to the interaction wave-structure. This effect could be related to unexplained 3-dimensional effects.

For the EOF temporal extrapolation the same methodology explained in Section 6.1.1 for the 1D case is followed. Figure 6.18 shows the EOF temporal extrapolation performed using the Dynamic EOF method (top panel) and using the standard method (bottom panel).

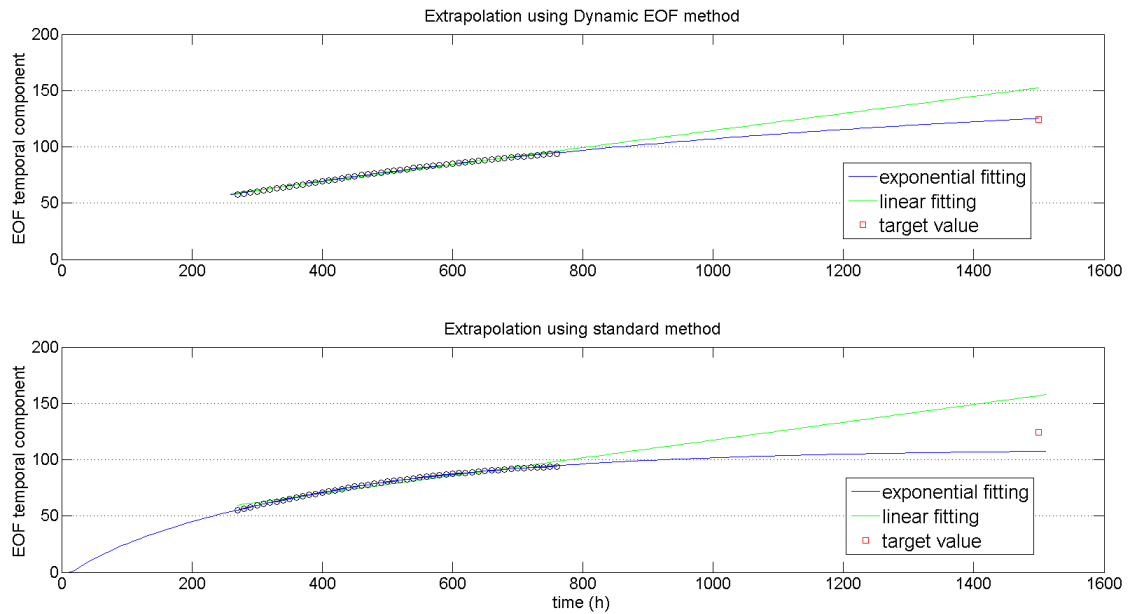


Figure 6.18. Temporal extrapolation using Dynamic EOF method (top panel) and standard method (bottom panel).

It can be seen that the dynamic EOF method yields better results also for the EOF temporal component extrapolation. Table 8 shows the values for the EOF temporal component extrapolation using both methods.

Table 8. 1st EOF temporal component values for 2D unit volumetric changes for individual cells.

1st EOF temporal component at t=1500h	Value	Error (%)
Calculated using the 1500h period	124.3	
Standard extrapolation	107.5	13.6
Dynamic EOF extrapolation	125.3	0.8
Calculated using the 750h period	93.82	24.6

Once both temporal and spatial EOF components are extrapolated, unit volumetric changes can be reconstructed at the target time $t=1500h$. As it was done for the 1D case, two reconstructions are done. One uses the Dynamic EOF extrapolation method and the other uses the standard EOF extrapolation technique with no spatial component extrapolation.

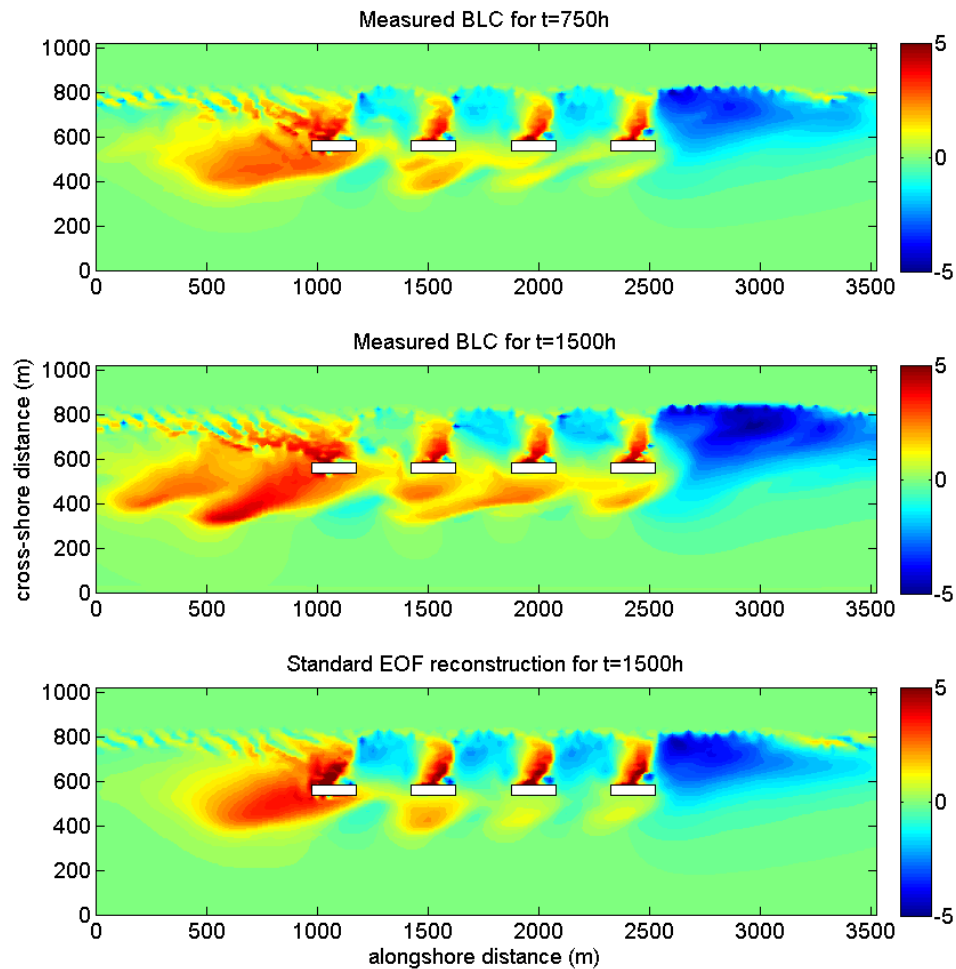


Figure 6.19. Extrapolation results at $t=1500h$ using the standard EOF method.

Figure 6.19 shows the measured unit volumetric changes for $t=750h$ (top panel), for $t=1500h$ (middle panel) and the reconstruction using the 1st EOF component with the standard EOF extrapolation method, meaning only temporal extrapolation is performed. From 750h to 1500h it can be seen that the accretion area at the left of the domain extends significantly to the left and the erosion area on the right of the domain extends significantly to the left. These changes were seen in the EOF spatial component corresponding to those periods. The reconstruction using the standard EOF extrapolation method with no spatial extrapolation is not able to catch this trend and it only represent higher values of accretion and erosion where there was accretion and erosion already at $t=750h$. However it is not able to catch the moving erosion and accretion patterns. It also can be see that accretion on the seaside of the breakwaters has increased significantly from $t=750h$ to $t=1500h$ but the standard extrapolation is not able to represent this feature either, providing similar values to those find at $t=750h$.

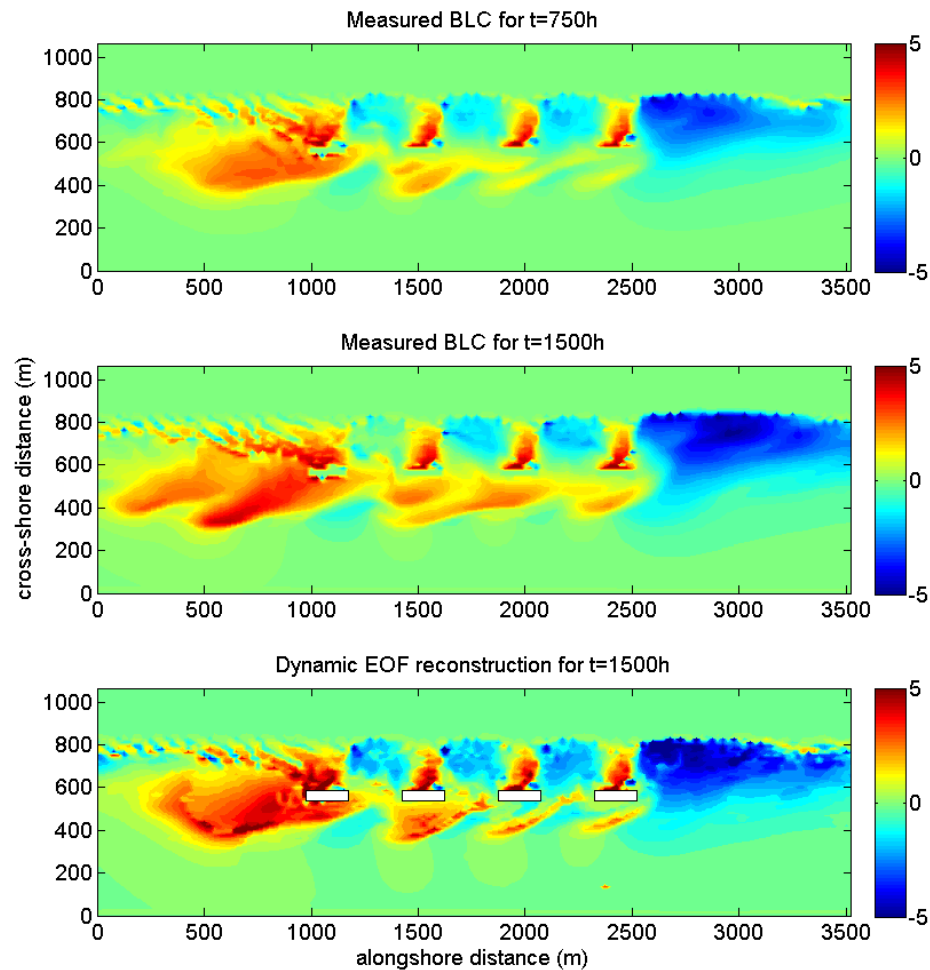


Figure 6.20. Extrapolation results at $t=1500h$ using the Dynamic EOF method.

Figure 6.20 shows the measured unit volumetric changes for $t=750h$ (top panel), for $t=1500h$ (middle panel) and the reconstruction using the 1st EOF component with the Dynamic EOF extrapolation method

The bottom panel represents the extrapolation done with the Dynamic EOF method. It can be seen how the extension on both the accretion and erosion areas on the left and right of the domain have been accurately represented by the Dynamic EOF method. Also the enlargement of the sandbars on the seaside of the breakwaters is well represented.

In order to statistically understand these results the error (%) between measured and extrapolated values are calculated for each cell (72x142) and both the dynamic EOF extrapolation method and the standard EOF method with no spatial extrapolation. Figure 6.21 shows that the dynamic EOF method is significantly reducing the error for the extrapolation measurements when compared with the standard EOF extrapolation method.

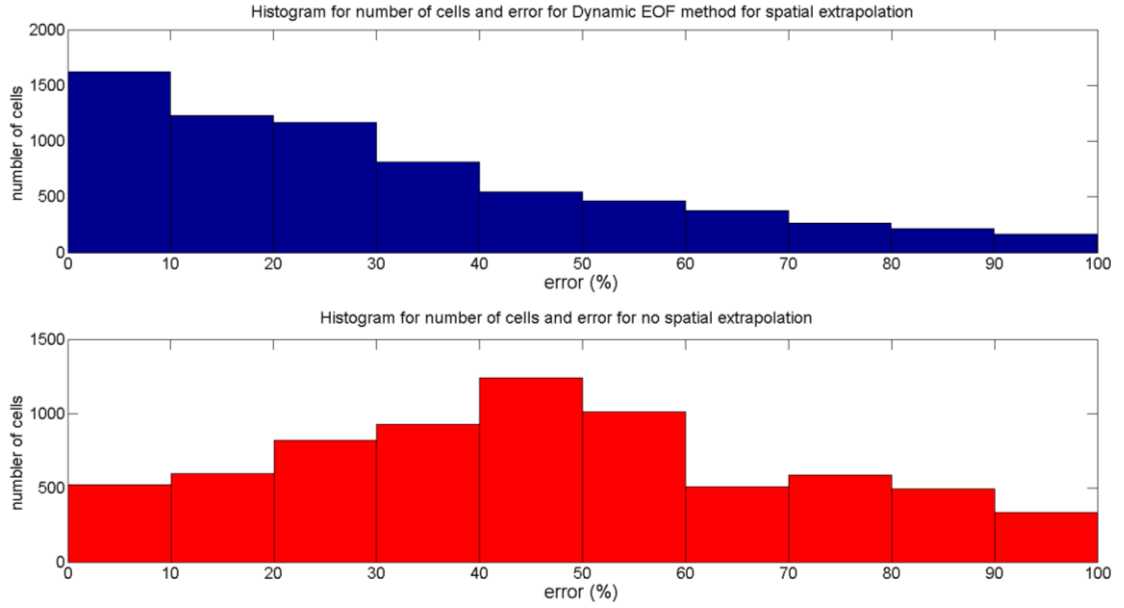


Figure 6.21. Difference (percentage) between measured and extrapolated unit volumetric changes at $t=1500h$ for both the Dynamic EOF extrapolation method (blue) and the standard EOF extrapolation method (red).

The approach considered in this section, improves greatly the simple methodology followed for the 1D case. It takes into consideration more than one function for fitting and also considers different fitting intervals, increasing the accuracy of the extrapolation. It also considers different number of points to be used for extrapolation for each location in the domain. Limitations of the method lie now on the consistency of dataset used but this is an inherent limitation to any EOF analysis.

6.4 DYNAMIC EOF METHOD ADVANTAGES AND LIMITATIONS

One of the main differences between the EEOF method and the proposed methodology is that the EEOF method applies the traditional EOF method once and the proposed methodology applies the traditional EOF method N_{LAG} times. However, the proposed methodology applies the traditional EOF method to smaller matrices than the EEOF, becoming N_{LAG} times computationally cheaper.

Given a variable, V_i^j , defined at the spatial position i and time j , where $i = 1:L_x$ and $j = 1:L_T$ and being N_{LAG} the number of maps, D_T the temporal gap between maps and $LAG = N_{LAG} \times D_T$, the EEOF calculates the EOF components from a matrix M with dimensions $M = [i * N_{LAG}, j - N_{LAG} * D_T + 1]$. In the process, eigenvectors of the matrix $F = M \times M^t$ are obtained. F dimensions are $F = [i * N_{LAG}, i * N_{LAG}] = i^2 \times N_{LAG}^2$

The proposed methodology calculates the EOF components for N_{LAG} matrices $M^{p=1:N_{LAG}}$ with dimensions $M^{p=1:N_{LAG}} = [i, 1: j - LAG + D_T * p]$. For each matrix M^p , the matrix $F^p = M^p \times M^{p^t}$ with dimensions $F = [i, i] = i^2$ is used to calculate the EOF components. As the method uses N_{LAG} matrices, the total dimension is $i^2 \times N_{LAG}$.

Therefore, the proposed methodology is N_{LAG} times computationally cheaper when calculating the EOF components, overcoming the downside of the computational cost limitation of the EEOF allowing much higher spatial i and temporal N_{LAG} resolution studies. Additionally, the EEOF does not provide means to extrapolate the spatial component quantitatively.

Complex EOF (CEOF) is able, in principle, to describe moving patterns within the spatial domain. CEOF produces spatial and temporal components in a similar manner as the traditional EOF method, with the main difference that spatial components are decomposed into real and the imaginary parts, also named as amplitude and phase. This feature causes two difficulties. On the one hand, any extrapolation method proposed will have to be applied to both phase and amplitude, making the process more complex. Moreover, classic EOF components, temporal and spatial, are sometimes difficult to interpret. Dividing the spatial components into phase and amplitude makes the interpretation process even harder, which has been reason for some authors to discard this method when applied to coastal morphology (Larson et al., 2003). The proposed methodology is able to represent moving patterns while keeping the analysis as simple to interpret as possible.

The proposed methodology offers the advantages of EEOF and CEOF as it is capable of defining the temporal evolution of the spatial components as well as describing moving trends within the domain, while overcoming the main difficulties of those methods. The proposed methodology is computationally less expensive than the EEOF and easier to interpret than the CEOF.

- The novelty of the proposed methodology is to allow extrapolating both temporal and spatial EOF components in order to enhance the accuracy of the predictions beyond the original period L_T .

-
- Improves the definition of moving features.
 - Allows analysing each location in the spatial domain independently and describing different functions for each location.
 - Allows knowing the degree of uncertainty for the behaviour followed at each location, which help understanding the system behaviour.
 - Overcomes the downside of the computational cost limitation of the EEOF allowing much higher spatial and temporal resolution studies.

The limitations of the method are mainly related to general EOF method issues and forecasting issues. The EOF components are obtained for certain conditions. If those conditions change significantly in the future, the obtained prediction will not yield accurate results. On the other hand, linear and exponential functions only were considered in this work. For different cases, different functions might be needed in order to describe other behaviours. The proposed methodology has been applied here to data obtained from a numerical model, which means high resolution data in time and space. This might be a limitation in other situations when data is limited both in time and space. However, as discussed in the literature review, data collection techniques are rapidly improving and the availability of quality data in the future will facilitate the application of the proposed methodology.

In order to assess the capabilities of the proposed methodology, it has been applied to the results from the numerical simulations presented in Chapters 5: Data Generation. Two approaches have been considered. The first approach applies the methodology to a simpler 1D case. This methodology and results were presented and published in the Proceeding of the 34th International Conference of Coastal Engineering (Alvarez and Pan 2014). The second approach applies the methodology to a 2D case including significant refinements for increased precision and was presented in the 3rd IMA International Conference on Flood Risk and published in the Water Science and Engineering journal (Alvarez and Pan 2016). Both approaches are explained and discussed in the following sections.

6.5 SUMMARY

This chapter described the usage of COAST2D to generate morphological changes around a shore-parallel breakwater scheme. Modelled data has been analysed by using the EOF method. It has been shown that EOF components extrapolation is possible and allows reconstructing the variable in study beyond the training period. Current methodologies extrapolate the EOF temporal component only. The present study proposes that extrapolating the EOF spatial component also yields to better results. This idea has been applied to two different case studies, 1D and 2D unit volumetric changes, with successful results. The proposed methodology shows it is possible to extrapolate EOF spatial components. While the 1D case proposed a very simple extrapolation technique that might not work well in more complex cases, the 2D case showed these difficulties can be overcome. Two functions were used for the 2D case extrapolation with a total of 8 different fittings per location. This methodology can be modified for each case, by considering more than 2 functions or varying the subset for fitting. Also a correlation threshold is included in order to reduce the possibility of non-sense results when extrapolating.

7 CONCLUSIONS AND FUTURE RESEARCH

This thesis proposed a methodology, dynamic EOF method, for EOF components extrapolation in order to study the impact of coastal defence structures on the nearshore morphodynamics. The dynamic EOF method consists of applying the standard EOF method to several subintervals within the training period in order to identify the temporal evolution of the EOF spatial components. The subintervals are also used to extrapolate the EOF temporal components. Both extrapolated EOF spatial and temporal components are used to reconstruct results beyond the training period. Results showed the dynamic EOF method reduces the error of the extrapolation results when compared to the methods applied in the relevant literature where only EOF temporal components are extrapolated. A review of the main results obtained and conclusions derived from this study is presented below

7.1 CONCLUSIONS

A process-based model was used to generate the high quality data needed to apply the Dynamic EOF method. COAST2D was chosen for its proven capabilities to represent the morphological changes around coastal defence structures. However, previous experience in COAST2D was limited in terms of spatial and temporal scales. Further validation was required to assure it was capable to work efficiently within the spatial and temporal scales required for this study. Once the model was validated it was used to simulate morphological changes on a domain containing four shore-parallel breakwaters. Finally, data from the model was used to feed the Dynamic EOF method. The conclusions from the usage of COAST2D in this study are summarised as:

1. COAST2D has adequately represented shoreline changes over a 4-month period and a 10km coastal stretch including two groynes. These values for temporal and spatial scales are higher than any other in previous experience, both for temporal and spatial scales. These results increase the confidence on the capabilities of COAST2D to simulate morphological changes surrounding coastal defence structures.
2. COAST2D has also been used to represent morphological changes around a set of four shore-parallel breakwaters during a period of 1500h. Results show the impact

of these structures on the shoreline and confirm the ability of COAST2D to represent morphological changes around coastal defence structures. The period of 1500h has proven to be adequate to study steady wave conditions as the system has enough time to reach the equilibrium under such conditions. However, longer periods with mixed conditions should be studied to fully understand the complexities behind the shore-parallel breakwater schemes.

Empirical Orthogonal Functions (EOF) method has been applied to study the impact of shore-parallel breakwaters on the nearshore morphodynamics. Different datasets, obtained from the process-based numerical models and representing different variables were used to feed the EOF method. The main findings are outlined as follows:

1. Shoreline changes obtained from the model can be difficult to study with the EOF method due to different issues. Firstly, depending on the wave conditions used for the simulations, the shoreline behind the breakwaters may form horn-shaped salients or tombolos. From a mathematical point of view, these shapes are non-bijective. The EOF method requires the function to be analysed to be bijective. Some simplifications can be done to overcome this issue but then the particularities of specific wave conditions would be missed. Also, the grid size and temporal output setup may lead to sudden ‘jumps’ on the shoreline shape which translate into sudden changes in the EOF components making its interpretation more difficult.
2. Volumetric changes are an ideal variable to be directly studied with the EOF method. In this study both 1D and 2D volumetric changes were studied. The 1D case study is simpler and provides means to represent shoreline changes. However due to its 1D nature some features as sandbars can be overlooked and represented as a non-realistic shoreline advance. The 2D case is ideal to study morphological changes around a set of shore-parallel breakwater as changes occurred both in the alongshore and cross-shore directions. Results show that although typically shoreline advance and recession are the more significant changes caused by these structures, the EOF spatial component values show there are two areas significantly affected by the structures when oblique waves are acting. These areas are a large accretion area upstream the first structure and a large erosion area downstream the breakwater scheme.

As discussed in the literature review, other authors have extrapolated EOF components in order to predict the variable of study beyond the training period. This extrapolation is typically performed by extrapolating the EOF temporal component only and using the EOF spatial component obtained from the training period. In order to improve the accuracy of the forecasting when using EOF extrapolated results a new methodology, the Dynamic EOF method has been developed and applied in this study. The main findings are summarised as:

1. As contrary to previous experience the EOF spatial component can be successfully extrapolated using the dynamic EOF method.
2. The Dynamic EOF method also provides means to increase the accuracy of the EOF temporal extrapolation.
3. Results show that the reconstructions done using the Dynamic EOF method yields better results than the reconstruction done using the standard EOF method extrapolation. The increased accuracy of these reconstructions is due the individual increased accuracy of the extrapolated EOF spatial and EOF temporal components.
4. 1D and 2D morphological changes have been reconstructed at $t=1500h$ using a training period of $750h$. Although is difficult to compare different studies as the quality and quantity of the data varies significantly, it is remarkable to note that the present study significantly increased the validation/calibration ratio described so far. Also Figure 6.21 shows that the Dynamic EOF method significantly reduces the error of the extrapolation when compared to the standard EOF method extrapolation techniques.
5. The limitations of the Dynamic EOF method are mainly related to data availability. The Dynamic EOF method requires a large enough number of temporal surveys able to capture the changes experimented by the system. Otherwise, the method will not be able to accurately define those trends and extrapolate into the future. There are other limitations on the application of the Dynamic EOF method on this work which are on inherent to the method itself. For instance the functions used for extrapolation are simple exponential and linear functions. More complex functions might be needed to adapt to more complex changes.

7.2 FUTURE RESEARCH

The following recommendations for future research are proposed.

- As it was described only linear and exponential functions were considered for data extrapolation. Even if these functions were appropriate to describe the evolution in this particular case study, different functions could be used. The Dynamic EOF method will therefore benefit from a more in-depth study of extrapolation techniques, like considering additional fitting functions that can adapt to more complex patterns, other than linear and exponential, even if the basis for the Dynamic EOF method would remain the same.
- This study has focussed on developing the Dynamic EOF method which has been applied to one particular case study. Nevertheless, six different cases were defined and simulated. It remains to be seen whether relationships can be described between the EOF components and the wave conditions. A potential area of research is to relate wave conditions with a certain bathymetry reaction. Once this has been done for several sea conditions, a statistical analysis could be done relating long-term wave series with long-term morphological changes.
- This study revealed that the areas of major changes are not only the salients and embayments as typically defined but also the areas upstream and downstream of the structures. These areas should be taken into account when designing breakwaters schemes not focusing only on the embayment erosion and the length of the salients. Other features were observed just offshore the breakwaters that would require further study.
- In order to study the effect of different parameters such as gran size or wave conditions the method should be applied to different cases. This approach will provided the opportunity to compare results and assess the impact of each parameter on the coastal morphodynamics.
- It was shown that depth of closure values definition is not obvious in a scheme of shore-parallel breakwaters. Further investigation of these values will help to better understand the morphological changes induced by these structures.
- New data collection techniques such as LiDAR for bathymetry acquisition around breakwaters (Jackson et al. 2015) or GPS drogues to measure currents around shore-parallel breakwaters (Phillips et al. 2013) are encouraging examples to think

that field data is going to be available in more quantity and better quality in the near future, allowing for more detailed data-driven studies like the one proposed in this thesis.

- Finally, the EOF method has been, and is currently applied to different areas of knowledge, not only coastal morphology. In the same way, the Dynamic EOF method can be applied to any other field.

8 REFERENCES

- Alvarez, F. and Pan, S. (2014) 'Modelling long-term coastal morphology using EOF method', *Coastal Engineering Proceedings*, (34).
- Alvarez, F. and Pan, S. (2016) 'Predicting coastal morphological changes with empirical orthogonal function method', *Water Science and Engineering*, 9(1), 14-20.
- Alvarez, F., Pan, S., Coelho, C. and Baptista, P. (2016 to be submitted) 'Modelling of shoreline changes at Aveiro, Portugal using a process-based numerical model: COAST2D'.
- Amoudry, L. O. and Souza, A. (2011) 'Deterministic coastal morphological and sediment transport modeling: A review and discussion', *Reviews of Geophysics*, 49(2).
- Angeloudis, A., Ahmadian, R., Falconer, R. and Bockelmann-Evans, B. (2016) 'Numerical model simulations for optimisation of tidal lagoon schemes', *Applied Energy*, (165), 522-536.
- Aubrey, D. G. (1985) 'The quantitative description of beach cycles', *Marine Geology*, 69, 155-170.
- Aubrey, D. G. (1979) 'Seasonal Patterns of onshore/offshore sediment movement', *Journal of Geophysical Research*, 84(C10).
- Baptista, P., Coelho, C., Pereira, C., Bernardes, C. and Veloso-Gomes, F. (2014) 'Beach morphology and shoreline evolution: Monitoring and modelling medium-term responses (Portuguese NW coast study site)', *Coastal Engineering*, 84, 23-37.
- Carvalho, J. P. F. (2004) 'Coastal and dune systems rehabilitation - The case of Quiaios-Mira coastal zone of Portugal', *Ecological Engineering Applied to Environmentl Restoration in Mediterranean Areas, CIHEAM*.
- CERC (1984) 'Coastal Engineering Research Center. Shore protection manual. '.
- Commission, E. (2004) 'Living with coastal erosion in Europe. Results from the EuroErosion study', *Office for Official Publications of the European Communities*.

Conscience website '<http://www.conscience-eu.net/index.htm>'.

- Dally, W. R. and Pope, J. (1986) 'Detached breakwaters for shore protection. Technical report', *TECHNICAL REPORT CERC-86-1. Waterways Experiment Station, Corps of Engineers*.
- De Vriend, H. J. (1987) 'Two- and three-dimensional mathematical modelling of coastal morphology', *Delft Hydraulics Communication*, (No 377).
- de Vriend, H. J., Capobianco, M., Chesher, T., de Swart, H. E., Latteux, B. and Stive, M. J. F. (1993) 'Approaches to long-term modelling of coastal morphology; a review', *Coastal Engineering*, 21, 225-269.
- Dean, R. G. and Dalrymple, R. A. (2004) 'Coastal Processes with Engineering Applications', *Cambridge University Press*.
- DEFRA (2005) 'Charting Progress: An Integrated Assessment of the State of UK Seas', *Defra Publications*.
- DEFRA (2002) 'Safeguarding our seas. A strategy for the Conservation and Sustainable Development of our Marine Environment.'
- DEFRA (2006) 'Shoreline management plan guidance. Volume 1: Aims and requirements'.
- Dick, J. E. and Dalrymple, R. A. (1984) 'Coastal Changes at Bethany Beach, Delaware', *Coastal Engineering Proceedings*.
- Dolphin, T. J., Vincent, C. E., Bacon, J. C., Dumont, E. and Terentjeva, A. (2012) 'Decadal-scale impacts of a segmented, shore-parallel breakwater system', *Coastal Engineering*, 66, 24-34.
- Du, Y., Wang, S., Liu, C., Zhou, H., Pan, S., Yin, S., Mao, Z. and Yang, S. (2012) 'Modelling shore-parallel breakwater effects on coastal morphology in various wave and tidal conditions at Sea Palling', *Proceedings of the Twenty-second (2012) International Offshore and Polar Engineering Conference*.
- Du, Y. L., Pan, S. Q. and Chen, Y. P. (2010) 'Modelling the effect of wave overtopping on nearshore hydrodynamics and morphodynamics around shore-parallel breakwaters', *Coastal Engineering*, 57(9), 812-826.

-
- Environment Agency (2008) 'Environment Agency. Coastal Adaptation Project: Review of international best practice.'
- Environment Agency (2010a) 'Environment Agency. Modelling the effect of nearshore detached breakwaters on sandy macro-tidal coasts'.
- Environment Agency (2011) 'Adapting to Climate Change: Advice for Flood and Coastal Erosion Risk Management Authorities.'
- Environment Agency (2010b) 'Essex and South Suffolk Shoreline Management Plan 2'.
- European Environment Agency (2009) 'European Environment Agency. Coastal erosion patterns in Europe. <http://www.eea.europa.eu/data-and-maps/figures/coastal-erosion-patterns-in-europe>'.
- EuroSION (2004) 'EuroSION: Living with Coastal Erosion in Europe. Results from the EuroSION Study. European Commission.', *Office for Official Publications of the European Communities*.
- Eurostat. Unit E1, F., Agro-environmental and rural development (2009) 'Key figures for coastal regions and sea areas', *Eurostat, Statistic in focus*.
- Fairley, I., Davidson, M., Kingston, K., Dolphin, T. and Phillips, R. (2009) 'Empirical orthogonal function analysis of shoreline changes behind two different designs of detached breakwaters', *Coastal Engineering*, 56(11-12), 1097-1108.
- Fleming, C. and Hamer, B. (2000) 'Successful implementation of an offshore reef scheme', *Coastal Engineering*.
- Gao, G., Falconer, R. and Lin, B. (2013) 'Modelling importance of sediment effects on fate and transport of enterococci in the Severn Estuary, UK', *Marine Pollution Bulletin*, 67, 45-54.
- Gee, N. (2005) 'Coastal Management, Sea Palling, Norfolk.', *Geography review*, 10-13.
- Hallermeir, R. J. (1978) 'Uses for a Calculated Limit Depth to Beach Erosion', *Proceeding in 16th Coastal Engineering Conference*, pp. 1493-1512.

- Hanson, H., Aarninkhof, S., Capobianco, M., Jimenez, J. A., Larson, M., Nicholls, R., Plant, N. G., Southgate, H. N., Steetzel, H., Stive, M. J. F. and De Vriend, H. J. (2003) 'Modelling of coastal evolution on yearly to decadal time scales', *Journal of Coastal Research*, 19(4), 790-811.
- Hanson, H., Brampton, A., Capobianco, M., Dette, H. H., Hamm, L., Laustrup, A., Lechuga, A. and Spanhoff, R. (2002) 'Beach nourishment projects, practices, and objectives—a European overview'.
- Hanson, H., Larson, M., Kraus, N. C. and Gravens, M. B. (2006) 'Shoreline response to detached breakwaters and tidal current: comparison of numerical and physical models.', *Proceeding in 30th International Conference of Coastal Engineering*.
- Horrillo-Caraballo, J. M., Karunaratna, H. U., Reeve, D. E. and Pan, S. (2014) 'A hybrid-reduced physics modelling approach applied to the deben estuary, UK.', *Coastal Engineering Proceedings*, (34).
- Hsu, T. W., Liaw, S. R., Wang, S. K. and Ou, S. H. (1986) 'Two-dimensional empirical eigenfunction model for the analysis and prediction of beach profile changes'.
- Jackson, N. L., Harley, M. D., Armaroli, C. and Nordstrom, K. F. (2015) 'Beach morphologies induced by the breawaters with different orientations', *Geomorphology*, (239), 48-57.
- JMC (1986) 'Handbook of offshore breakwater design. River Bureau of the Ministry of Construction, Japanese Government. Japanese Ministry of Construction'.
- Jolliffe, I. T. (2004) 'Principal Component Analysis, Second Edition.', *Springer*.
- Kamphuis, J. W. (2002) 'Alongshore transport of sand', *Proceeding in 28th Coastal Engineering Conference*.
- Kamphuis, J. W. (2010) 'Introduction to coastal engineering and management, 2nd ed.', *World scientific press*.
- Karunaratna, H., Horrillo-Caraballo, J. M., Ranasinghe, R., Short, A. D. and Reeve, D. (2012) 'An analysis of cross-shore profile evolution of a sand and composite sand-gravel beaches', *Coastal Engineering Proceedings*.

- Karunarithna, H., Kuriyama, Y., Mase, H., Horrillo-Caraballo, J. M. and Reeve, D. E. (2015) 'Forecasts of seasonal to inter-annual beach change using a reduced physics beach profile model', *Marine Geology*, 365, 14-20.
- Karunarithna, H., Reeve, D. and Spivack, M. (2008) 'Long-term morphodynamic evolution of estuaries: An inverse problem', *Estuarine, Coastal and Shelf Science*, 77(3), 385-395.
- Kraus, N. C., Larson, M. and Wise, R. A. (1998) 'Depth of Closure in Beach-fill Design', *Coastal Engineering Technical Note, CETN II-40*.
- Larson, M., Capobianco, M., Jansen, H., Rozynski, G., Southgate, H. N. and Stive, M. J. F. (2003) 'Analysis and modeling of field data on coastal morphological evolution over yearly and decadal time scales. Part 1: Background and linear techniques', *Journal of Coastal Research*, 19(4).
- Larson, M. and Kraus, N. C. (1994) 'Temporal and spatial scales of beach profile change, Duck, North Carolina', *Marine Geology*, 117(1-4), 75-94.
- Liang, G., White, T. E. and Seymour, R. J. (1992) 'Complex Principal Component Analysis of seasonal variation in nearshore bathymetry', *Coastal Engineering Proceedings*.
- Lorenz, E. N. (1956) 'Empirical Orthogonal Functions and Statistical Weather Prediction'.
- Losada, M. A., Medina, R., Vidal, C. and Roldan, A. (1991) 'Historical Evolution and Morphological Analysis of "El Puntal" Spit, Santander (Spain)', *Journal of Coastal Research*, 7(3).
- Loureiro, C., Ferreira, Ó. and Cooper, J. A. G. (2012) 'Geologically constrained morphological variability and boundary effects on embayed beaches', *Marine Geology*, 329-331, 1-15.
- Mangor, K. (2004) 'Shoreline Management Guidelines', *DHI Water and Environment*, 294.
- Marchand, M. E. (2010) 'Concepts and science for coastal erosion management. Concise report for policy makers.', *Deltares, Delft*.

-
- Masselink G., Russel, P. (2013) ' Impacts of climate change on coastal erosion. Concise report for policy makers.', Marine Climate Change Impacts Partnership. Science Review 2013: 71-86.
- Medina, R., Losada, M. A. and Vidal, C. (1994) 'Temporal and spatial relationship between sediment grain size and beach profile'.
- Merrifield, M. A. and Guza, R. T. (1990) 'Detecting propagating signals with Complex Empirical Orthogonal Functions: a cautionary note', *Journal of Physical Oceanography*, 20, 1628-1633.
- Miller, J. K. and Dean, R. G. (2007a) 'Shoreline variability via empirical orthogonal function analysis: Part I temporal and spatial characteristics', *Coastal Engineering*, 54(2), 111-131.
- Miller, J. K. and Dean, R. G. (2007b) 'Shoreline variability via empirical orthogonal function analysis: Part II relationship to nearshore conditions', *Coastal Engineering*, 54, 130-150.
- Munoz-Perez, J. J., Medina, R. and Tejedor, B. (2001) 'Evolution of longshore beach contour lines determined by E.O.F. method', *Scientia Marina*, 65(4), 393-402.
- Navarra, A. and Simoncini, V. (2010) 'A guide to Empirical Orthogonal Functions for Climate Data Analysis', *Springer*.
- Navarro, M., Munoz-Perez, J. J., Roman-Sierra, J., Tsoar, H., Rodriguez, I. and Gomez-Pina, G. (2011) 'Assessment of highly active dune mobility in the medium, short and very short term', *Geomorphology*, 129(1-2), 14-28.
- Nicholls, R.J., Vega-Leintert, A.C., (2013) ' Potential Implications of Sea-Level Rise for Great Britain' *Journal of Coastal Research*, 24(2), 342–357. *West Palm Beach (Florida), ISSN 0749-0208*.
- Pan, S. (2011) 'Modelling beach nourishment under macro-tide conditions', *Journal of Coastal Research*, (64), 2063-2067.
- Pan, S., Horrillo-Caraballo, J. M., Reeve, D. and Simmonds, D. (2013) 'Morphological modelling of V-shaped submerged breakwaters', *Coasts, Marine Structures and Breakwaters*.

-
- Pan, S., Li, M., Zhu, Y., O'connor, B. A., Vincent, C. E., Taylor, J. A., Dolphin, T. J. and Bacon, J. C. (2005) 'Effect of shore-parallel breakwaters on coastal morphology under storm conditions', *International Conference on Coastlines, structures and breakwaters 2005*.
- Pan, S., MacDonald, N., Williams, J., O'connor, B. A., Nicholson, J. and Davies, A. M. (2007) 'Modelling the hydrodynamics of offshore sandbanks'.
- Pelnard-Considére (1956) 'Essai de Theorie de l'Evolution des Forms de Rivages en Plage de Sable et de Galets', *Fourth Journess de l'Hydralique, les energies de la Mer, Question III*, 289-298.
- Phillips, M. R., Vincent, C. E., Bell, P., Dolphin, T. and Bacon, J. C. (2013) 'Use of GPS and X-Band Radar to track tidal currents around the shore parallel breakwaters at Sea Palling, Norfolk, UK.', *Journal of Coastal Research*, (56), 1832-1837.
- Pilarczyk, K. W. and Zeidler, R. B. (1996) 'Offshore breakwaters and shore evolution control', *Offshore breakwaters and shore evolution control. Chapter 6: Structural design*.
- Pope, J. and Dean, J. L. (1986) 'Development of design criteria for segmented breakwaters.', *Proceedings, 20th International Conference on Coastal Engineering*, 2144-2158.
- Pruszek, Z. (1993) 'The analysis of beach profile changes using Dean's method and empirical orthogonal functions', *Coastal Engineering*, 19, 245-261.
- Reeve, D. E., Chadwick, A. J. and Fleming, C. (2011) 'Coastal Engineering, processes, theory and design practice, 2nd edition', *Spon press*.
- Reeve, D. E., Horrillo-Caraballo, J. M. and Magar, V. (2008) 'Statistical analysis and forecasts of long-term sandbank evolution at Great Yarmouth, UK', *Estuarine, Coastal and Shelf Science*, 79(3), 387-399.
- Reeve, D. E. and Karunaratna, H. (2011) 'A statistical-dynamical method for predicting estuary morphology', *Ocean Dynamics*, 61(7), 1033-1044.
- Reeve, D. E., Karunaratna, H., Pan, S., Horrillo-Caraballo, J. M., Rozynski, G. and Ranasinghe, R. (2016) 'Data-driven and hybrid coastal morphological prediction methods for mesoscale forecasting', *Geomorphology*, (256), 49-67.

- Reeve, D. E., Li, B. and Thurston, N. (2001) 'Eigenfunction Analysis of Decadal Fluctuations in Sandbank Morphology at Gt Yarmouth', *Journal of Coastal Research*, 17(2), 371-382.
- Roelvink, J. A. (2006) 'Coastal morphodynamic evolution techniques', *Coastal Engineering*, 53(2-3), 277-287.
- Rosati, J. D. (1990) 'Functional design of breakwaters for shore protection: Empirical methods', *Coastal Engineering Research Centre*.
- Rusu, E. and Guedes-Soares, C. (2015) 'Influence of a new quay on the wave propagation inside the Sines harbour', *Maritime Technology and Engineering - Proceedings of MARTECH 2014: 2nd International Conference on Maritime Technology and Engineering*.
- Short, A. D. and Trembanis, A. C. (2004) 'Decadal Scale Patterns in Beach Oscillation and Rotation Narrabeen Beach, Australia—Time Series, PCA and Wavelet Analysis', *Journal of Coastal Research*, 20(2), 523-532.
- Silva, R., Baptista, P., Veloso-Gomes, F., Coelho, C. and Taveira-Pint, F. (2009) 'Sediment grain size variation on a coastal stretch facing Morth Atlantic (NW Portugal)', *Journal of Coastal Research*, SI 56 (Proceedings of the 10th International Coastal Symposium), 762-766.
- Soulsby, R. (1997) 'Dynamics of Marine Sands: A manual for practical applications', *Thomas Telford Editions*.
- The Guardian (2014) 'Rail services could take months to return to normal after storm damage', <https://www.theguardian.com/uk-news/2014/feb/11/rail-services-storm-damage-repairs-london-cornwall>.
- Thomalla, F. and Vincent, C. E. (2001) 'Beach response to shore-parallel breakwaters at Sea Palling, Norfolk, UK', *Coastal and Shelf Science*, 56(2), 203-212.
- Thomalla, F. and Vincent, C. E. (2004) 'Designing Offshore Breakwaters Using Empirical Relationships: A Case Study from Norfolk, United Kingdom'.
- Turki, I., Medina, R., Gonzalez, M. and Coco, G. (2013) 'Natural variability of shoreline position: Observations at three pocket beaches', *Marine Geology*, 338(0), 76-89.

-
- USACE (2003) 'Coastal engineering manual. ', *U.S. Army corps of engineers. Engineer Manual 1110-2-1100.*
- Van Rijn, L. C. (2011) 'Coastal erosion and Control', *Ocean and Coastal Management*, 54(12), 867-887.
- Walstra, R. J. R., Hoekstra, R., Tonnon, P. K. and Ruessink, B. G. (2013) 'Input reduction for long term morphodynamic simulations in wave-dominated coastal settings', *Coastal Engineering*, 77, 57-70.
- Wang, B. and Reeve, D. E. (2010) 'Probabilistic modelling of long-term beach evolution near segmented shore-parallel breakwaters', *Coastal Engineering*, 57(8), 732-744.
- Weare, B. C. and Nasstrom, J. S. (1982) 'Examples of Extended Empirical Orthogonal Function Analyses', *Monthly Weather Review*, 110, 481-485.
- Welsh Coastal Monitoring Centre (2011). ' *First Annual Report 2010/11*'
- Wijnberg, K. M. and Terwindt, J. H. J. (1995) 'Extracting decadal morphological behaviour from high-resolution, long-term bathymetric surveys along the Holland coast using eigenfunction analysis', *Marine Geology*, 126, 301-330.
- Winant, C. D., Inman, D. L. and Nordstrom, C. E. (1975) 'Description of seasonal beach changes using empirical eigenfunctions', *Journal of Geophysical Research*, 80(15).
- Yuhi, M., Dang, M. H. and Umeda, S. (2013) 'Comparison of accelerated erosion in riverbed and downstream coast by EOF analysis', *Journal of Coastal Research*, (SPEC. ISSUE 65), 618-623.

